ENCLOSURE 2

M170261

GNF2 Advantage Generic Compliance with NEDE-24011-P-A (GESTAR II), NEDO-33270, Revision 9, December 2017

Non-Proprietary Information – Class I (Public)

IMPORTANT NOTICE

This is a non-proprietary version of NEDC-33270P, Revision 9, which has the proprietary information removed. Portions of the document that have been removed are indicated by white space with an open and closed bracket as shown here [[ ]].

Global Nuclear Fuel

A Joint Venture of GE,Toshiba, & Hitachi

NEDO-33270
Revision 9
December 2017

Non-Proprietary Information - Class I (Public)

GNF2 Advantage
Generic Compliance with NEDE-24011-P-A (GESTAR II)

INFORMATION NOTICE

This is a non-proprietary version of the document NEDC-33270P, Revision 9, which has the proprietary information removed. Portions of the document that have been removed are indicated by an open and closed bracket as shown here [[ ]].

IMPORTANT NOTICE REGARDING CONTENTS OF THIS REPORT

PLEASE READ CAREFULLY

The only undertakings of Global Nuclear Fuel-Americas, LLC (GNF-A) with respect to information in this document are contained in contracts between GNF-A and its customers, and nothing contained in this document shall be construed as changing those contracts. The use of this information by anyone other than those participating entities and for any purposes other than those for which it is intended is not authorized; and with respect to any unauthorized use, GNF-A makes no representation or warranty, and assumes no liability as to the completeness, accuracy, or usefulness of the information contained in this document.

TABLE OF CONTENTS

Page

LIST OF TABLES

LIST OF FIGURES

EXECUTIVE SUMMARY

This report presents generic information relative to the GNF2 fuel design and analyses of GE Boiling Water Reactors for which GNF provides fuel. The scope of assessments is in accordance with the fuel licensing acceptance criteria as specified in NEDE-24011-P-A, General Electric Standard Application for Reactor Fuel (GESTAR II) (Reference 1) and is often called the Amendment 22 process. The criteria in GESTAR II establish the basis for evaluating new fuel designs, developing the critical power correlation for these designs, and determining the applicability of generic analyses. This process has been applied in the licensing of the GE14, GE12, GE13, and GE11 fuel designs, References 2 through 5, respectively.

In addition to the generic information documented herein, the fuel introduction process includes two additional activities: plant specific cycle-independent New Fuel Introduction (NFI) analyses, and cycle-unique analyses. The NFI report documents the cycle-independent plant specific analyses for use by the Licensee as input to the plant's 10 CFR 50.59 evaluation of the new fuel introduction. The cycle-unique analyses, which are part of the normal reload process, are documented in the Supplemental Reload Licensing Report (SRLR).

GNF2 was designed for mechanical, nuclear, and thermal-hydraulic compatibility with the other GNF fuel designs. The design has features of the currently operating GE10, GE11/13 and GE12/14 fuel including pellet-cladding interaction resistant barrier cladding, high performance spacers, part length rods, thick corner/thin wall channel, and axial enrichment loading. The GNF2 design is a 10x10 array with 92 fuel rods and two large central water rods, eight long part length fuel rods, and six short part length fuel rods. The part length rod configuration improves efficiency and reactivity margins.

This document contains the update to the GNF2 licensing basis to the PRIME (Reference 59) thermal-mechanical (T-M) methodology. The GESTR-M T-M bases remain valid, subject to their limitations, and are moved to Appendix A. As noted in Reference 59, the transition from GESTR-M to PRIME inputs for the downstream codes will be completed in accordance with the transition plan in NEDO-33173, Supplement 4-A, *Implementation of PRIME Models and Data in Downstream Methods*, September 2011 (Reference 60). The downstream analyses presented in

Revision 4 are based on GESTR-M models and inputs. The evaluation of PRIME Implementation on GNF2 Amendment 22 Compliance is included as Appendix D.

As stated in GESTAR II, "Fuel design compliance with the fuel licensing acceptance criteria constitutes USNRC acceptance and approval of the fuel design without specific USNRC review." All of the criteria defined in GESTAR II have been met for the GNF2 fuel design.

REVISIONS

Number	Purpose of Revision
0	Initial documentation of GNF2 Advantage compliance with GESTAR II
1	The following minor error corrections and editorial changes have been made: Page 2-2 and 2-4 Clad thickness is corrected to [[ ]]. Pre-pressurization is rounded to [[ ]] (Also Page 3-15 in Section 3.2.) Active fuel length for different BWR products is clarified. Page 2-3 The 1st sentence in the 2nd paragraph was confusing and not necessary and was deleted. Page 2-6 (Table 2-1) Corrected Figure 1-2 to Figure 2-2. Corrected GE14 FLR to [[ ]] Pellet diameter units corrected to mm. The CGE natural U specifications are not key aspects of the design and are subject to variations. The natural U rows have been deleted. Page 2-9 Figure 2-3 FLR plenum length is corrected to [[ ]] LPLR plenum length is corrected to [[ ]] SPLR plenum length is corrected to [[ ]] Page 2-11 (Figure 2-5) Line for bottom of active fuel is misplaced. Page 3-14 and 3-19 The GNF2 Power-Exposure Envelope is modified consistent with MFN 07-040 Supplement 2, August 28, 2008 (Reference 58). This is accomplished by making a modification to Figure 3-6, GNF2 Power Exposure Envelope and to the text in Section 3.1.4. Section 3.8 Updated consistent with NEDC-33292P, Revision 2, "GEXL17 Correlation for GNF2 Fuel," December 2007 Page 3-93 Updated number of data points. Page 3-96 Table 3-21 updated additive constants. Page 3-98 Updated concluding mean ECPR and standard deviation.
2	Added description of BWR 2 related changes. Section 2.2 - Modified to add GNF2 for BWR2 Table 2-1 - Modified to add BWR2 Section 3.2.1 – Modified to include GNF2 for BWR2 Figure 3-7 – Added New Figure for BWR2 Table 3-7 – Added New Table for BWR2 Section 3.2.6 - Modified to include GNF2 for BWR2 Section 3.2.9 - Modified to include GNF2 for BWR2 Section 3.2.10 - Modified to include GNF2 for BWR2 Section 3.5 – Modified to include the GNF2 cosine pressure drop data up to 8 MW bundle power. It was based on inlet-peak testing and the max bundle power tested for pressure drop was 6 MW.

	Section 3.8 – Modified to update the information regarding GEXL17 (the statistics of the latest revision of GEXL17 with the cosine critical power data) Section 4 – Modified to add BWR2 Section 5 – Modified to add BWR2 Section 6 – Modified to update some of the References
3	Modified Executive Summary and Section 1.0, Introduction, to indicate that Revision 3 is implementing the PRIME methodology for the T-M fuel design. However, the downstream analyses continue to use the GESTR-Mechanical (GESTR-M) models and inputs. Modified Section 2.1, 2.2.4, 2.2.5, and Figure 2-7 to indicate that the Defender Debris Filter is now defined as standard equipment on the GNF2 fuel assembly [[ ]] Modified Section 3.1.1.7 to include the PRIME methodology Modified Section 3.1.4 to clarify exposure limitations Incorporated the PRIME Thermal-Mechanical (T-M) methodology and revised GESTAR Amendment 33 bases into Section 3.2, updated sections 3.2.1, 3.2-3.2.4, 3.2.6 through 3.2-10 Moved the GESTR-Mechanical basis to Appendix A. The GESTR-Mechanical basis as described in Appendix A continues to be a valid T-M basis, but will not be used for future GNF2 applications Reference 58 - Replaced the MFN 07-040 Supplement 2, August 28, 2008 citation with the GESTAR II Amendment 32 submittal and its Safety Evaluation Added Reference 59 – the PRIME basis references Added Reference 60 – the downstream code transition plan Added Appendix A, GESTR-M Thermal-Mechanical Bases Added Appendix B, PRIME Based GNF2 LHGR Envelopes Added Appendix C, GESTR-M Based GNF2 LHGR Envelopes
4	Executive Summary and Section 1.0 - Updated references to Reference 60 to reflect the approved version. Executive Summary and Sections 1.0, 4.0, and 5.0 - Updated references to Revision 3 to reflect the current revision of this report. [[ ]] Figure 2-4 – Updated the figure in response to the GNF2 spacer design change [[ ]] Tables 3-27 and 3-28 – Updated the values Tables 3-29 and 3-30 – Added these new tables. Renumbered Tables 3-29, 3-30, and 3-31 from Revision 3 to Tables 3-31, 3-32, and 3-33 Figure 3-34 - Deleted Section 3.7.1 – Modified text to be more concise [[ ]] Section 3.12.3 – Added this new section on the fuel enthalpy analysis [[ ]]

	Section 6.0 – Updated Reference 1 to the current revision of GESTAR II, updated Reference 60 to reflect the approved version, and added Reference 61 – GE Fuel Bundle Designs Appendix A, Figure A-2 – Corrected the peak LHGR value at the 45 GWd/MTU peak pellet exposure Appendices B and C – Added clarifying language regarding the values in Tables B-1 through B-4 and C-1 through C-4. Appendix C, Table C-3 – Corrected the pellet power at Knee 2 Appendix C, Table C-4 – Corrected the pellet power at Knee 2 for all rod/section
5	Executive Summary and Section 1.0: Added reference to Appendix D. Section 3.2.1: Adding wording pertaining to alternate GNF2 channel designs. Figure 3-8: Added figure for alternate GNF2 channel designs. Added Appendix D, Evaluation of PRIME Implementation on GNF2 Amendment 22 Compliance.
6	Added Appendix E, Evaluation for Slightly Enriched Blankets in GNF2.
7	Added Appendix F, Evaluation of Improvements to Debris Filter and Spacer.
8	Table 2-1: Revised the GE14 and GNF2 Fuel Column Geometric Stacking Factor Standard.
9	Section 3.1.1.4: Transient Simulator subsection: Updated to reflect that TRACG04 (Reference 27) has been approved by the NRC and contains limitations that have been addressed by the method. Section 3.3.2: Deleted an inaccurate statement pertaining to low void conditions. Figure 3-33: Corrected the location of the vertical line for the lower bound of the mass flux range. Section 6.0: Updated Reference 27 to the current NRC-approved version.

ACRONYMS AND ABBREVIATIONS

Term	Definition
AOO	Anticipated Operational Occurrence
APRM	Average Power Range Monitor
ATWS	Anticipated Transient Without Scram
BOC	Beginning Of Cycle
BOEC	Beginning of Equilibrium Cycle
BOL	Beginning of Life
BT	Boiling Transition
BWR	Boiling Water Reactor
BWROG	BWR Owners Group
CDA	Confirmation Density Algorithm
CPPU	Constant Pressure Power Uprate
CPR	Critical Power Ratio
DIVOM	Delta CPR over Initial MCPR Versus Oscillation Magnitude
DRC	Doppler Reactivity Coefficient
ΔCPR	Delta Critical Power Ratio
[[	]]
ECCS	Emergency Core Coolant System
EOC	End Of Cycle
EOC – 3K	End Of Cycle – 3000 MWd/MTU
EOEC	End of Equilibrium Cycle
EOL	End of Life
EOP	Emergency Operating Procedure
EPU	Extended Power Uprate
FMCPR	Final Minimum Critical Power Ratio
FWCF	Feedwater Controller Failure Event
FWHOOS	Feedwater Heating Out-of-Service
FSAR	Final Safety Analysis Report
GE	General Electric Company
GESTAR II	General Electric Standard Application for Reload Fuel, (Current Revision: NEDE-24011-P-A-18, April 2011)
GEXL	General Electric Critical Quality versus Boiling Length Correlation
GESTR	General Electric Stress and Thermal Analysis of Fuel Rods
HBB	Hard Bottom Burn
HCOM	Hot Channel Oscillation Magnitude
ICPR	Initial Critical Power Ratio
LHGR	Linear Heat Generation Rate
LTS	Long Term Solution for Stability
LOCA	Loss Of Coolant Accident
LTR	Licensing Topical Report
LPRM	Local Power Range Monitor
MAPLHGR	Maximum Average Planar Linear Heat Generation Rate

Term	Definition
MOP	Mechanical Overpower
MOC	Middle of Cycle
MOEC	Middle of Equilibrium Cycle
MCPR	Minimum Critical Power Ratio
MELLLA+, M+	Maximum Extended Load Line Limit Analysis Plus
Methods LTR	Applicability of GE Methods to Expanded Operating Domains Licensing Topical Report
MTC	Moderator Temperature Coefficient
MNCP	A General Monte Carlo N-Particle Transport Code
NFI	New Fuel Introduction
NRC	Nuclear Regulatory Commission
ODYN	1-D Transient Model
ODYSY	GE Best-Estimate Frequency Domain Stability Code
OLMCPR	Operating Limit MCPR
OLTP	Original Licensed Thermal Power
OPRM	Oscillation Power Range Monitor
Option II	Stability Detect and Suppress Long Term Solution for BWR/2
Option III	Stability OPRM-Based Detect and Suppress Long Term Solution
PANACEA	Current GE BWR Core Simulator
PCT	Peak Cladding Temperature
PLR	Part Length Rod
PRIME	The PRIME Model for Analysis of Fuel Rod Thermal – Mechanical Performance, NEDC-33256P, NEDC-33257P, and NEDC-33258P
PU	Power Uprate
SAFDLs	Specified Acceptable Fuel Design Limits
SDM	Shutdown Margin
SE, SER	Safety Evaluation Report
SLMCPR	Safety Limit MCPR
SRLR	Supplemental Reload Licensing Report
TGBLA	Current GE BWR lattice physics code
T-M	Thermal-Mechanical
TOP	Thermal Overpower
TIP	Traversing In-Core Probes
TR	Topical Report
TRACG	Transient Reactor Analysis Code (GE proprietary version)
UTL	Upper Tolerance Limit
1-D	One Dimensional
3-D	Three Dimensional

1.0 INTRODUCTION

This report presents generic information relative to the GNF2 fuel design and analyses of GE Boiling Water Reactors for which GNF provides fuel. The organization and scope of assessments is in accordance with the fuel licensing acceptance criteria as specified in GESTAR II (NEDE-24011-P-A, General Electric Standard Application For Reactor Fuel) and often called the Amendment 22 process. The Amendment 22 process was approved by the NRC in July 1990 (Reference 6). The fuel licensing acceptance criteria included in GESTAR II establishes the basis for evaluating new fuel designs, developing the critical power correlation for these designs, and determining the applicability of generic analyses to these new designs. Compliance with the fuel licensing acceptance criteria constitutes USNRC acceptance of the fuel design without specific USNRC review. This process has been previously applied to the GE14 fuel design (Reference 2), GE12 fuel design (Reference 3), GE13 fuel design (Reference 4), and the GE11 fuel design (Reference 5). This document updates the GNF2 licensing basis to the PRIME (Reference 59) thermal-mechanical (T-M) methodology. The GESTR-M T-M bases remain valid, subject to their limitations, and are moved to Appendix A. As noted in Reference 59, the GESTR-M to PRIME transition for the downstream codes will be completed in accordance with the transition plan in NEDO-33173, Supplement 4-A, *Implementation of PRIME Models and Data in Downstream Methods*, (Reference 60). The downstream analyses presented in Revision 4 are based on GESTR-M models and inputs. The evaluation of PRIME Implementation on GNF2 Amendment 22 Compliance is included as Appendix D.

In addition to the generic information documented herein, the fuel introduction process includes two additional activities: plant specific cycle-independent new fuel introduction analyses, and cycle-unique analyses. The New Fuel Introduction report (Section 4.2) documents the cycle-independent plant specific analyses for use by the Licensee as input to the plant's 10 CFR 50.59 evaluation of the new fuel introduction. The cycle-unique analyses, which are part of the normal reload process, are documented in the Supplemental Reload Licensing Report (SRLR).

The fuel licensing criteria from GESTAR II are included in the applicable sections. The features and design characteristics of the GNF2 fuel bundle are described in Section 2.0. The evaluations, meeting the requirements of GESTAR II, are presented in Section 3.0. Each section or sub-section of Section 3.0 includes the requirement from GESTAR II. Section 4.0, Licensing Application, describes the manner in which the Licensees use this report.

2.0 GNF2 FUEL BUNDLE DESIGN

GNF2 is very similar to the GE14 design licensed under the GESTAR II process (Reference 1). Table 2-1 provides a summary of the GNF2 design as compared to the GE14 design.

A GNF2 bundle schematic is shown in Figure 2-1. The GNF2 design consists of 92 fuel rods and two large central water rods contained in a 10x10 array. The two water rods encompass eight fuel rod positions. Eight of the fuel rods terminate just past the [[ ]] and are designated as long part length fuel rods. Six fuels rods terminate just past the [[ ]] and are designated as short part length fuel rods. Eight fuel rods are used as tie rods. The GNF2 lattice arrangement is shown in Figure 2-2. The rods are spaced and supported by the upper and lower tie plates and eight spacers over the length of the fuel rods. For GNF2, the channel interacts with the Lower Tie Plate (LTP) to [[ ]]

The fuel rods consist of high-density ceramic UO_2 or (U, Gd)O_2 fuel pellets stacked within Zircaloy-2 cladding. The cladding will generally have an inner zirconium liner. The fuel rod is evacuated and backfilled with helium. Fuel rod dimensions are given in Table 2-1.

2.1 NEW DESIGN FEATURES

GNF2 was designed for mechanical, nuclear, and thermal-hydraulic compatibility with the other GNF fuel designs. The design includes many features of the GE10, GE11/13 and GE12/14 fuel including pellet-cladding interaction resistant barrier cladding, high performance spacers, part length rods, thick corner/thin wall channel, and axial enrichment loading. New or improved features included in GNF2 are:

- Part length rod configuration (both lattice position and axial extent) that improves efficiency and reactivity margins
- Eight Alloy X-750 spacers with reduced pressure drop and improved resistance to boiling transition as compared to the Zircaloy ferrule spacer
- New fuel rod design with increased uranium content
- Optional Debris Shield Lower Tie Plate (LTP)

- Defender Debris Filter LTP as standard equipment.

A discussion of each of these new design features is provided below.

2.2 FUEL ASSEMBLY CONFIGURATION

The 10x10 fuel assembly configuration is described above and shown in Figure 2-1 and Figure 2-2. The GNF2 design operates at a LHGR comparable to previous designs (GE11 and GE13), and higher than the GE14 design. The barrier fuel cladding is utilized to avoid capacity factor losses due to recommended operating restrictions associated with Pre-Conditioning Interim Operating Management Recommendations (PCIOMR). The zirconium barrier liner that has been incorporated in GE6 through GE14 designs is standard in the GNF2 design. [[

]] The combination and number of part length rods as well as the lengths of part length rods has been optimized. The GNF2 optimization maximizes the fuel assembly weight while maintaining pressure drop and stability characteristics compatible with existing BWR fuel designs. [[

]]

2.2.1 Part Length Rods

Fourteen (14) part length fuel rods (PLRs) are selectively located in the lattice as shown in Figure 2-2. Eight of these PLRs are approximately two thirds the length of the full-length rods. The longer part length rods terminate [[

]] These shorter part length rods terminate [[

]]

[[

]] Figure 2-3 provides a nominal description of the GNF2 fuel rod configuration.

2.2.2 Spacers

The GNF2 fuel design uses eight Alloy X-750 spacers [[

]] The spacers are shown in Figure 2-4. The spacer spring force is established to avoid fretting wear on the fuel rods due to fuel rod vibration. Flow diversion devices have been added to the top of the spacer to improve thermal hydraulic characteristics in the two-phase flow region. The axial distribution of the spacers is shown in Figure 2-5.

The GNF2 bundle design uses a [[

]]

2.2.3 GNF2 Advantage Fuel Rod

The high energy GNF2 fuel rod has the following characteristics:

- [[

]]

The GNF2 Advantage fuel rod has evolved from GNF's proven 10x10 fuel rod design methodology and extensive in-reactor experience. The GNF2 fuel rod was designed to provide increased bundle uranium mass while maintaining the same reliability performance as existing designs. The GNF2 Advantage fuel rod thermal mechanical limits have been defined to meet the same Specified Acceptable Fuel Design Limits (SAFDLs) as the GE14 fuel rod. [[

]]

2.2.4 Debris Shield Lower Tie Plate

The Debris Shield Lower Tie Plate is an optional lower tie plate design that is available for the GNF2 Advantage product line. A primary design consideration in the development and application of foreign material mitigation devices, such as the Debris Shield or Defender LTP, is to ensure equivalent hydraulic resistance, which is the primary LTP characteristic affecting licensing evaluations. The GNF2 LTP is equivalent to previous designs with respect to pressure drop loss coefficients and this has been confirmed with full-scale tests. The debris shield lower tie plate provides enhanced foreign material protection by reducing the pore size of the filter with respect to earlier debris filter lower tie plate designs.

The debris shield LTP (Figure 2-6) is an assembly [[

]] The plate has been designed to reduce the introduction of foreign material (wire, springs, drill turnings, etc) into the assembly. The Debris Shield LTP protects the GNF2 assembly from foreign material that may be located in the bottom plenum of the reactor vessel. Fuel failures have been identified as resulting from foreign objects interacting with the fuel cladding. Foreign material introduced to the fuel assembly may become lodged in the fuel

assembly structure. Once lodged in the fuel assembly structure, flow induced vibration of the object can cause fretting wear on the rods. The Debris Shield LTP reduces the probability of foreign material related fuel rod failures by reducing the size and quantity of foreign material that can enter the fuel assembly from the bottom plenum of the reactor vessel.

2.2.5 Defender Debris Filter Lower Tie Plate

The Defender Debris Filter LTP (Figure 2-7) is an assembly consisting [[

]] The Defender Debris Filter has been designed to provide a more effective debris filter relative to the Debris Shield Lower Tie Plate. [[

]] as shown in Figure 2-7. [[

]] The Defender Debris Filter and its LTP have been designed to have equivalent hydraulic resistance as other GNF lower tie plates and is interchangeable with other GNF 10x10 LTP designs.

2.2.6 [[ ]]

[[

]]

Table 2-1 GE14 and GNF2 Dimensions

Fuel Assembly	GE14	GNF2
Total number of fuel rods	92	No Change
Full length	78	No Change
Partial length	14 total, Single Length	14 total, Two Lengths
Long Part Length Rod (LPLR)	14	8
Short Part Length Rod (SPLR)	0	6
Lattice Array	Figure 2-2	Figure 2-2
Rod to rod pitch (cm)	[[	]]
Number of water rods	2	No Change
Typical Assembly weight (kgU)	[[	
BWR/2-3 Full Length Rod (mm)		
BWR/4-6 Full Length Rod (mm)		
Long Part Length Rod (LPLR) (mm)		
Short Part Length Rod (SPLR) (mm)		
Fuel Rod		
Cladding material		
Typical BWR/2-3 Assembly active fuel length (mm)		
Typical BWR/4-6 Assembly active fuel length (mm)		
LPLR Active Fuel Length (mm)		
SPLR Active Fuel Length (mm)		
Cladding tube diameter, outer (cm)		
Cladding tube wall thickness (cm)		
Pellet diameter, outer (mm)		
Fuel pellet density (PD) standard		
Fuel column Geometric Stacking Factor (GSF) standard		
Helium Backfill Pressure BWR/2		
Helium Backfill Pressure BWR/3-6		
Fuel column stack density (g/cc)		
Water Rod		
Cladding material		
Cladding diameter, outer (cm)		
Cladding wall thickness (cm)		]]
Spacer		
Number of spacers	8	No Change
Axial locations	See Reference 2 Figure 1-6	See Figure 2-5
Material	Zircaloy ferrule and bands with Alloy X-750 springs	Alloy X-750

[1] [[ ]]

[2] Gd_2O_3 Concentration, percent by weight (GC)

Figure 2-1 GNF2 Fuel Bundle Assembly

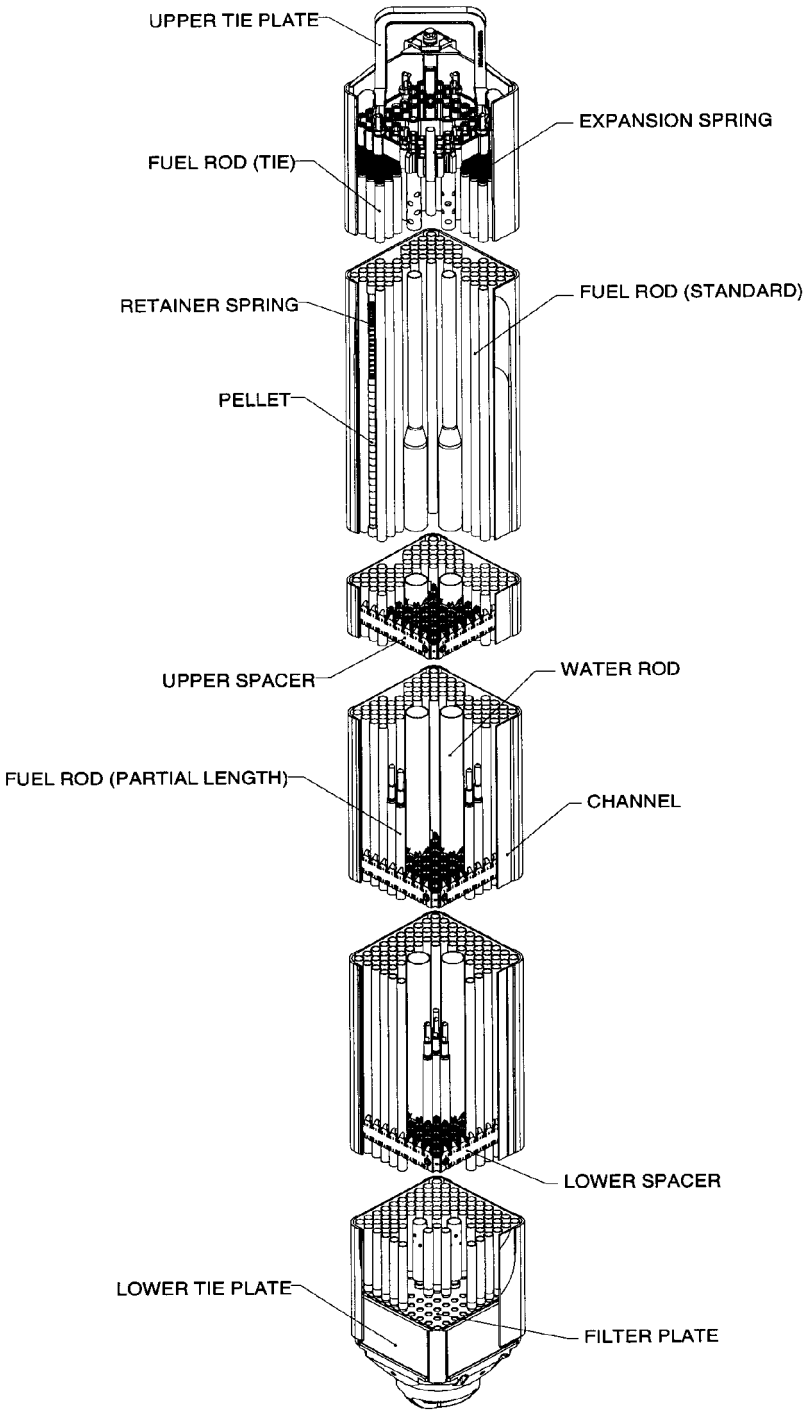

Figure 2-2 Lattice Arrangement

[[

]]

Figure 2-3 GNF2 Fuel Rods

[[

]]

Figure 2-4 GNF2 Spacer

[[

]]

Figure 2-5 GNF2 Axial Spacer Locations

[[

]]

Figure 2-6 GNF2 Debris Shield LTP Assembly

[[

]]

Figure 2-7 Defender Debris Filter LTP

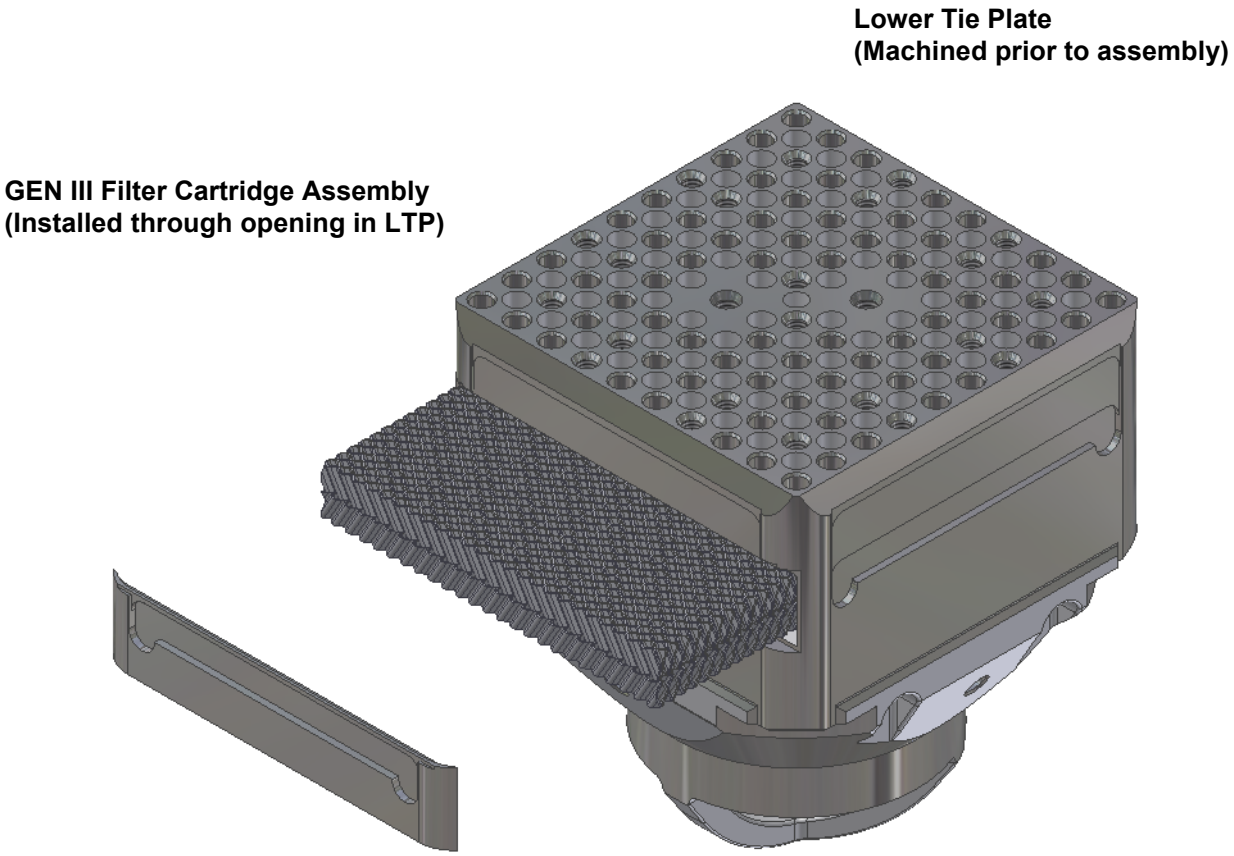

3.0 EVALUATION

The fuel licensing acceptance criteria included within GESTAR II are established for evaluating new fuel designs, developing critical power correlation for these designs, and determining the applicability of generic analyses to these new designs. GNF2 fuel design compliance with the fuel licensing acceptance criteria constitutes USNRC acceptance and approval of the fuel design without specific USNRC review.

This process has been previously applied to the GE14 and GE12 10x10 fuel designs, and GE13 and GE11 9x9 fuel designs. NRC audits of the previous applications of the GESTAR II new fuel process are documented in References 7 and 8. Prior to the GE14 compliance report, NRC-GE interactions (References 9, 10, and 11) resulted in process clarification and some minor changes to the original analysis methods. The following bulleted items provide the status of the technical subjects in the GE14 compliance report relative to the GNF2 fuel:

- **Stability Analyses:** The GNF2 generic licensing compliance stability checks have been performed using the methods defined by the BWR Owners Group and approved by the NRC (Reference 12). In addition, the stability analyses that establish the acceptability of the setpoints and define the backup protection regions are now performed on a cycle specific basis.
- **Pressurization Transient Analyses:** GE accounts for the time variation of the axial power shape during pressurization transients. The procedure for doing this has been approved by the NRC (References 7 and 13). In addition, both the ODYN and TRACG methods directly determine the change in axial power shape during a pressurization event. The limiting pressurization events are performed on a cycle specific basis.
- **Control Blade Insertion:** Generic compliance with this criterion is determined by calculating the magnitude of the bundle lift during a combined seismic and LOCA loading for a reference approved design in a reference plant. As was done for GE14, the GNF2 evaluation used a standard reference plant that shows significant lift with a referenced approved fuel design.
- **Doppler Reactivity Coefficient:** In the same manner as GE14 and previous fuel designs, a bounding calculation using an infinite lattice was performed to demonstrate that the Doppler coefficient remains negative for GNF2. Section 3.3.1 describes the analysis approach and assumptions. The GE11 NRC audit report (Reference 7) noted that the GE11 compliance report (Reference 5) described in some detail the analysis procedure, including calculations for an equilibrium core of GE11 and for the limiting

point in the cycle considering all modes of expected operation, to demonstrate that the negative Doppler reactivity coefficient required by the acceptance criterion is maintained.

- **Fuel Handling Accident:** In cases where the refuel accident may not be confirmed as bounding, an alternate criterion requiring the performance of a new analysis has been specified (Reference 8). Section 3.13 of this document provides information necessary for each licensee to satisfy the alternate criterion. This is accomplished by adjusting their current FSAR basis for such variables as number of failed rods and the power of the damaged bundles. However, this event depends on a number of factors that may have changed over the history of the plant. Therefore, this event will be evaluated during the plant specific cycle-independent NFI of GNF2 (See Section 4.2).

The GESTAR II fuel licensing acceptance criteria and the bases for compliance of GNF2 fuel with these criteria are presented in the following subsections.

3.1 GENERAL CRITERIA

3.1.1 NRC-Approved Models

GESTAR II Section 1.1.1.A: "NRC-approved analytical models and analysis procedures will be applied."

NRC approved methodologies as documented in GESTAR II have been used to demonstrate compliance for each of the analyses required in Subsection 3.2 through Subsection 3.14. Analytical models and analysis procedures for the evaluation of each criterion will be described in each respective section of this report.

This section addresses the applicability of the current methods and methodologies to the GNF2 fuel design. Most approved methodologies include an engineering computer program (ECP) that encodes part or all of each methodology within an algorithmic framework. For the most commonly used ECPs, discussion of any effects of the unique characteristics of GNF2 has been included. In particular, the unique characteristics of GNF2 that the methods must address are the multiple lengths of part length rods. Generally, the codes are unaffected by these characteristics given flexibility of their modeling, input structure, or representation of these characteristics in the approved methodology. A partial demonstration of the continued applicability of the methods to the GNF2 geometry and characteristics has been provided.

3.1.1.1 Nuclear Methods

Lattice Physics

TGBLA06 (Reference 14) is the two-dimensional transport corrected diffusion theory model used to model the details of nuclear transport at the lattice level. While the fundamental methodology for TGBLA06 will not be changed from that approved by the NRC, the TGBLA06 ECP required a modification to properly model GNF2. [[

]]

[[

]]

Figures 3-1 and 3-2 demonstrate the applicability of TGBLA06 using direct comparisons to Monte Carlo (MCNP, Reference 16) at 0.0 exposure. [[

]] The average reactivity bias for all cases at each moderator density is provided in Figure 3-1. For reference, the 1σ spread of a small set of GE14 designs are also provided. The small impact of analyzing the GNF2 designs is well within the accepted levels of uncertainty in lattice physics modeling. Figure 3-2 extends this comparison to standard deviation of pin-by-pin fission density differences between MCNP and TGBLA06. It is concluded that the introduction of GNF2 is not significant to the TGBLA lattice physics methodology.

Figures 3-3 and 3-4 demonstrate the capability of TGBLA06 at [[ ]] This lattice average exposure corresponds to approximately [[

]]. This analysis is completed by applying the high exposure isotopics from TGBLA06 within MCNP. [[

]] These results indicate that the method performs well and that no abrupt changes in code performance versus exposure are expected.

[[

]]

Figure 3-1 TGBLA06 Reactivity Benchmark for GNF2, solid line, at BOC (GE14 1σ uncertainty band, dashed line)

[[

]]

Figure 3-2 TGBLA06 Fission Density Benchmark for GNF2, solid line, at BOC (GE14 1σ uncertainty band, dashed line)

[[

]]

Figure 3-3 TGBLA06 Reactivity Benchmark for GNF2, solid line, at high exposure (GE14 1σ uncertainty band, dashed line)

[[

]]

Figure 3-4 TGBLA06 Fission Density Benchmark for GNF2, solid line, at high exposure (GE14 1σ uncertainty band, dashed line)

Steady-State Core Simulator

PANAC11 (Reference 14) is the three-dimensional core simulator utilized for design, licensing, and core monitoring. PANAC11 correctly handles varying axial geometry in nuclear and thermal-hydraulic modeling through use of its lattice dependent geometry, nodal thermal-hydraulic properties, and axial meshing routines. This allows PANAC11 to handle multiple PLR, varying water rod diameter, and other axially varying features when modeled at the bundle/lattice library level.

PANAC11, like other GNF thermal-hydraulic codes, uses the "New Dix" void-quality correlation in its thermal-hydraulics treatment and accounts for bundle leakage and water rod flow by parameterized input from ISCOR simulations. As explained further in Section 3.1.1.2, the New Dix void quality correlation has been shown to be applicable to GNF2.

3.1.1.2 Thermal-Hydraulic Methods

ISCOR09 (Reference 17) is a thermal-hydraulic core analysis program wherein different fuel types can be designated to represent various types of bundles within a core. The introduction of various PLR rod heights, such as in GNF2, or other axially varying features, such as axially varying thick/thin channels, can be readily handled by ISCOR09 since parameters can be varied axially to account for changes in the number of rods, water rod diameters, etc. in the lattice at different axial locations. [[

]]

The GE void correlation has previously been shown to be applicable for all GE BWR fuel designs, including 10x10 lattices with part length rods. [[

]] Qualification of advanced designs like GE12, GE14, and GNF2 has been evaluated with full-scale experimental pressure drop data described in Section 3.5. Correct prediction of the pressure drop requires accurate prediction of the void fraction throughout the length of the bundle. In addition, the void fraction correlation is indirectly qualified via comparison with sub-channel analysis methods as

show in Figure 3-5. Therefore, the GE void fraction correlation forming the basis for all currently approved methodologies is applicable to GNF2 fuel designs.

[[

]]

Figure 3-5 Axial Void Calculation on GNF2 at High Power Conditions from the Dix Correlation and Sub-channel Based Calculation

3.1.1.3 Safety Limit

The facets of the SLMCPR calculation include discussion of the adaptive technology, establishment of uncertainties, and method of SLMCPR calculation. (References 18 and 19)

Adaption

The adaptive methodology is applied within PANAC11. There are no changes to this methodology as a result of introduction of GNF2.

Uncertainties

There is no change to the SLMCPR uncertainties for GNF2 application. In accordance with the safety evaluation for the SLMCPR methodology, the uncertainties must be verified for new fuel designs. These restrictions are evaluated in Section 3.6. The verification of the pin power/R-factor uncertainty is also supported by the analysis in Section 3.1.1.1.

SLMCPR Calculation

GESAM02 embodies the implementation of the revised SLMCPR methodology using PANAC11 physics models to calculate CPR distribution (References 18, 19, and 20). There are no changes required to determine the SLMCPR for GNF2.

3.1.1.4 Transient Analysis

Interface and Collapse

CRNC-06 (References 21 and 22) collapses the 3-D cross sections supplied by PANAC11 into 1-D cross section fits acceptable for ODYNM10 or ODYNV09 (References 21, 22, and 23). The resulting cross section fits and thermal-hydraulic information is collected and stored on the CRNC-06 output file for ODYNM10/ODYNV09 and other codes to read. Detailed GNF2 axial geometry information is written under auxiliary dataset names. The capabilities of both PANAC11 and CRNC-06 to perform this function are adequate for the modeling of GNF2.

Transient Simulator

ODYNM10/ODYNV09 (References 21, 22, and 23) retrieves cross section information and thermal-hydraulic information from the CRNC-06 output file. [[

]] The thermal-hydraulics and void correlation implemented in ODYN is applicable to GNF2.

TRACG02 (References 24, 25, and 26) and TRACG04 (Reference 27) are also approved for use for transients (Anticipated Operational Occurrences). Simulation of GNF2 does not pose

challenges to the modeling capabilities of this technology, and all fuel type specific limitations have been addressed for this method.

Hot Bundle Simulation

TASC-03 (Reference 28) is a single hot channel thermal hydraulic analysis code and requires detailed bundle geometry input that designates different types of rod groups within the bundle. The two types of PLR within GNF2 can be handled in TASC-03 by designating an additional PLR rod group and giving the required geometry inputs. TASC-03 also uses the "New Dix" void quality correlation. This void correlation has been shown to be acceptable for application to GNF2 fuel bundles. The approved methodology is applicable to GNF2.

3.1.1.5 Stability

ODYSY05 (Reference 29) is capable of modeling axially varying bundle designs. This is accomplished by requiring axial geometry to be specified through input on a nodal basis. The multiple part-length rod inputs for GNF2 must be calculated outside the code and provided as input to ODYSY. This void correlation has been shown to be acceptable for application to GNF2 fuel bundles. The approved methodology is applicable to GNF2.

3.1.1.6 Channel Bow

The methodology used to assess the impact of channel bow on R-Factor (Reference 30), and thus critical power continues to be applicable because the mechanical behavior of the channel is not changing (Section 3.2.5) The effect on individual rod power peaking continues to be evaluated as a function of the degree of channel bow. While numerical sensitivities of the critical power will differ between the various fuel types, GNF2 included, the process continues to be applicable. The cross section of the thick-thin region of the Zircaloy (the entire channel, except for the ends) is almost identical to the prior thick-thin channels. The ends of the channels do not play a large role in channel bow.

3.1.1.7 Thermal-Mechanical Methods

An important part of the GNF2 design and licensing bases is the fuel rod thermal-mechanical design and licensing analyses. These design and licensing analyses for the prior GE8 through GE14 fuel designs were performed with the GNF GESTR-Mechanical fuel rod thermal-mechanical performance model (References 31, 32, and 33), supplemented with GESTR-LOCA analyses to provide inputs to the Loss-of-Coolant Accident analyses. (GESTAR II-US Supplement Section S.2.2.3.2) The PRIME model (Reference 59), GESTR-Mechanical model, and GESTR-LOCA model have been applied to the GNF2 design as well. A discussion of the PRIME thermal-mechanical compliance is provided in Section 3.2 and GESTR-Mechanical thermal-mechanical compliance is provided in Appendix A.

3.1.1.8 LOCA Analysis Methods

The LOCA analysis models (GESTAR II-US Supplement Section S.2.2.3.2) and application methodology with respect to GNF2 are discussed in Section 3.11. No modifications are needed for application to the GNF2 fuel design.

3.1.2 Lead Use Assemblies

GESTAR II Section 1.1.1.B: "New design features will be included in lead use assemblies."

The new design features of GNF2 relative to previously approved designs are described in detail in Section 2.0.

Four (4) prototypical GNF2 Lead Use Assemblies (LUAs) have been loaded into the KKM plant in Switzerland and began operation in September, 2005.

Four (4) prototypical GNF2 LUAs have also been loaded into the Peach Bottom plant in the United States and began operation in October, 2005. NEDC-33144P, Rev. 1, *GNF2 Lead Use Assembly (LUA) for Peach Bottom Atomic Power Station, Unit 3*, January 2005 has been provided to USNRC per the requirements of Letter, T.A. Ippolito (NRC) to R.E. Engel (GE), *Lead Test Assembly Licensing*, September 23, 1981.

In addition, four (4) GNF2 LUAs have been loaded into the Forsmark-3 reactor in Sweden and began operation in May, 2006. These LUAs are prototypical with minor variations to accommodate the non-GE plant characteristics, such as having the channel attached to the nosepiece.

These lead use programs constitute compliance with this criterion.

3.1.3 Post-Irradiation Fuel Examination

GESTAR II Section 1.1.1.C: "The generic post–irradiation fuel examination program approved by the NRC will be maintained (GESTAR References 1–3 and 1–4)."

The generic post-irradiation fuel examination program approved by the NRC for previous fuel designs will be maintained for GNF2. [[

]] Descriptions of the NRC-approved fuel examination program required for new fuel designs, and subsequent revisions to the program, were documented in correspondence between GE and the NRC listed below.

1. 1. Letter, J.S. Charnley (GE) to C.H. Berlinger (NRC), Post Irradiation Fuel Surveillance Program, November 23, 1983. (GESTAR Reference 1-3)
2. Letter, L.S. Rubenstein (NRC) to R.L. Gridley (GE), Post Irradiation Fuel Surveillance, January 18, 1984.
3. Letter, J.S. Charnley (GE) to L.S. Rubenstein (NRC), Fuel Surveillance Program, February 29, 1984.
4. Letter, J.S. Charnley (GE) to L.S. Rubenstein (NRC), Additional Details Regarding Fuel Surveillance Program, May 25, 1984.
5. Letter, L.S. Rubenstein (NRC) to R.L. Gridley (GE), Acceptance of GE Proposed Fuel Surveillance Program, June 27, 1984. (GESTAR Reference 1-4)
6. Letter, Glen A. Watford (GNF-A) to R. Pulsifer/R. Caruso (NRC), "GNF Fuel Surveillance Plan" FLN-2001-009, May 7, 2001.

A peripheral visual inspection of irradiated bundles is performed after final discharge, targeted for normal end-of-life exposures, for reload assemblies of a new fuel design. [[

]] The practice has been to couple the confirmatory end-of-life surveillance examinations with other examination programs that may be ongoing.

These requirements will be carried out for the GNF2 fuel design. The fuel examination program meets GNF's commitment to the NRC and provides evidence that the bundles have performed as expected.

3.1.4 New Fuel-Related Licensing Issues

GESTAR II Section 1.1.1.D: "New fuel related licensing issues identified by the NRC will be evaluated to determine if the current criteria properly address the concern; if necessary, new criteria will be proposed to the NRC for approval."

On August 31, 1994, the NRC issued Information Notice 94-64 (Reference 34) that discussed information obtained on the performance of high burnup fuel. The notice expresses concern that the data does not support the current licensing limits for certain accidents and beyond design basis events (ATWS). In the GE11 NRC audit report (Reference 7), the auditors commented: "...the ATWS evaluation did not include consideration of the new issues regarding power oscillations that have been identified by the ATWS/stability studies currently in progress. The criteria and the GE11 design should be reexamined for adequacy with respect to fuel related impact on the conclusions of these studies when they are complete."

Studies have been completed by the BWROG to assess the impact of oscillations on the consequences of an ATWS and to evaluate the effectiveness of operator actions to mitigate the effects of oscillations (Reference 35). The studies were based on a bounding 8x8 fuel design and

showed that "...the level of safety expected from the requirements of 10 CFR 50.62 is not compromised because of stability." and that "Operator actions to inject boron and reduce reactor water level were...the best options for mitigating oscillations in ATWS events."

Additional ATWS Instability studies have been performed for the Maximum Extended Load Line Limit Analysis Plus (MELLLA+) operating domain expansion (Reference 36). The increased power-flow map upper boundary for the MELLLA+ domain expansion has the potential to increase the severity of the ATWS and ATWS Instability events. The Reference 36 analysis of GE14 fuel at the MELLLA+ upper boundary shows that the response is similar to the boron injection mitigation results shown in the previous Reference 35. The results demonstrate that boron injection effectively eliminates oscillations and provides safe shutdown of the reactor. The GNF2 10x10 fuel design is very similar to the GE14 and therefore the conclusions regarding the mitigation of the ATWS Instability event are not expected to be different (See Section 4.1).

This report does not seek to extend operation of GNF2 beyond an exposure limit of [[
]] peak pellet. [[

]]

3.1.5 NRC Separate Review

GESTAR II Section 1.1.1.E: "If any of the criteria in Subsection 1.1 are not met for a new fuel design, that aspect will be submitted for review by the NRC separately."

All of the criteria specified in Subsections 1.1 of GESTAR II are met by the GNF2 fuel design as documented in this report. Therefore, there are no aspects of the GNF2 design that require a separate review by the NRC.

3.2 THERMAL-MECHANICAL

The Thermal-Mechanical (T-M) analysis of the GNF2 fuel assembly fuel rod and assembly components is performed to demonstrate compliance with the criteria identified in Subsection 1.1.2 of GESTAR II.

The GNF2 analyses utilize the following two processes from Section 1.1.2.A. of GESTAR II:

1. Either worst tolerance assumptions are applied or probabilistic analyses are performed to determine statistically bounding results (i.e. upper 95% confidence).
2. Operating conditions are taken to bound the conditions anticipated during normal steady–state operation and anticipated operational occurrences.

The GNF2 fuel rod and assembly component analyses were performed in accordance with the above guidance to demonstrate compliance to the fuel design criteria in Section 1.1.2.B of GESTAR II. The T-M design criteria from GESTAR II are illustrated in Table 3-1 with the corresponding subsection of this document. The criteria and subsections that apply to fuel rod T-M design are identified in Table 3-2.

The GNF2 fuel rod definition includes three variable application parameters, which may vary for different plants and for different energy utilization plans. The following table illustrates the application parameters and an example of a set that may be applied for a specific design.

Fuel Rod Variable Application Parameters:	Example Values
Fuel rod as fabricated internal fill-gas pressure	[[ ]] MPa
Active fuel column length	Any design reflected in Table 2-1
Local fuel linear heat generation rate [[ ]]	Figure 3-6 and Figure 3-7

Compliance of the fuel rod response with Subsections 3.2.1, 3.2.6, 3.2.9, and 3.2.10 is confirmed for specific sets of the three application parameters by performing exposure-dependent T-M analyses with appropriate consideration of anticipated operational overpower occurrences. The compliance analyses confirm that the criteria are satisfied for all exposures from beginning of life to design discharge exposure. Compliance with Subsection 3.2.8 is confirmed generically

for the most limiting set of application parameters. GNF2 compliance with the fuel rod T-M acceptance criteria shall be reconfirmed for each set of application parameters utilized for GNF2 core designs.

The GNF2 fuel rod thermal-mechanical analyses are performed using NRC-approved analytical models. The model applied to the fuel rod analyses in this Section was the PRIME (Reference 59) thermal-mechanical performance model as documented in Section 2.2 of NEDE-24011-P-A, General Electric Standard Application For Reactor Fuel, GESTAR II. [[

]] GNF2 thermal-mechanical analyses performed with the GESTR-Mechanical model, also documented in Section 2.2 of NEDE-24011-P-A, remain valid within the limits of applicability and are provided in Appendix A.

Table 3-1 GESTAR Fuel Thermal-Mechanical Design Criteria

Section 3.2 Subsection	GESTAR Subsection	GESTAR Criteria
3.2.1 Stress, Strain, Fatigue	1.1.2.B.i	The fuel rod and fuel assembly component stresses, strains, and fatigue life usage shall not exceed the material ultimate stress or strain and the material fatigue capability.
3.2.2 Fretting	1.1.2.B.ii	Mechanical testing will be performed to ensure that loss of fuel rod and assembly component mechanical integrity will not occur due to fretting wear when operating in an environment free of foreign material.
3.2.3 Metal Thinning	1.1.2.B.iii	The fuel rod and assembly component evaluations include consideration of metal thinning and any associated temperature increase due to oxidation and the buildup of corrosion products to the extent that these effects influence the material properties and structural strength of the components.
3.2.4 Fuel Rod Internal Hydrogen Content	1.1.2.B.iv	The fuel rod internal hydrogen content is controlled during manufacture of the fuel rod consistent with ASTM standards C776-83 and C934-85 to assure that loss of fuel rod mechanical integrity will not occur due to internal cladding hydriding.
3.2.5 Fuel Rod/Channel Bow	1.1.2.B.v	The fuel rod is evaluated to ensure that fuel rod or channel bowing does not result in loss of fuel rod mechanical integrity due to boiling transition.
3.2.6 Cladding Pressure Loading	1.1.2.B.vi	Loss of fuel rod mechanical integrity will not occur due to excessive cladding pressure loading.
3.2.7 Control Rod Insertion	1.1.2.B.vii	The fuel assembly (including channel box), control rod and control rod drive are evaluated to assure control rods can be inserted when required.
3.2.8 Cladding Creep Collapse	1.1.2.B.viii	Loss of fuel rod mechanical integrity will not occur due to cladding collapse into a fuel column axial gap.
3.2.9 Fuel Center Temperature	1.1.2.B.ix	Loss of fuel rod mechanical integrity will not occur due to fuel melting.
3.2.10 Cladding Plastic Strain During AOOs	1.1.2.B.x	Loss of fuel rod mechanical integrity will not occur due to pellet-cladding mechanical interaction.

Table 3-2 Fuel Rod Thermal-Mechanical Design Criteria

Criterion	Subsection	Governing Equation
The cladding creepout rate ($\dot{\varepsilon}_{cladding\_creepout}$), due to fuel rod internal pressure, shall not exceed the fuel pellet irradiation swelling rate ($\dot{\varepsilon}_{fuel\_swelling}$).	3.2.6	$\dot{\varepsilon}_{cladding\_creepout} \le \dot{\varepsilon}_{fuel\_swelling}$
The maximum fuel center temperature (T_{center}) shall remain below the fuel melting point (T_{melt}).	3.2.9	$T_{center} < T_{melt}$
Range 1 – [[ ]] Range 2 – [[ ]]	3.2.10	Range 1: [[ ]] Range 2: [[ ]]
The fuel rod cladding fatigue life usage ($\sum_i \frac{n_i}{n_f}$ where n_i=number of applied strain cycles at amplitude ε_i and n_f=number of cycles to failure at amplitude ε_i) shall not exceed the material fatigue capability.	3.2.1	$\sum_i \frac{n_i}{n_f} \le 1.0$
Cladding structural instability, as evidenced by rapid ovality changes, shall not occur.	3.2.8	No creep collapse
Cladding effective stresses (σ_e) shall not exceed the failure stress (σ_f) and cladding effective strains (ε_e) shall not exceed the failure stress strain (ε_f).	3.2.1	$\sigma_e < \sigma_f$, $\varepsilon_e < \varepsilon_f$
The as-fabricated fuel pellet evolved hydrogen (C_H is content of hydrogen) at greater than 1800 °C shall not exceed prescribed limits.	3.2.4	[[ ]]

3.2.1 Stress, Strain, Fatigue

GESTAR II Section 1.1.2.B.i: "The fuel rod and fuel assembly component stresses, strains, and fatigue life usage shall not exceed the material ultimate stress or strain and the material fatigue capability."

Fuel Rods

The fuel rod stress analysis was performed for the limiting application parameters as defined in Subsection 3.2. The analysis was performed using a Monte Carlo statistical method to calculate the effects of [[

]]

For each calculation, the stresses are combined into an effective stress using the Von Mises theory and compared with the appropriate design limit to produce a design ratio. [[

]] such as shown in the reference power-exposure envelope of Figure 3-6 and Figure 3-7. Table 3-3 and Table 3-4 summarize the calculated cladding stress design ratios for the power versus exposure envelopes listed in Appendix B.

[[ ]]

Figure 3-6 GNF2 for BWR/3-6 Power-Exposure Envelope

[[ ]]

Figure 3-7 GNF2 for BWR/2 Power-Exposure Envelope

Table 3-3 Results of Cladding Stress Analysis for BWR/3-6 Fuel Rod

Fuel Rod Type	Period	Design Ratio at Rated Power	Design Ratio at Overpower
[[			
			]]

Table 3-4 Results of Cladding Stress Analysis for BWR/2 Fuel Rod

Fuel Rod Type	Period	Design Ratio at Rated Power	Design Ratio at Overpower
[[			
			]]

These analyses demonstrated that the GNF2 fuel rod stresses do not exceed the failure strength of the material.

Inputs to these fuel rod cladding statistical stress analyses are obtained from the fuel rod thermal-mechanical performance model PRIME as documented in GESTAR II.

Fatigue evaluations of fuel rod designs are performed for the application parameters using the analysis methodology as defined in Subsection 3.2 of this document. These evaluations demonstrate with large conservatism that the cladding fatigue usage does not exceed the cladding fatigue capability. Therefore, loss of fuel rod mechanical integrity due to cladding fatigue will not occur.

[[

]]

Channels

The GNF2 fuel channel (Figure 3-8) is open at the bottom and makes a sliding seal fit on the lower tieplate surface. At the top of the channel, two opposite corners have welded tabs. These tabs support the weight of the channel on the upper tieplate posts. One of the tabs is drilled for attaching the channel fastener to the bundle. [[

]]

[[

]]

The GNF2 channel has been evaluated by finite element analyses. These analyses demonstrate that the stresses and strains are well below the failure strength at operating conditions. The channel wall pressure differential required to cause material yielding is [[

]] for the thinner and thicker channel offerings, respectively. For each new channel application, it is confirmed that the specific plant pressures do not exceed the channel capability. A fatigue analysis was also performed which addressed the cyclic pressure duty due to normal and transient operation.

[[

]]

Figure 3-8 GNF2 Fuel Channel Alternate Designs

Spacers

Cyclic testing for seismic loading demonstrates that the GNF2 spacer stresses and strains do not exceed failure values and that the fatigue capability is not exceeded. Because the seismic loads are well in excess of any operational or handling loading and because there is no significant deformation or fracture of the spacer under seismic loadings, the GNF2 spacer is demonstrated to meet the requirements of this Subsection.

The spacer fatigue test consists of loading the spacer in [[

]] The results of the tests are then used to determine the design margin to failure. The test results show the maximum loads that are acceptable, [[

]] and the minimum loads that cause failures. [[

]]

Table 3-5 Maximum Successful & Failure Loads

Configuration Description	Maximum Successful Load (kN)	Failure Load (kN)
[[		
		]]

[[

]]

The spacer deformation test consists of testing [[

]] The load is the maximum fuel spacer component load experienced in the postulated combined safe shutdown, earthquake and loss-of-coolant-accident. [[

]] In all cases, the gap changes were small compared to the initial gap; therefore the coolability of the bundle will not be compromised.

Because the seismic loads are in excess of any operational or handling loading and because significant deformation or fracture of the spacer was shown to not occur even under seismic loadings, the GNF2 spacer is demonstrated to meet the requirements of this Subsection.

Water Rods

The GNF2 assembly is designed with two large circular water rods that are centrally located and occupy eight fuel rod lattice positions. A typical spacer–positioning water rod is shown in Figure 3-9.

The water rods are hollow Zircaloy tubes with several holes around the circumference near each end to allow coolant to flow through the rod. The number and diameter of the inlet holes at the lower end control the water rod flow. [[

]] Similar to the fuel rods, an expansion spring is located between the water rod shoulder and upper tieplate to allow for differential axial expansion.

Demonstration that the water rod stresses and strains do not exceed failure strength and that the fatigue capability will not be exceeded is shown by stress analyses that address handling and fit up loading.

A limiting pressure differential stress analysis is also provided in response to Subsection 3.2.6 requirements. The water rod tubing was evaluated for a steady state differential wall pressure of [[ ]]. The Zircaloy material properties at operating conditions appropriate for this analysis are: Yield Strength = [[ ]] at 288ºC

Tensile Strength = [[ ]] at 288ºC

The water rod tube membrane stress was determined from S = Pr/t.

Where: S = membrane stress

P = pressure differential

r = mean tubing radius

t = tubing wall thickness

The maximum stress occurs in the large diameter portion of the water rod.

Therefore; [[ ]]

Because all stresses are well below yield strength and since there is no significant cyclic loading, the fatigue capability is not exceeded.

When the water rod is subjected to maximum handling and shipping loads, the stress due to axial compression is of concern. A static structural analysis was run in ANSYS to determine the equivalent stress throughout the water rod. [[

]] This very localized stress is [[ ]] but does not compromise the integrity of the water rod. A linear buckling analysis was performed in ANSYS. The buckling load was found to be [[ ]] times the applied load. The finite element analysis of the GNF2 water rod demonstrates that the design adequately sustains the design shipping and handling loads.

[[

]]

Figure 3-9 Water Rod

Tie Plates

Demonstration that the GNF2 upper and lower tieplates do not exceed failure strength was shown by stress analyses that addressed the maximum handling loads. The loads are the largest loads on these components except for seismic and fuel lift loadings that are addressed in Subsection 3.2.7. The upper and lower tie plates are not subjected to any significant cyclic loadings and fatigue capability is therefore not exceeded.

Upper Tie Plate

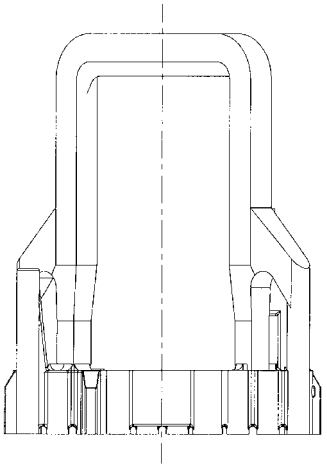

Lower Tie Plate

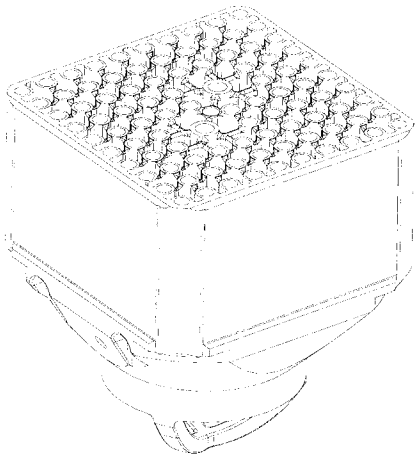

Appropriate material properties for Type-304 Stainless Steel for the upper tieplate stress evaluations are:

Yield Strength = [[ ]] at 38º C
Tensile Strength = [[ ]] at 38º C

The limiting loading on the upper tieplate occurs during fuel handling when the fuel assembly is lifted by the grapple that is attached to the upper tieplate handle. The loads that are evaluated are [[ ]] For this analysis, the GNF2 fuel assembly weight, which includes the fuel bundle, channel, and channel fastener weights, is assumed to be [[ ]] in air (a conservative assumption with respect to the typical weight of an assembly [[( ]]). Therefore, the upward loading on the upper tieplate is [[ ]] for this condition.

The upper tieplate was evaluated by finite element analysis using the ANSYS® code. The model utilizes [[

]]

An upward vertical load of [[ ]] was applied at the edge of the grapple interface with the upper tieplate handle (20 mm from the center of the handle). The downward load from the channel of [[ ]] was applied at the channel post location. Note that this is conservative relative to the channel weight of [[ ]]. The upward loading from the expansion springs is also modeled ([[ ]]). The remainder of the upward vertical load was [[

]]

The maximum bending stress in the grid portion of the tieplate (corrected for minimum dimensions) based on these loading was determined to be [[ ]].

A finite element analysis, using three dimensional beam elements, was also used to evaluate the stresses in the handle. The maximum stress in the handle occurs at the center of the horizontal portion of the handle. Correcting the stresses for minimum dimensions results in a stress equal to [[ ]]. This stress is above the yield strength, but much less than the tensile strength. The acceptability of exceeding the yield strength in the center of the handle is addressed by the mechanical handling load test described below.

A mechanical test was performed to assure that excessive deformation or fracture will not occur when the UTP handle is subjected to a [[ ]] load. Tie plates tested were restrained vertically at the eight tie rod locations and an upward load on the handle with a simulated fuel grapple was applied. The test tie plates were subject to a load approximately twice the [[ ]] load and then inspected for grid deformation and deformation of the handle. Previous tests for the GE14

tie plate, which has handle geometry essentially identical to the GNF2 upper tie plate, show a maximum handle deformation of only [[ ]].

The limiting loading condition on the lower tieplate is due to seating of the fuel assembly into the core or into the fuel storage racks. The load that is evaluated is [[ ]] distributed over the tieplate surface. This load is conservative relative to a design basis load of 4.2 times the assembly weight minus the lower tie plate weight i.e., [[ ]]. The lower tieplate was evaluated by a finite element analysis using the ANSYS code. The model utilizes ¼ symmetry and consists of [[ ]] elements. Three dimensional beam elements were used to model the lower tie plate structure. The element cross-section properties were calculated from the nominal drawing dimensions. The side wall was considered as rigid due to its relatively large thickness and depth, therefore no vertical displacement and no rotation along the axis of side wall are assumed. The maximum bending stress (corrected for minimum section dimensions) was determined to be [[ ]]. These lower tieplate analysis results demonstrate that the lower tieplate stresses are well below the yield strength.

The above analysis demonstrates that the GNF2 upper and lower tieplates are not expected to experience excessive deformation or failure during service.

3.2.2 Fretting

GESTAR II Section 1.1.2.B.ii: "Mechanical testing will be performed to ensure that loss of fuel rod and assembly component mechanical integrity will not occur due to fretting wear when operating in an environment free of foreign material."

The GNF2 fuel assembly was tested to assure that the design features do not result in a significant increase in flow induced vibration (FIV) response and thereby do not increase the potential for fretting. The method used to demonstrate the adequacy of the fuel assembly from a FIV perspective was to compare the vibration response of the GNF2 design with the GE14 design during FIV tests. The response comparison was based on accelerometer data from various locations in the fuel assemblies. The GE14 fuel assembly's performance is considered acceptable based upon its reliable performance in reactor operation.

[[

]] The acceleration signals were recorded and then analyzed to perform direct comparisons of RMS and maximum response between GE14 and GNF2 over a range of flow conditions. Each configuration was tested over a range of flow rates, from [[ ]] to approximately [[ ]] of in-reactor rated mass flow.

The results of the FIV tests shown in Figure 3-10 show that there are no significant differences in the peak acceleration response of the GNF2 fuel and water rods compared to the performance of the GE14 fuel and water rods. The GNF2 FIV test results also demonstrate the acceptable performance of the part length fuel rods and adjacent rods. The differences in fuel rod, lower tieplate, channel-lower tie plate interface and spacer designs show no significant effect on FIV performance when compared to the GE14 design.

[[

]]

Figure 3-10 GNF2 & GE14 FIV Test Result Comparison

Based on the FIV test program, the performance of the GNF2 fuel design meets the fretting design requirements.

3.2.3 Metal Thinning

GESTAR II Section 1.1.2.B.iii: "The fuel rod and assembly component evaluations include consideration of metal thinning and any associated temperature increase due to oxidation and the buildup of corrosion products to the extent that these effects influence the material properties and structural strength of the components."

Metal thinning of the Zircaloy components due to corrosion will result in higher stresses being calculated at end of life if the loading conditions do not change. The increase in stress is more than offset, in this case, by the increase in material strength due to irradiation. However, the fatigue strength of the Zircaloy components is not increased with irradiation. Where the load cycling is potentially significant, the effects of corrosion are explicitly addressed. Corrosion thinning effects were consequently addressed in the fuel rod stress and fatigue analyses and in the channel fatigue analysis described in Subsection 3.2.1. Subsections 3.2.3.1 and 3.2.3.2 describe the methods applied for consideration of metal thinning.

3.2.3.1 Metal Thinning Effects On Zircaloy Cladding

Zircaloy cladding tubes undergo oxidation at slow rates during normal reactor operation. This oxidation causes thinning of the cladding tube wall and introduces a resistance to the fuel rod-to-coolant heat transfer. Corrosion products present in the reactor coolant system also tend to deposit on the fuel rod cladding outer heat transfer surface. This corrosion product deposition also introduces a resistance to the fuel rod-to-coolant heat transfer. In the extensive GNF operational history database, fuel rod failures have not occurred due to cladding corrosion without the presence of an augmenting factor such as an aggressive crud-induced localized corrosion environment. Therefore, no specific value of cladding oxide thickness can be identified to correspond to fuel rod failure; however, cladding oxidation does affect the overall strength of the cladding through loss of structural material and reduced material strength due to higher temperature. Therefore, all fuel rod evaluations explicitly include the amount of cladding

metal thinning and the cladding temperature increase due to cladding oxidation and the buildup of corrosion products based on the results summarized in Table 3-6.

Table 3-6 Cladding Oxidation and Corrosion Product Buildup

	Radial Thickness (mm)	
	Mean	**Standard Deviation**
Beginning-of-Life		
Cladding Oxidation	[[	
Corrosion Product Buildup		
End-of-Life (8 years)		
Cladding Oxidation		
Corrosion Product Buildup		]]

These results are based on numerous field measurements through September 2002 at 14 plants, as well as numerous field measurements that continue to support these results, representing normal GNF experience, excluding cases involving specific water chemistry issues outside of normal operating experience. The data above was generated with a best-fit estimate based on the data set mentioned above.

[[

]]

[[

]]

Figure 3-11 Projected GNF2 Cladding Hydrogen Content vs. Exposure

[[

]]

3.2.3.2 Metal Thinning Effects On Zircaloy Channels

The effects of metal thinning have been considered in a GNF channel fatigue and stress rupture analysis. This analysis shows that the GNF2 channel is structurally adequate, with respect to

fatigue and stress rupture, for a bounding design basis pressure differential and a maximum lifetime of [[ ]].

Metal thinning as a result of oxidation for the fatigue and stress rupture analysis is modeled by consideration of the thermal and irradiation components in a BWR environment. Metal thinning is modeled according to the following relationship.

[[ ]]

where Z_{total} is the oxidation on each side of the channel wall.

Considering metal thinning, a channel pressure differential of [[ ]] was used to determine the limit of pressure differential that exceeds a total damage of 1.0. The damage is calculated as the sum of the fatigue and rupture stress life consumed under a series of events and conditions. By definition a damage value of 1.0 indicates failure. Minimum channel thickness is assumed at t=0 in the analysis. An initial thickness of [[ ]] mm is utilized as compared to the nominal values of [[ ]] mm. Figure 3-12 depicts a channel cross-section and the nominal thickness.

[[

]]

Figure 3-12 Channel Cross Section

As a result of these analysis, which included metal thinning, a fatigue damage and stress rupture damage summation of less than 1.0 for both corner and thickness transitions was determined to be acceptable for differential pressures less than [[ ]].

These analyses demonstrate the adequacy of the GNF2 design and the methods for resisting the effects of metal thinning due to corrosion. The methods are applied for Zircaloy-2 and Zircaloy-4 variants of the GNF2 product.

3.2.4 Fuel Rod Internal Hydrogen Content

GESTAR II Section 1.1.2.B.iv: "The fuel rod internal hydrogen content is controlled during manufacture of the fuel rod consistent with ASTM standards C776-83 and C934-85 to assure that loss of fuel rod mechanical integrity will not occur due to internal cladding hydriding."

The pellet specifications include a requirement that limits the maximum amount of hydrogen that is allowed to be present in the manufactured fuel pellets. This limit is consistent with or less than that specified by ASTM standards C776-83 and C934-85. Manufacturing processes for the fuel rod and its components include controls to ensure that the hydrogen limit is met and are designed to avoid spurious sources of hydrogen in the fuel rod.

3.2.5 Fuel Rod/Channel Bow

GESTAR II Section 1.1.2.B.v: "The fuel rod is evaluated to ensure that fuel rod or channel bowing does not result in loss of fuel rod mechanical integrity due to boiling transition."

Analysis Procedures for Incorporating Channel Bow Effects in Critical Power Evaluations

Channel bow effects are incorporated in critical power evaluations by modifying the bundle R-factor to include changes in local peaking caused by channel bowing. The model is described in the GE report MFN086-89 submitted by letter to the NRC November 15, 1989 and in additional information contained in MFN041-90, May 3, 1990, and MFN109-90, Sep. 26, 1990. The methodology has been approved by the NRC letter, Acceptance for Referencing of Topical Report Titled "GE-Nuclear Energy Report MFN086-89," to J.S. Charnley (GE) from A.C. Thadani (NRC), Jan. 11, 1991.

Channel Bow Compliance

Loss of mechanical integrity due to boiling transition is prevented because all critical power evaluations in the plant process computer and other licensing analyses include an allowance for channel bow effects according to approved methods described above.

Rod Bow Compliance

Reference 37 describes a large program to characterize the extent of rod bowing in BWR fuel along with full scale thermal hydraulic experiments on 8x8 assemblies to investigate the potential impact on Boiling Transition due to rod bow. This program included poolside measurements of over 1000 assemblies and concluded that significant rod bowing did not exist in BWR fuel. Furthermore, the thermal hydraulic testing did not observe any significant impact on critical power.

This original work was supplemented with additional full scale testing of 9x9 assemblies. The results of this testing, described in Reference 38, were verbally communicated to NRC. In summary, a very improbable configuration was tested in which the critical rods in a reference test were bowed to contact just upstream of the onset of Boiling Transition. This testing again concluded that rod bowing does not degrade the margins to Boiling Transition even in this highly improbable circumstance. The results of these two programs are considered applicable to 10x10 fuel. As such, standard critical power limits are sufficient to prevent loss of mechanical integrity due to Boiling Transition even in the presence of rod bow. As stipulated in Reference 37, NRC will be notified if rod-to-rod gap closures greater than 50% are observed.

Compliance with requirement has been met.

3.2.6 Cladding Pressure Loading

GESTAR II Section 1.1.2.B.vi: "Loss of fuel rod mechanical integrity will not occur due to excessive cladding pressure loading."

Evaluations of fuel rod designs are performed for the application parameters using the analysis methodology as referenced in Subsection 3.2 of this document. These evaluations demonstrate

that the cladding creepout rate due to fuel rod internal pressure will not exceed the irradiation-swelling rate of the fuel pellet. Therefore, loss of fuel rod mechanical integrity due to excessive pressure loading will not occur.

In this section, cladding lift-off is defined as the separation of the cladding from the pellet. Cladding lift-off evaluations are used to ensure that the criterion in Item 1 of Table 3-2 is met. For the cladding lift-off evaluation, fuel rod internal pressure for the maximum duty fuel rods is determined using the PRIME thermal-mechanical performance model in conjunction with the standard error propagation statistical method. [[

]] The standard error propagation analysis results in a mean and standard deviation for the fuel rod internal pressure at uniformly spaced exposure points throughout the design lifetime. [[

]] This design ratio has been calculated at several exposure points for the maximum duty fuel rod for each fuel rod type present in the fuel bundle.

Table 3-7 and Table 3-8 summarize the PRIME results for the cladding lift-off evaluation for some of the key rod types for BWR/3-6 and BWR/2 respectively. Because all design ratios are less than 1.0, it is assured, [[

]]

Table 3-7 GNF2 for BWR/3-6 Fuel Rod Cladding Lift-Off Results

		Rod Internal Pressure (MPa)		Critical Pressure (MPa)		
Fuel Rod Type	Exposure where Design Ratio is Max., GWd/MTU	Mean	Standard Deviation	Mean	Standard Deviation	Max. 95% Confidence Design Ratio
[[						
						]]

Table 3-8 GNF2 for BWR/2 Fuel Rod Cladding Lift-Off Results

		Rod Internal Pressure (MPa)		Critical Pressure (MPa)		
Fuel Rod Type	Exposure where Design Ratio is Max., GWd/MTU	Mean	Standard Deviation	Mean	Standard Deviation	Max. 95% Confidence Design Ratio
[[						
						]]

3.2.7 Control Rod Insertion

GESTAR II Section 1.1.2.B.vii: "The fuel assembly (including channel box), control rod and control rod drive are evaluated to assure control rods can be inserted when required."

The fuel assembly is evaluated to assure that component deformations are not severe enough to prevent control rod insertion and that vertical uplift forces will not unseat the lower tie plate such that the resultant loss of lateral fuel bundle positioning would prevent control rod insertion. This evaluation is performed considering the combined effects of Safe Shutdown, Earthquake and Loss-of-Coolant Accident loadings on fuel assembly deformation and lift-off.

Assurance that component deformations are not excessive is provided by primary load stress analyses and tests of the components. These evaluations are based on un-irradiated material properties at operating temperature. The loads used in the evaluation of the fuel assembly components are derived from enveloping values of combined horizontal and vertical acceleration of the fuel assembly. All component stress evaluations have minimum margins of at least [[ ]] because the limit is specified to be [[ ]] times ultimate. The channel buckling has the same margin as was demonstrated previously in NEDE-21175-3-P-A (Reference 39). The existing plant seismic analysis results for the fuel assembly are checked to assure that fuel loadings do not exceed the enveloping values.

Assurance that vertical uplift forces will not unseat the fuel assembly such that loss of lateral fuel bundle positioning could occur was provided by a nonlinear fuel lift analysis as described in detail in NEDE-21175-3-P-A. The GNF2 fuel design, while visibly different from the previous fuel designs for which the lift analysis was initially performed, is dynamically similar when modeled. Because of this dynamic similarity, no significant difference in the fuel lift behavior was expected. This conclusion was confirmed by explicitly modeling the GNF2 fuel design in a typical BWR plant that has been extensively studied for previous fuel design changes. The study plant was selected because it showed potential fuel lift with previous fuel designs.

Separate from consideration of the combined effects of Safe Shutdown Earthquake and Loss of Coolant Accident loads on control rod insertability, considerations also arise for control rod insertability during normal operation due to any channel-control blade interference that may result from irradiation-induced channel bulge and channel bow deformations. The primary control for channel-control blade interference is provided by the Plant Technical Specifications surveillance where actions are specified both (1) to ensure control rod drive scram performance is consistent with requirements, and (2) to appropriately disposition instances where control rod operability, including channel control blade interference effects, is less than adequate. These plant technical specification requirements will continue to be applied with GNF2. Additionally, the guidance, as documented in MFN 06-355, “Update to GE Surveillance Program for Channel-Control Blade Interference Monitoring”, September 28, 2006, remains applicable and will be

similarly applied to operating plants with GNF2 fuel to mitigate any elevated levels of channel-control blade interference.

3.2.8 Cladding Collapse

GESTAR II Section 1.1.2.B.viii: "Loss of fuel rod mechanical integrity will not occur due to cladding collapse into a fuel rod column axial gap."

The condition of an external coolant pressure greater than the fuel rod internal pressure provides the potential for elastic buckling or possibly even plastic deformation if the stresses exceed the material yield strength. Fuel rod failure due to elastic buckling or plastic collapse has never been observed in commercial nuclear reactors. However, a more limiting condition that has been observed in commercial nuclear reactors is cladding creep collapse. This condition occurs at cladding stress levels far below that required for elastic buckling or plastic deformation. In the early 1970s, excessive in-reactor fuel pellet densification resulted in the production of large fuel column axial gaps in some PWR fuel rods. The high PWR coolant pressure in conjunction with thin cladding tubes and low helium fill gas pressure resulted in excessive fuel rod cladding creep and subsequent cladding collapse over fuel column axial gaps. Such collapse occurs due to a slow increase of cladding initial ovality due to creep resulting from the combined effect of reactor coolant pressure, temperature and fast neutron flux on the cladding over the axial gap. Since the cladding is unsupported by fuel pellets in the axial gap region, the ovality can become large enough to result in elastic instability and cladding collapse.

It is noted in this PWR experience that, although complete cladding collapse was observed in some cases, cladding fracture did not occur in any case, therefore fuel rod failure by this mechanism is not expected. However, the GNF design basis includes ensuring that fuel rod failure will not occur due to cladding collapse into a fuel column axial gap. The creep collapse analysis procedure applied to the GNF2 fuel design is documented in NEDC 33139P-A, "Cladding Creep Collapse Licensing Topical Report", July 2005. The analysis consists of a detailed finite element mechanics analysis of the cladding.

The topical report confirmed that creep collapse will not occur for GNF fuel designs as long as design and operation parameters are within the ranges addressed by the generic analyses in the topical report. An evaluation has been performed to confirm that the GNF2 design and operation parameters are bounded by the generic analyses. Thus, it is concluded that creep collapse of freestanding cladding (cladding unsupported by fuel pellets) will not occur for the GNF2 design.

3.2.9 Fuel Melting

GESTAR II Section 1.1.2.B.ix: "Loss of fuel rod mechanical integrity will not occur due to fuel melting."

Evaluations of fuel rod designs are performed for the application parameters using the analysis methodology referenced in Subsection 3.2 of this document. These evaluations demonstrate that the fuel center temperature will not exceed the fuel melting temperature. Therefore, loss of fuel rod mechanical integrity due to fuel melting will not occur.

Numerous irradiation experiments have demonstrated that extended operation with significant fuel pellet central melting does not result in damage to the fuel rod cladding. However, the fuel rod performance is evaluated to ensure that fuel rod failure due to fuel melting will not occur. To achieve this objective, the fuel rod is evaluated to ensure that fuel melting during normal steady-state operation and anticipated operational occurrences is not expected to occur. This fuel temperature limit is specified to ensure that sudden shifting of molten fuel in the interior of fuel rods, and subsequent potential cladding damage, can be positively precluded.

The fuel center temperature evaluation is performed using the PRIME thermal-mechanical performance model in conjunction with the standard error propagation statistical method [[

]]. The standard error propagation analysis results in a mean and standard deviation for the fuel center temperature during AOOs at uniformly spaced exposure points throughout the design lifetime. These results are used to specify a Thermal Overpower (TOP) limit that assures with 95% confidence that the fuel center temperature will not exceed the fuel melting temperature for the maximum duty fuel rod during an AOO at any point in the licensed design lifetime of the fuel.

[[

]]

3.2.10 Pellet-Cladding Mechanical Interaction

GESTAR II Section 1.1.2.B.x: "Loss of fuel rod mechanical integrity will not occur due to pellet-cladding mechanical interaction."

Evaluations of fuel rod designs are performed for the application parameters using the analysis methodology as defined in Subsection 3.2 of this document. These evaluations demonstrate that the cladding circumferential strain due to pellet-cladding mechanical interaction during an AOO will not exceed the cladding circumferential strain limit. Therefore, loss of fuel rod mechanical integrity due to pellet-cladding mechanical interaction will not occur.

After the initial rise to power and the establishment of steady-state operating conditions, the pellet-cladding gap will eventually close due to the combined effects of cladding creep-down, fuel pellet irradiation swelling, and fuel pellet fragment outward relocation. Once hard pellet-cladding contact has occurred, a rapid power increase, such as would occur during an AOO, will result in cladding outward diametral deformation due to the fuel pellet thermal expansion. The extent of deformation depends on the extent of irradiation exposure, the magnitude of the power increase, and the final peak power level. This (high strain rate) deformation can be a combination of (a) plastic deformation during the power increase due to the cladding stress exceeding the cladding material yield strength, and (b) creep deformation during the elevated power hold time due to creep-assisted relaxation of the high cladding stresses. [[

]]

The cladding strain evaluation is performed using the PRIME thermal-mechanical performance model in conjunction with worst tolerance assumptions. The fabrication parameters important to the analysis are all biased to the fabrication tolerance limit in the direction that produces the most severe result. Other input parameters conservatively biased for this analysis include (a) cladding corrosion, and (b) corrosion product (crud) buildup on the cladding outer surface. These analyses result in cladding strain during AOOs at uniformly spaced exposure points throughout the design lifetime. These results are used to specify a Mechanical Overpower (MOP) limit that assures that the fuel circumferential strain will not exceed the specified strain limit for the maximum duty fuel rod during an AOO at any point in the design lifetime of the fuel. [[

]]

[[

]]

Table 3-9 GNF2 for BWR/3-6 Circumferential Cladding Strain Results

[[						
						]]

Table 3-10 GNF2 for BWR/2 Circumferential Cladding Strain Results

[[						
						]]

3.3 NUCLEAR

3.3.1 Doppler Reactivity Coefficient

GESTAR II Section 1.1.3.A: "A negative Doppler reactivity coefficient shall be maintained for any operating conditions."

Analysis Description

The Doppler Reactivity Coefficient (DRC) is of high importance in reactor safety. The Doppler reactivity coefficient is a measure of the reactivity change associated with a change in the temperature of the fuel material. An increase in fuel temperature causes an increase in the absorption of resonance energy neutrons and a decrease in reactivity. The DRC of a core is a function of the average of the bundle Doppler reactivity coefficients. A negative DRC provides instantaneous negative reactivity feedback to any rise in fuel temperature, on a gross or local basis, and thus assures the tendency of self-control for the BWR.

The DRC characteristics for GNF2 were determined by using the NRC-approved [[

]]

[[

]]

[[

]] The results of the calculations demonstrate that the DRC becomes more negative as the fuel temperature decreases.

The DRC in units of pcm/K is defined as follows:

$$DRC = \frac{10^5 \left(k_{T_1} - k_{T_0} \right)}{k_{T_0} \left(T_1 - T_0 \right)}$$

where

T_0 = Reference temperature (Kelvin)

T_1 : = Elevated temperature (Kelvin)

k_{T_0} := Eigenvalue at reference temperature

k_{T_1} : = Eigenvalue at elevated temperature

Typical values are shown in Figure 3-13. The zero void fraction value is illustrated in the figure since it corresponds to the least negative DRCs. Hot Doppler reactivity coefficients calculated as explained above range from approximately [[ ]]

[[

]]

Figure 3-13 Typical Behavior for Doppler Reactivity Coefficient (Hot, Uncontrolled, Zero Void Fraction)

Conclusion

The GNF2 Doppler reactivity coefficient is negative for any operating conditions thus meeting the requirement of GESTAR II Section 1.1.3.A.

3.3.2 Moderator Void Coefficient

GESTAR II Section 1.1.3.B: "A negative core moderator void reactivity coefficient resulting from boiling in the active flow channels shall be maintained for any operating conditions."

The moderator void coefficient of reactivity is associated with the change in moderating capability of the in-channel water. The analysis performed to calculate the moderator void coefficient used the lattice physics code TGBLA06 and the three-dimensional core simulator PANAC11 (Reference 14). [[

]] Thus, this analysis is applicable to BWR types 2 through 6. The ABWR, ESBWR, and non-GE plants would have to be evaluated separately.

The generic moderator coefficient analyses included the following considerations:

1. [[

]]

The core eigenvalue is calculated at various temperatures from [[

]] The void coefficient, which is the change in reactivity divided by the change in void fraction, is calculated for each of these moderator temperatures. This was performed at three exposures thru the cycle:

Beginning Of Cycle (BOC): Zero Exposure

Middle Of Cycle (MOC): [[ ]]

End Of Cycle (EOC): [[

]]

The following characteristics were selected in order to obtain a bounding condition:

1. [[

]]

A GNF2 equilibrium fuel cycle with a [[

]]

All of the nuclear libraries included cold libraries with moderator temperatures at [[

]]

The void coefficient is calculated as follows:

$$\alpha_v \equiv \frac{d\rho}{dv} \approx \frac{1}{k}\frac{dk}{dv} \approx \frac{1}{k_{v_0}}\left(\frac{k_{v_1} - k_{v_0}}{v_1 - v_0}\right)$$

where:

ρ = Reactivity
k_{v1} = Eigenvalue at 5% in-channel void fraction
k_{v0} = Eigenvalue at 0% in-channel void fraction
v_0 = Zero in-channel void fraction
v_1 = [[ ]] in-channel void fraction

In order to obtain a critical control blade configuration, [[

]]

At each exposure and moderator temperature, a critical control blade configuration was established [[

]] Figures 3-14, 3-15, and 3-16 summarize the results.

[[

]]

[[

]]

Figure 3-14 GNF2 Void Coefficient at BOC

[[

]]

Figure 3-15 GNF2 Void Coefficient at MOC

[[

]]

Figure 3-16 GNF2 Void Coefficient at EOC

Conclusion

It is concluded that the GNF2 void coefficient of reactivity is negative for any operating conditions.

3.3.3 Moderator Temperature Coefficient

GESTAR II Section 1.1.3.C: "A negative moderator temperature coefficient shall be maintained for temperatures equal to or greater than hot standby."

The moderator temperature coefficient is associated with the change in moderating capability of the water. A negative moderator temperature coefficient during power operation provides inherent protection against power excursions. Hot standby is the condition under which the BWR core coolant has reached operating pressure and the temperature at which boiling has begun. Once boiling begins, the moderator temperature remains essentially constant in the boiling regions.

The analysis performed to calculate the moderator temperature coefficient used the lattice physics code TGBLA06 and the three-dimensional core simulator PANAC11 (Reference 14). The analysis used to demonstrate that it is negative for temperatures equal to or greater than hot standby was performed [[

]] Thus, this analysis is applicable to BWR types 2 through 6. The ABWR, ESBWR, and non-GE plants would have to be evaluated separately.

A GNF2 [[

]]

The core eigenvalue is calculated at various temperatures from [[

]] The moderator temperature coefficient, which is the change in reactivity divided by the change in moderator temperature, was calculated for each of these temperatures. This was performed at three exposures thru the cycle:

- Beginning Of Cycle (BOC): Zero Exposure
- Middle Of Cycle (MOC): [[ ]]
- End Of Cycle (EOC): [[

]]

The moderator temperature coefficient is calculated by fitting the eigenvalue versus temperature to a quadratic curve and solving the differential equation of the quadratic expression. For each temperature, the [[ ]]

The MTC is defined as follows:

$$\alpha_T \equiv \frac{d\rho}{dT} \approx \frac{1}{k}\frac{dk}{dT}$$

where:

ρ: Reactivity
T: Moderator Temperature
k: Effective multiplication factor

The MTC is calculated by fitting the eigenvalue results to quadratic functions of temperature and differentiating with respect to temperature. That is, consider the eigenvalue as follows:

$$k = C_0 + C_1 * T + C_2 * T^2$$

Differentiating this equation and dividing by the eigenvalue yields the following expression:

$$\alpha_T = \frac{1}{k}\left(C_1 + 2C_2 * T\right)$$

[[

]] Again the results were tabulated and the moderator temperature coefficient calculated.

The generic analyses include the following considerations:

1. [[

]]

In order to obtain a critical control blade configuration, [[

]]

At each exposure and temperature, a critical control blade configuration was established. Then, maintaining this control blade configuration, all other temperatures were analyzed. Figures 3-17, 3-18, and 3-19 summarize the results.

[[

]]

[[

]]

Figure 3-17 GNF2 MTC with Critical Control Blades Configuration @ BOC

[[

]]

Figure 3-18 GNF2 MTC with Critical Control Blades Configuration @ MOC

[[

]]

Figure 3-19 GNF2 MTC with Critical Control Blades Configuration @ EOC

Conclusion

It is concluded that the GNF2 moderator temperature coefficient of reactivity is negative for moderator temperatures equal to or greater than hot standby.

3.3.4 Prompt Reactivity Feedback

GESTAR II Section 1.1.3.D: "For a super prompt critical reactivity accident (e.g. control rod drop accident) originating from any operating condition, the net prompt reactivity feedback due to prompt heating of the moderator and fuel shall be negative."

The mechanical and nuclear design of the fuel shall be such that the prompt reactivity feedback (requiring no conductive or convective heat transfer and no operator action) provides an automatic shutdown mechanism in the event of a super prompt incident such as a control rod drop accident. This characteristic will assure rapid termination of super prompt critical accidents with additional long-term void reactivity shutdown capability provided by the moderator void

feedback for those cases where heat transfer from the fuel to the moderator results in boiling in the active flow channel.

A model is developed relating moderator temperature and fuel temperature for a super prompt critical excursion. Enthalpy increases in moderator and fuel are given by the following expressions,

[[

]]

The GNF2 fuel mass is [[

]]

A super prompt reactivity excursion occurs in a time frame much too short to allow heat conduction from the fuel through the cladding to the moderator. The only mechanism for moderator heating is through fission neutron slowing and fission gamma absorption. [[

]]

Hence, the heating fractions are calculated as follows:

Emission Type	Recoverable Energy, MeV	Energy Deposition, MeV		
		Fuel	Moderator	Zircaloy
Fission fragments	[[			
Fission neutrons				
Prompt γ-rays				
Total				
Fractional				]]

Calculations of prompt reactivity insertion are made at the [[

]]

The lattice physics code TGBLA06 (Reference 14) is used to evaluate [[

]]

Figure 3-20 illustrates the change in eigenvalue [[

]] due to prompt heating of the moderator and fuel.

[[

]]

Figure 3-20 Prompt Reactivity Defect for a Typical GNF2 Lattice

The results demonstrate that the eigenvalues at [[

]]

Conclusion

It is concluded that the net prompt reactivity feedback due to prompt heating of the moderator and fuel is negative.

3.3.5 Power Coefficient

GESTAR II Section 1.1.3.E: "A negative power coefficient, as determined by calculating the reactivity change due to an incremental power change from a steady state base power level, shall be maintained for all operating power levels above hot standby."

The power coefficient is defined as the rate of change in reactivity as the core power changes while all other core boundary conditions (control rod distribution, core inlet coolant flow, core inlet coolant enthalpy, reactor system pressure) remain constant.

A negative power coefficient provides an inherent negative feedback mechanism to provide more reliable control of the plant during power maneuvers. The power coefficient is effectively the combination of Doppler, void and moderator temperature coefficients of reactivity.

Conclusion

For the GNF2 fuel design, each of these three components has been shown to be negative for all operating power levels above hot standby. Therefore, a negative power coefficient is assured for all operating power levels above hot standby.

3.3.6 Cold Shutdown Margin

GESTAR II Section 1.1.3.F: "The plant shall be calculated to meet the cold shutdown margin requirement for each plant cycle specific analysis."

The core must be capable of being made subcritical with margin in the most reactive condition throughout an operating cycle with the most reactive control rod in its full out position and all other control rods fully inserted. The typical values of cold shutdown margin required by plant Technical Specifications are 0.38% $\Delta k/k$ or 0.25% $\Delta k/k$, depending on the specific plant. Shutdown margin is dependent upon the core loading. It is calculated for each plant cycle prior to the operation of that cycle.

Conclusion

The calculations demonstrating compliance with this requirement will be performed for every reload of GNF2 fuel. The results of the cycle specific calculations will be documented in the reload license report for that cycle.

3.3.7 Fuel Storage

GESTAR II Section 1.1.3.G: "The effective multiplication factor for new fuel designs stored under normal and abnormal conditions shall be shown to meet fuel storage limits by demonstrating that the peak uncontrolled lattice k-infinity calculated in a normal reactor core configuration meets the limits provided in Section 3 of GESTAR II (Reference 1) for GE-designed regular or high density storage racks."

The basic criterion associated with the storage of both irradiated and new fuel is that the effective multiplication factor of fuel stored under normal conditions will be less than or equal to 0.90 for regular density racks and less than or equal to 0.95 for high-density racks including all biases and uncertainties. Credible abnormal storage conditions are limited to a k_{eff} of less than or equal to 0.95 including all biases and uncertainties. For GE designed fuel storage racks, [[

]] assures satisfaction of the most stringent requirements of the set specified in Section 3.5 of GESTAR II (Reference 1).

The analysis performed to calculate the lattice k_∞ to confirm compliance with the above criterion uses the lattice physics portion of the methods described in Reference 15. These NRC-approved lattice physics models are encoded into the TGBLA Engineering Computer Program. One of the outputs of the TGBLA is the lattice k_∞ of a specific nuclear design for a given set of input state parameters (void fraction, control state, fuel temperature) (Reference 14). A description of the requirements and the analytical process to calculate the fuel storage reactivity requirements is contained in Section 3.5 of GESTAR II (Reference 1). This analytical process includes a series of Monte Carlo calculations using MCNP (Reference 16) [[

]] consistent with the requirements of ANSI/ANS 57.2-1983 (Reference 40) and shown to meet the k_∞ reactivity criteria noted above.

Compliance of GNF2 fuel with the k_∞ limits specified above will be confirmed for each GNF2 lattice as part of the design process. Documentation that this criterion has been met will be contained in the fuel design information report that defines the maximum lattice k_∞ for each final bundle nuclear design.

3.4 NEW FUEL DESIGN LICENSING EVALUATION

Section 2.4 from US NRC SE: "Licensing evaluations of new fuel designs will include generic analyses of a large BWR/4 or BWR/5 plant at limiting points of the cycle for an equilibrium loading of the new fuel design to assure that (1) nuclear design criteria are satisfied, and (2) safety limit MCPR values are correct. In addition, Chapter 15 safety analyses are performed for each reload application on a cycle-specific basis for (3) limiting anticipated operational occurrences and (4) bounding accidents. The cycle-specific plant (5) operating limit MCPR is determined and the effect of the new fuel design on previously evaluated accidents must be reconfirmed or reanalyzed."

Compliance with each of these criteria are performed in accordance with the methodologies as described in NEDE-24011-P-A-15 and are documented in the subsections of this report as well as other licensing documentation supporting new fuel introduction and cycle operation.

(1) **Nuclear Design Criteria:** Compliance with this criterion is documented in Subsection 3.3. In addition, cycle-specific nuclear design criteria are confirmed for each operating cycle.

(2) **Safety Limit MCPR:** Safety Limit MCPR is now calculated for each unique core loading. (Reference 20) This criterion is no longer meaningful for the generic new fuel design evaluations, but is satisfied by performing the cycle-specific SLMCPR calculation.

(3) **Anticipated Operational Occurrences:** Compliance with this criterion is documented in Subsection 3.7. Per GESTAR II, limiting AOOs are analyzed on a cycle-specific basis.

(4) **Accidents:** Compliance with this criterion is documented in Subsection 3.3.4 (super prompt critical feedback), Subsection 3.11 (loss of coolant accident), Subsection 3.12 (rod drop accident), and Subsection 3.14 (anticipated transient without scram).

(5) **Operating Limit MCPR:** Compliance with this criterion is documented in Subsection 3.7. The plant OLMCPR is established by considering the limiting AOOs for each operating cycle.

3.5 THERMAL-HYDRAULIC

GESTAR II Section 1.1.4: "Flow pressure drop characteristics shall be included in plant cycle specific analyses for the calculation of the Operating Limit Minimum Critical Power Ratio."

Because of the channeled configuration of BWR fuel assemblies, there is no bundle-to-bundle cross flow inside the core and the only issue of hydraulic compatibility of the various bundle types in a core is the bundle inlet flow rate variation and its impact on margin to the Operating Limit MCPR. The coupled thermal-hydraulic-nuclear analyses performed each cycle for each plant to determine fuel bundle flow and power distribution use the various bundle pressure loss coefficients to determine the flow distribution required to maintain total core pressure drop boundary conditions to be applied to all fuel bundles. The margin to the thermal limits of each fuel bundle is determined using this consistent set of bundle flow and power.

The GNF2 fuel assembly design incorporates the use of nickel-based, Ni-Cr-Ti alloy grid type spacers with special flow wings designed for improved critical power performance. The pressure drop characteristics of the GNF2 spacers are based on the pressure drop data from full-scale testing of the GNF2 fuel assembly. Production spacers were used in the full-scale test assembly with no modifications. The measured pressure drops include static head, wall friction, acceleration pressure drop, and form losses. The loss coefficients were evaluated in a manner consistent with the steady state thermal hydraulic analysis methodology documented in Section 4.2 of GESTAR II (Reference 1). The test assembly and the measurement scheme for obtaining differential pressures are shown in Figure 3-21. Test data were obtained at [[

]]

Table 3-11 provides measured pressure drops across the bundle height from [[ ]] to [[ ]] cm ([[ ]] to [[ ]] inches) as well as comparisons to the predictions. Figure 3-22 summarizes the results graphically. The comparison of the predicted vs. measured pressure drop for [[ ]] tests over a range of thermal-hydraulic conditions resulted in a mean error for the [[ ]]
Therefore, it is concluded that the models and methods used for the determination of pressure

drop in the GNF2 fuel assembly accurately predict the test data over a wide range of power and flow conditions.

Conclusion: The unique GNF2 fuel assembly hydraulic characteristics have been developed and confirmed by the test comparisons discussed above. These unique GNF2 hydraulic characteristics are used in all analysis models and methods where the fuel assembly hydraulics are needed. For cores of mixed assembly types, the hydraulics are uniquely represented for each assembly type. Therefore, the flow-pressure drop characteristics for each fuel assembly type (including GNF2) present in a plant are included in all plant cycle specific analyses for the calculation of the Operating Limit Minimum Critical Power Ratio.

Table 3-11 Spacer Test Results

Run	Pressure (psia)	Mass Flux (Mlb/ hr-ft^2)	Bundle Power (MW)	Inlet Temp (°F)	Measured ΔP (psid)	Predicted ΔP (psid)	Predicted-Measured ΔP (psid)
[[							

Run	Pressure (psia)	Mass Flux (Mlb/ hr-ft^2)	Bundle Power (MW)	Inlet Temp (°F)	Measured ΔP (psid)	Predicted ΔP (psid)	Predicted-Measured ΔP (psid)

]]

Average	[[	
Standard Deviation		]]

[[

]]

Figure 3-21 Spacer Test Configuration

[[

]]

Figure 3-22 Spacer Test Results and Predictions

3.6 SAFETY LIMIT MCPR

3.6.1 Confirmation of Applicability

GESTAR II Section 1.1.5.A: "A cycle-specific Safety Limit MCPR will be calculated on a cycle-specific basis following the steps in 1.1.5.B (of GESTAR II)."

The Safety Limit MCPR will be established on a cycle-specific basis following the calculational process steps in 1.1.5.B of GESTAR II. It will be calculated prior to the operation of that cycle

to confirm that the Safety Limit MCPR value to be used for that cycle, which is incorporated into the supplemental reload licensing report, is applicable.

The NRC SE for NEDC-32694P-A (Reference 19) provides four actions to follow whenever a new fuel design is introduced. These four conditions are listed in Section 3 of the SE. In the last paragraph of Section 3.2.2 of the Technical Evaluation Report included in the SE are the statements "GE has evaluated this effect for the 8x8, 9x9, and 10x10 lattices and has indicated that the R-Factor uncertainty will be increased … to account for the correlation of rod power uncertainties" and "it is noted that the effect of the rod-to-rod correlation has a significant dependence on the fuel lattice (e.g., 9x9 versus 10x10). Therefore, in order to insure the adequacy of the R-Factor uncertainty, the effect of the correlation of rod power calculation uncertainties should be reevaluated when the NEDC-32601P (Reference 18) methodology is applied to a new fuel lattice." Therefore, the definition of a new fuel design is based on the lattice array dimensions (e.g., NxN). Because GNF2 is a 10x10, and the evaluations in NEDC-32694P-A includes 10x10, then these four actions are not applicable to GNF2.

3.7 OPERATING LIMIT MCPR EVALUATION

Section 3.7 summarizes the analyses performed for GNF2 fuel to demonstrate the applicability of cycle/plant specific and generic MCPR and LHGR analyses described in Section 4 (of GESTAR II).

3.7.1 Cycle-Specific Analysis

GESTAR II Section 1.1.6.A: "Plant operating limit MCPR is established by considering the limiting anticipated operational occurrences for each operating cycle."

Anticipated Operational Occurrences (AOO's) are classified as transient events of moderate frequency and must be analyzed with NRC approved methods. AOO events are analyzed to establish the reactor system response, including the calculation of the Operating Limit Minimum Critical Power Ratio (OLMCPR).

The operating limit MCPR is established by adding (with appropriate statistical adjustment factors) the change in the MCPR (ΔCPR) for the limiting analyzed AOO to the safety limit MCPR. The calculational process for determining the Safety Limit MCPR is documented in Subsection 3.6.

The AOO scenarios that are analyzed are listed below with the corresponding Standard Review Plan (SRP) Section.

Section	Event
15.1.1 – 15.1.4	Decrease in feedwater temperature, increase in feedwater flow, increase in steam flow and inadvertent opening of a steam generator relief or safety valve.
15.2.1 – 15.2.5	Loss of external load; turbine trip; loss of condenser vacuum; closure of main steam isolation valve (BWR); and steam pressure regulator failure (closed)
15.2.6	Loss of non-emergency AC power to the station auxiliaries.
15.2.7	Loss of normal feedwater flow.
15.3.1 - 15.3.2	Loss of forced reactor coolant flow, including trip of pump motor and flow controller malfunctions.
15.4.4 – 15.4.5	Startup of an inactive loop or recirculation loop at an incorrect temperature, and flow controller malfunction causing an increase in BWR core flow rate.
15.5-1 - 15.5.2	Inadvertent operation of ECCS and chemical and volume control system malfunction that increases reactor coolant inventory.
15.6.1	Inadvertent opening of a BWR pressure relief valve.

Cycle Specific Operating Limit MCPR Analytical Models and Analysis Procedures

The primary NRC-approved methods used in the calculation process of the delta CPR during a pressurization AOO include: (1) lattice physics models (TGBLA, Reference 14); (2) three-dimensional core simulator (PANACEA, Reference 14); (3) one-dimensional transient model (ODYN, References 21, 22, and 23) in conjunction with (4) transient hot channel model (TASC, Reference 28); or with (5) an advanced realistic combination one-dimensional and three-dimensional method (TRACG, References 24, 25, 26, and 27) and (6) GEXL critical power correlation (described in Subsection 3.8). Calculations performed in support of the results in this section have been analyzed with ODYN and TASC models. Calculations using the TRACG model will be performed on a plant/cycle specific basis.

The nuclear libraries for the GNF2 fuel are generated by TGBLA and then are used as input to PANACEA. PANACEA, based on the cycle-specific reference core-loading pattern, calculates the core state and the nuclear parameters for input to the plant transient model, ODYN or

TRACG. The ODYN methodology has been applied to the analyses in this section to calculate the time-dependent plant response to the prescribed transient using a one-dimensional (axial) representation of the core. The time-dependent parameters calculated by ODYN include core pressure, core pressure drop, core inlet flow rate, core inlet flow enthalpy, core fission power level and core axial fission power shape.

These ODYN output parameters are then used to determine the input to TASC for further analysis of the thermally limiting GNF2 bundle. The primary output of TASC is the change in calculated critical power ratio during the limiting pressurization transient. For GNF2, the CPR of the hot channel is calculated using the GEXL17 critical power correlation.

Loss of Feedwater Heating is analyzed using the steady-state nuclear methods (TGBLA and PANACEA). If the inadvertent HPCI startup is more limiting than the Loss of Feedwater Heating event, it is analyzed using the system transient models, ODYN and TASC or TRACG, if TRACG is the transient method applied to a plant.

The design process assures that an inadvertent rotation of a fuel bundle will not result in violation of the Safety Limit MCPR by calculating nominal and rotated bundle average R-factors as a function of exposure for each new bundle. From these results, delta R-factors and delta powers are constructed, and the maximum delta R-factors and the corresponding delta power are input to the analysis that determines the Operating Limit MCPR (OLMCPR).

The rod withdrawal error and fuel misloading errors are also evaluated on a cycle specific basis (see Subsection 3.7.2).

A description of the Operating Limit MCPR calculational process is contained in Section S.2.2.1 of NEDE-24011-P-A-16-US, the US Supplement to GESTAR II (Reference 1).

Cycle Specific Operating Limit Compliance: The OLMCPR is dependent upon the cycle-specific core loading pattern. The OLMCPR is calculated prior to operation of that cycle and incorporated into the supplemental reload license report (SRLR).

3.7.2 Generic Analysis

GESTAR II Section 1.1.6.B: "For each new fuel design, the applicability of generic MCPR analyses described in Section 4 (of GESTAR II) or in the country specific supplement to this base document shall be confirmed for each operating cycle or a plant-specific analysis will be performed."

In addition, to the MCPR statement in GESTAR II above, GE confirms the applicability of generic LHGR analyses for each operating cycle or a plant specific analysis will be performed.

Rod Withdrawal Error

Generic event analysis results have been calculated for the Rod Withdrawal Error. A plant cycle specific evaluation will be performed for the GNF2 fuel design using NRC approved methods. The plant/cycle specific result is then compared to the generic event analyses. If the calculated limit is less than the generic event analyses, then the generic limit is applied. If the calculated limit is greater than the generic event analyses the calculated value is considered in the determination of the rated OLMCPR.

A description of the cycle specific rod withdrawal error analysis process is contained in Section S.2.2.1.5 of NEDE-24011-P-A-16-US, the US Supplement to GESTAR II (Reference 1).

Mislocated Fuel Loading Error

A mislocated bundle analysis to determine the potential influence of the GNF2 critical power correlation and the GNF2 fuel design will be performed for the first introduction of a reload batch of GNF2 into a BWR. This check may also include the elimination of this anticipated operational occurrence. [[

]]

Off-Rated (Partial Power/Flow) Thermal Limits

The operating limit MCPR (OLMCPR) must be increased for the low core flow and low core power conditions to provide assurance that the fuel will not approach boiling transition in the

event of an AOO at a low flow/power condition. Fuel LHGR operating limits are decreased for the low core flow and low core power conditions to provide assurance that the fuel rod thermal-mechanical design and safety bases are not exceeded in the event of an AOO at the low flow/power condition. Extensive analyses have been performed for the low flow/power condition for many fuel designs and many plant/cycles. From the resulting database, a generic partial flow/power set of thermal limits has been established which is termed generic. Applicability of the generic partial flow/power thermal limits to the GNF2 fuel design, including the generic limits for non-ARTS plants (K_f) and for ARTS plants ($MCPR_f$, $MCPR_p$, $LHGRFAC_f$, and $LHGRFAC_p$) have been evaluated and documented in this section.

The off-rated thermal limits are a function (multiplier) of the rated power/flow, cycle and plant-unique limits. Any significant impact due to changes in fuel design will be reflected in this rated condition operating limit, and therefore indirectly in the off-rated limits.

The off-rated limits are primarily determined by non-fuel plant system parameters (bypass capacity, feedwater and recirculation runout capacity, steamline volumes, etc.), which affect core-wide transient responses. Therefore, any fuel design changes resulting from GNF2 fuel would have a second order effect on these core-wide transient responses.

These considerations, coupled with the calculations performed for GNF2 and comparisons of the generic off-rated thermal limits, confirms the applicability of the generic off-rated thermal limits to GNF2.

The off-rated generic limits are justified based on the results reported in this section. The calculations consist of a series of transient analyses at the power and flow conditions that define the off-rated MCPR and LHGR operating thermal limits. These limits ensure the integrity of the fuel during any transient regardless of the initial conditions of the core. The analyses are sufficient to cover all BWR/2-6 plants with $MCPR_f$, $LHGRFAC_f$ and $LHGRFAC_p$ limits. In addition, the K_f limits have been confirmed for non-ARTS plants.

The plants chosen for these analyses are described below. These were selected due to their high power density as these plants and core designs incorporate the latest Extended Power Uprate and the extended operating domain features of MELLLA+.

Model	BWR/6	BWR/4
Number of bundles	[[	
Thermal power, MWt		
Rated Core flow, kg/sec		
Core Flow Range, % of rated		
Power density, kW/l		]]

The applicability of the generic partial power and flow dependent thermal limits to GNF2 fuel have been confirmed by comparing the calculated off-rated conditions thermal limits with the generic limits established with the introduction of ARTS.

Transient Types Considered

The following transient types have been considered (the transient classification is based on Section 2 of GESTAR II):

- Pressurization transients: Load Rejection without Bypass (LRNBP) and Turbine Trip without Bypass (TTNBP) are potentially limiting. The Pressure Regulator Controller Failure (PRFDS) for BWR/6 is classified as an accident since it implies the failure of both the primary and secondary regulators and therefore is not included in thermal limits determination (Reference 1).
- Excess of coolant inventory transients: Feedwater Controller Failure (FWCF).
- Core flow increase transients for flow dependent limits determination: the Slow Flow Runout (SFRO) is analyzed since historically it determines both MCPR and LHGR flow dependent limits. The Idle Recirculation Loop Startup (IRLS) and the Fast Flow Runout (FFRO) are also reviewed.
- Core subcooling increase transients: historically these are not limiting.
- Core flow decrease transients are not analyzed since they are not limiting.

For a description of the transients see Section 2 of GESTAR II. A more detailed description is given in the plant UFSARs.

Flow Dependent Limits

[[

]]

$MCPR_f$

[[

]] In all cases the GNF2 results are bounded by the generic limits that have been employed with the introduction of ARTS Power and Flow dependent limits.

[[

]]

$LHGRFAC_f$

[[

]] The generic LHGRFAC limits are shown to bound the BWR/4 and BWR/6 based LHGRFAC results. It can be concluded that the GNF2 response for these cores with the additional conservatism added that the results are not worse than the original ARTS flow dependent LHGRFAC limit. [[

]]

Based on this analysis it can be concluded that the generic $LHGRFAC_f$ limits are conservative for GNF2.

Idle Recirculation Loop Startup and Fast Recirculation Flow Runout

These transients have been analyzed for both BWR/4 and BWR/6 at several power/flow points. ODYN is used to perform these analyses.

[[

]] the MCPR results are bounded by the generic $MCPR_f$ limits, and well bounded by the power dependent MCPR generic limits.

[[

]]

Non ARTS Plants K_f Limit

The BWR 2/3/4/5 K_f limits are covered by the ARTS $MCPR_f$ limits provided that the OLMCPR is higher than following the values: [[

]]

Flow Dependent Limits Summary

[[

]]

Power Dependent Limits

ARTS and BWR/6 plants operate with generic power dependent MCPR and LHGR limits. Extensive transient analyses at various power and flow conditions are performed in determining these limits. The operating limit MCPR (OLMCPR) must be increased for low core power conditions. The power dependent LHGR operating limits are decreased for the low core power conditions.

Power Dependent MCPR Limits

[[

]] As a result of dissimilar plant designs and setpoints, there are significant differences in the requirements at low power conditions. These off-power $MCPR_p$ limits are dependent on whether the power is greater than or less than the bypass power, Pbypass. The bypass power set point is not the same for all plants and usually varies somewhere between 22% and 40% power. Above Pbypass, where automatic scram on turbine stop valve closure and fast turbine control valve closure occurs, a Kp trend function is calculated. [[

]]

Power Dependent LHGRFAC$_p$ Limits

The LHGRFAC$_p$ is determined by pressurization transient analyses performed with ODYN for three GNF2 core configurations at several offrated conditions using bounding inputs for the fleet for parameters described below. [[

]]

The results of the analyses will then be evaluated for the required $LHGRFAC_p$ that would be needed to meet fuel centerline melt and cladding circumferential strain limits. The required LHGRFAC would then be compared to the generic ARTS and BWR/6 limits above the core power where the SCRAM on turbine control/stop valves is bypassed (P_{bypass}). [[

]] The generic $LHGRFAC_p$ limits are acceptable [[

]]

Power Dependent Limits Summary

The power dependent off-rated limits are primarily determined by non-fuel plant system parameters (bypass capacity, feedwater capacity, and steamline volumes, etc.), which affect core-wide transient responses. Therefore, any fuel design changes would have a second order effect on these core-wide transient responses.

In the previous sections it has been demonstrated that the generic power dependent $LHGRFAC_p$ limits are appropriate for application to GNF2. This is demonstrated in Figure 3-32.

[[

]]

Table 3-12 BWR/4 Equilibrium Limiting MCPR Results for SFRO Transient

		Calculated	**Generic**	Calculated	**Generic**	Calculated	**Generic**	Calculated	**Generic**
Power (%)	Flow (%)	$MCPR_f$- 102.5% Max Flow	$MCPR_f$ 102.5% Max flow	$MCPR_f$- 107% Max Flow	$MCPR_f$ 107% Max Flow	$MCPR_f$- 112% Max Flow	$MCPR_f$- 112% Max Flow	$MCPR_f$- 117% max Flow	$MCPR_f$- 117% max Flow
[[									
									]]

Table 3-13 BWR/4 Equilibrium Limiting MCPR Results for MELLLA+ SFRO Transient

		Calculated	**Generic**	Calculated	**Generic**	Calculated	**Generic**	Calculated	**Generic**
Power (%)	Flow (%)	$MCPR_f$- 102.5% max Flow	$MCPR_f$- 102.5% max Flow	$MCPR_f$- 107% max Flow	$MCPR_f$- 107% max Flow	$MCPR_f$- 112% max Flow	$MCPR_f$- 112% max Flow	$MCPR_f$- 117% max Flow	$MCPR_f$ 117% max Flow
[[									
									]]

Table 3-14 BWR/6 Equilibrium Limiting MCPR Results for SFRO Transient

		Calculated	**Generic**	Calculated	**Generic**	Calculated	**Generic**	Calculated	**Generic**
Power (%)	Flow (%)	$MCPR_f$- 102.5% Max Flow	$MCPR_f$ 102.5% Max flow	$MCPR_f$- 107% Max Flow	$MCPR_f$ 107% Max Flow	$MCPR_f$- 112% Max Flow	$MCPR_f$- 112% Max Flow	$MCPR_f$- 117% max Flow	$MCPR_f$- 117% max Flow
[[									
									]]

Table 3-15 BWR/6 Equilibrium Limiting MCPR Results for MELLLA+ SFRO Transient

		Calculated	**Generic**	Calculated	**Generic**	Calculated	**Generic**	Calculated	**Generic**
Power (%)	Flow (%)	$MCPR_f$- 102.5% max Flow	$MCPR_f$- 102.5% max Flow	$MCPR_f$- 107% max Flow	$MCPR_f$- 107% max Flow	$MCPR_f$- 112% max Flow	$MCPR_f$- 112% max Flow	$MCPR_f$- 117% max Flow	$MCPR_f$ 117% max Flow
[[									
									]]

Table 3-16 BWR/4 Equilibrium Core LHGRFAC$_f$ SFRO Results

	Calculated	**Generic**	Calculated	**Generic**	Calculated	**Generic**	Calculated	**Generic**
Flow (%)	102.5% Max Flow	102.5% Max Flow	107% Max Flow	107% Max Flow	112% Max Flow	112% Max Flow	117% Max Flow	117% Max Flow
[[								
								]]

The Table represents the minimum limits observed for each of the flow points represented as calculated from BOC, MOC, EOC-3K and EOC exposures.

Table 3-17 BWR/4 Transition Core LHGRFAC$_f$ SFRO Results

	Calculated	**Generic**	Calculated	**Generic**	Calculated	**Generic**	Calculated	**Generic**
Flow (%)	102.5% Max Flow	102.5% Max Flow	107% Max Flow	107% Max Flow	112% Max Flow	112% Max Flow	117% Max Flow	117% Max Flow
[[								
								]]

The Table represents the minimum limits observed for each of the flow points represented as calculated from BOC, MOC and EOC exposures.

Table 3-18 BWR/6 Equilibrium Core LHGRFAC$_f$ SFRO Results

	Calculated	**Generic**	Calculated	**Generic**	Calculated	**Generic**	Calculated	**Generic**
Flow (%)	102.5% Max Flow	102.5% Max Flow	107% Max Flow	107% Max Flow	112% Max Flow	112% Max Flow	117% Max Flow	117% Max Flow
[[								
								]]

The Table represents the minimum limits observed for each of the flow points represented as calculated from BOC, MOC and EOC exposures.

Table 3-19 ΔCPR, TOP and MOP Results for IRLS for BWR/4 Equilibrium

Power (%)	Flow(%)	Exposure	ΔCPR	TOP	MOP	TOP/MOP* LHGRFAC	Generic $LHGRFAC_f$	Generic $LHGRFAC_p$
[[								
								]]

* Includes a [[ ]] conservatism factor.

Table 3-20 ΔCPR, TOP and MOP Results for IRLS for BWR/6 Equilibrium Core

Power (%)	Flow(%)	Exposure	ΔCPR	TOP	MOP	TOP/MOP* LHGRFAC	Generic $LHGRFAC_f$	Generic $LHGRFAC_p$
[[								
								]]

* Includes a [[ ]] conservatism factor.

Table 3-21 ΔCPR, TOP and MOP Results for FFRO for BWR/4 Equilibrium Core

Power (%)	Flow (%)	Exposure	ΔCPR	Req'd Kp*	Generic Kp	TOP	MOP	TOP** LHGRFAC	Generic $LHGRFAC_f$	Generic $LHGRFAC_p$
[[										
										]]

* The required Kp is conservatively calculated [[ ]]

** Includes a [[ ]] conservatism factor.

Table 3-22 ΔCPR, TOP and MOP Results for FFRO for BWR/6 Equilibrium Core

Power (%)	Flow (%)	Exposure	ΔCPR	Req'd Kp*	Generic Kp	TOP	MOP	TOP** LHGRFAC	Generic $LHGRFAC_f$	Generic $LHGRFAC_p$
[[										
										]]

* The required Kp is calculated [[ ]]

** Includes a [[ ]] conservatism factor .

Table 3-23 Power and Flow Conditions for Pressurization Transient Analysis Above P_{bypass}

Generic Analysis	
Power (%)	Flow (%)
[[	
	]]

Table 3-24 Limiting $LHGRFAC_p$ Results

P/F (%)	Limiting Case	$LHGRFAC_p$	
		Required	Generic
[[			
			]]

Figure 3-23 $MCPR_f$ Based on GNF2 Response to Slow Flow Runout

[[

]]

Figure 3-24 Change in Axial Power Shape During SFRO for BWR-4 GNF2 Equilibrium Core

[[

]]

Note: the initial power shapes are normalized to 1.0. The final power shapes are normalized to the final core power divided by the initial core power, to represent the actual power increase during the transient.

Figure 3-25 Change in Axial Power Shape During SFRO for BWR-6 GNF2 Equilibrium Core

[[

]]

Figure 3-26 GNF2 LHGRFAC$_f$ Limit Comparison for Maximum Flow of 102.5%

[[

]]

Figure 3-27 GNF2 LHGRFAC$_f$ Limit Comparison for Maximum Flow of 107.%

[[

]]

Figure 3-28 GNF2 LHGRFAC$_f$ Limit Comparison for Maximum Flow 112.%

[[

]]

Figure 3-29 GNF2 LHGRFAC$_f$ Limit Comparison for Maximum Flow 117.%

[[

]]

Figure 3-30 GNF2 MCPR for Flow Increase Transients Compared to Generic $MCPR_f$

[[

]]

Figure 3-31 Non-ARTS Plants K_f Comparison to Generic ARTS $MCPR_f$

[[

]]

Figure 3-32 Limiting $LHGRFAC_p$

[[

]]

3.8 CRITICAL POWER CORRELATION

3.8.1 New Fuel Design Features

GESTAR II Section 1.1.7.A: "The currently approved critical power correlation will be confirmed or a new correlation will be established when there is a change in wetted parameters of the flow geometry; this specifically includes fuel and water rod diameter, channel sizing and spacer design."

3.8.2 New Correlation Data

GESTAR II Section 1.1.7.B: "A new correlation may be established if significant new data exists for a fuel design(s)."

3.8.3 Critical Power Correlation Calculation

GESTAR II Section 1.1.7.C: "The criteria for establishing the new correlation are as follows:

A. The new correlation shall be based on full-scale prototypical test assemblies.
B. Tests shall be performed on assemblies with typical rod-to-rod peaking factors.
C. The functional form of the currently approved correlations shall be maintained.
D. Correlation fit to data shall be best fit.
E. One or more additional assemblies will be tested to verify correlation accuracy (i.e., test data not used to determine the new correlation coefficients).
F. Coefficients in the correlation shall be determined as described in Reference 1-5 or 1-6 of GESTAR II.
G. The uncertainty of the resulting correlation shall be determined by:

$$\sigma^2 = \frac{1}{N-1}\sum_{i=1}^{N}\left(\mu - ECPR_i\right)^2$$

Where:

σ = standard deviation

$\mu = \frac{1}{N}\sum_{i=1}^{N} ECPR_i$ = mean ECPR

N = Total number of data in both the data set used to determine the coefficients and the set used for verification

$ECPR$ = Calculated bundle critical power divided by experimentally determined bundle critical power."

Critical Power Correlation Results

The GEXL17 (NEDC-33292P, Revision 3, "*GEXL17 Correlation for GNF2 Fuel*," June 2009) database was obtained from Stern Laboratory tests of full-scale GNF2 bundle simulations. A statistical analysis has been performed for the GNF2 database used to develop the GEXL17 correlation, consisting of [[ ]] data points for [[ ]] different local peaking patterns. This correlation statistics were based on [[ ]] data points.

The GEXL17 correlation is valid for GNF2 fuel over the following range of state conditions:

- Pressure: [[ ]]
- Mass Flux*: [[ ]]
- Inlet Subcooling: [[ ]]
- R-factor: [[ ]]

[[

]]. Refer to the Figure 3-33.

Figure 3-33 Mass Flux vs. R-Factor Plane

[[

]]

In addition, there is an additive constant applied to each fuel rod location [[

]] For GNF2, the additive constants used in the design process are provided in Table 3-25. [[

]]

Table 3-25 GEXL17 Additive Constants for GNF2

Fuel Rod Lattice Position	Fuel Rod Additive Constant
[[	
	]]

[[

]]

The resulting GEXL17 correlation for the critical quality (dimensionless) applicable to GNF2 fuel is of the form: $X_C = \sum_{i=1}^{18} A_i V_i$ where the variables and their coefficients are defined in Table 3-26:

Table 3-26 GEXL17 Variables and Coefficients

i	V_i		A_i
1	[[		
2			
3			
4			
5			
6			
7			
8			
9			
10			
11			
12			
13			
14			
15			
16			
17			
18			]]

Where:

G = Mass flux in 10^6 pounds per hour per square foot (Mlb/hr-ft^2)

P = Pressure in pounds per square inch (psia)

DQ = Thermal diameter in inches

LB = Boiling length in inches

LA = Annular flow length in inches

R = R-factor

The terms that comprise the form of the correlation have been previously approved by the NRC. These terms are specifically identified in References 41 and 42.

Conclusion

The GNF2 fuel assembly has a different part length rod configuration and spacer design relative to previous fuel designs. Therefore, a new correlation has been established which is based on the same terms and form as the previous correlation. The new correlation, GEXL17, has been established based on significant new data for the GNF2 fuel design. Criteria a. through g. defined above have been used in the development of the GEXL17 correlation.

Based on the [[ ]] data points used to develop and verify the GEXL17 correlation statistics, the mean ECPR, μ, was determined to be [[ ]], with a standard deviation, σ, of [[ ]].

3.9 STABILITY

GESTAR II Section 1.1.8: "New fuel designs must satisfy either criterion A or B below:

A. The stability behavior, as indicated by core and limiting channel decay ratios, must be equal to or better than a previously approved GE BWR fuel design.
B. If the core and limiting channel decay ratios are not equal to or better than a previously approved GE fuel design, it must be demonstrated that there is no change to the exclusion zone."

The GNF2 fuel design was analyzed against both Criterion A and Criterion B of GESTAR II Section 1.1.8. Acceptance of the GNF2 fuel design is based on Criterion B.

Stability Analytical Models and Analysis Procedures

The stability compliance calculations utilize the approved ODYSY methodology (Reference 29). ODYSY is a frequency domain program that calculates both the core and channel decay ratios for a prescribed fuel design, plant configuration, and plant operating state.

Analysis with Respect to Criterion A

Previous fuel designs have demonstrated acceptable stability performance, thereby assuring that the new fuel designs also have acceptable performance. The fuel design comparative evaluation in Criterion A will be performed as follows:

1. [[

]]

The core and channel decay ratios for both fuel designs shall be calculated using identical operating state conditions for power, flow, inlet subcooling, axial and radial core power shapes, and core pressure.

The power-flow condition selected shall be on the rated power control rod line and near the point of minimum recirculation pump speed. The methods and procedures used to analyze both fuel designs shall be identical.

Calculations were performed to compare the GNF2 design with the earlier, NRC approved P8x8R fuel design. [[

]] The cycle exposure dependent decay ratio results for GNF2 and P8x8R are presented below in Table 3-27.

Table 3-27 Decay Ratios for Loose Inlet Orifice Plant

	Core			Channel
	BOEC	MOEC	EOEC	
GNF2	[[			
P8x8R				]]

(BOEC: Beginning of Equilibrium Cycle, MOEC: Middle of Equilibrium Cycle, EOEC: End of Equilibrium Cycle)

The plant analyzed had relatively "loose" inlet flow orifices. The GNF2 and P8x8R decay ratios for relatively "tight" inlet flow orifices are presented in Table 3-28.

Table 3-28 Decay Ratios for Tight Inlet Orifice Plant

	Core			Channel
	BOEC	MOEC	EOEC	
GNF2	[[			
P8x8R				]]

[[

]]

Analysis with Respect to Criterion B

For the same plant, the exclusion region analysis was performed for both GNF2 and P8x8R and both “loose” and “tight” inlet flow orifices. The exclusion region intercepts with the High Flow Control Line (HFCL) and Natural Circulation Line (NCL) are given in Tables 3-29 and 3-30.

Table 3-29 Exclusion Regions for Loose Inlet Orifice Plant

	P8x8R		GNF2	
	%P	%F	%P	%F
HFCL	[[			
NCL				]]

Table 3-30 Exclusion Regions for Tight Inlet Orifice Plant

	P8x8R		GNF2	
	%P	%F	%P	%F
HFCL	[[			
NCL				]]

Stability Compliance

As demonstrated in Tables 3-29 and 3-30, introduction of GNF2 to a plant operating with P8x8R does not cause the Exclusion Region to become larger. This validates the GNF2 stability performance under Criterion B of GESTAR II Section 1.1.8.

3.10 OVERPRESSURE PROTECTION ANALYSIS

GESTAR II Section 1.1.9: "Adherence to the ASME overpressure protection criteria shall be demonstrated on plant cycle specific analysis."

Overpressure Protection Analysis Acceptance Criterion

The ASME Boiler and Pressure Vessel Code, Section III, Class I, permits pressure transients up to 10% over design pressure for "upset conditions". Section III to the Code allows credit to be taken for the scram protection system as a pressure protection device when determining the required safety valve capacities for nuclear vessels.

The GE analysis to demonstrate vessel overpressure protection is performed assuming that all main steam isolation valves (MSIV) close inadvertently and that the MSIV position switch fails to initiate a scram. Using this low probability event definition, application of "emergency condition" limit is considered appropriate. However, GE conservatively applies the "upset" code requirements.

Overpressure Protection Analytical Models and Analysis Procedures

The primary methods of the transient analysis process used in the calculation of the vessel overpressure during an anticipated operational occurrence include: (1) lattice physics models (TGBLA, Reference 14); (2) three-dimensional core simulator (PANACEA, Reference 14); and

(3) one-dimensional transient model (ODYN, References 21, 22, and 23) or a combination one-dimensional/three-dimensional method (TRACG, References 24, 25, 26, and 27). All of these models are NRC-approved.

The nuclear behavioral libraries, for GNF2 fuel, are generated by TGBLA and then are used as input to PANACEA. PANACEA, based on the cycle-specific reference core loading pattern, calculates the core state and the nuclear parameters for input to the plant transient model, ODYN or TRACG. ODYN calculates the time-dependent plant response to the prescribed transient using a one-dimensional (axial) representation of the core and TRACG uses an advanced realistic combination one-dimensional and three-dimensional method. The output of ODYN and TRACG includes the vessel pressure.

Overpressure Protection Analysis Compliance

The calculated vessel pressure for MSIV inadvertent closure may be dependent upon the fuel design and core loading pattern. Compliance with the overpressure protection criterion is demonstrated by cycle-dependent analysis prior to the operation of that cycle.

A description of the criteria, models and procedure for vessel overpressure protection analysis is contained in Section S.3 of the US Supplement to GESTAR II (Reference 1).

3.11 LOSS-OF-COOLANT ACCIDENT ANALYSIS

The SAFER/GESTR-LOCA ECCS evaluation methodology is used to determine the effects of the postulated loss-of-coolant accident (LOCA) in accordance with the requirements of 10 CFR 50.46 and Appendix K. This methodology is NRC-approved and is described in Section S.2.2.3.2 of the US Supplement to GESTAR II (Reference 1) and its references. The SAFER/GESTR-LOCA evaluation methodology is used for all GE BWRs.

The SAFER/GESTR-LOCA methodology uses improved ECCS evaluation models along with a realistic application approach to calculate a licensing peak cladding temperature with margin substantiated by statistical considerations. Nominal values are used for most inputs, and Appendix K required inputs are utilized only for the limiting break in order to establish the

licensing basis values for comparison to the 10 CFR 50.46 limits. A description of the SAFER/GESTR methodology is contained in Sections S.2.2.3.2.4 and S.2.2.3.2.5 of the US Supplement to GESTAR II and its references. Four different GE computer codes are utilized to calculate LOCA analyses results. These models are briefly described below.

1. Short-Term Thermal-Hydraulic Model (LAMB)

The LAMB model (Reference 44) is used to analyze the short-term thermodynamic and thermal-hydraulic behavior of the coolant in the vessel during a postulated loss-of-coolant accident. In particular, this model predicts the core flow, core inlet enthalpy and core pressure during the blowdown prior to the end of lower plenum flashing. The detailed features of the fuel design do not significantly affect the system response; therefore, no modifications of this model are required for application to the GNF2 fuel design.

2. Transient Boiling Transition Model (TASC)

This model is used to evaluate the short-term thermal-hydraulic response of the coolant in the hot channel of the core during a postulated loss-of-coolant accident. In particular, the calculated time of boiling transition (the onset of loss of nucleate boiling) is used as input to the core heatup model of SAFER described later in this section. The details of the fuel design can impact the calculated time to boiling transition. The TASC code (Reference 28) is a single hot channel thermal hydraulic analysis code, which accepts detailed bundle geometry input that designates different types of rod groups within the bundle to explicitly model axially varying flow areas and heat transfer areas while incorporating the bundle specific critical power correlation described in Subsection 3.8. This model is the same one used for calculating the hot channel behavior during anticipated operational occurrences as described in Subsection 3.7. No modifications of this model are required for application to the GNF2 fuel design.

3. Long-Term Thermal-Hydraulic Model (SAFER)

This model is used to analyze the long-term thermal-hydraulic behavior of the coolant in the vessel for all breaks. The SAFER code (References 45-49) calculates the uncovery and reflooding of the fuel and the duration of spray cooling. This code provides a realistic nodal representation of the counter current flow limiting phenomena at all flow restrictions between the

core and adjacent regions and a realistic representation of the numerous leakage paths that exist in a BWR between the core and bypass regions. These leakage paths serve the important function of helping to refill the lower plenum and subsequently reflood the core region. Counter current flow limiting modeling in the SAFER code for the GNF2 configuration will be validated prior to plant specific application. The SAFER code also calculates realistic core heat transfer coefficients. The SAFER code employs a heatup model with a simplified radiation heat transfer correlation to calculate peak cladding temperature and local maximum oxidation. For calculated events in which the peak cladding temperature is substantially below design limits and no cladding perforations are expected to occur, the peak cladding temperature and local maximum oxidation fraction from SAFER can be used directly without recourse to additional calculations using the CORCOOL code. Detailed axial bundle geometry is not used in the SAFER methodology; therefore, no modifications of this model are required for application to the GNF2 fuel design.

4. Core Heatup Model (CORCOOL)

The CORCOOL model (Reference 45-49) solves the transient heat transfer equations for the highest power assembly, for the entire LOCA transient. The various heat transfer modes considered include nucleate boiling, film boiling (flow and pool), core spray heat transfer and thermal radiation. The introduction of GNF2 and its multiple PLR rod heights can be handled by the CORCOOL code since the CORECOOL model accounts for changes in the number of rods in the lattice at different axial locations by axially varying active flow within the channel. CORCOOL can accommodate the designation of separate PLR groups such that different PLR lengths can be input. PLR height for specific rod groupings within the bundle can be specified in the CORCOOL input. No modifications of this model are required for application to the GNF2 fuel design.

5. Best Estimate Fuel Rod Thermal Mechanical Model (GESTR–LOCA)

The GESTR-LOCA model (Reference 50) has been developed to provide best estimate predictions of the thermal performance of GE nuclear fuel rods experiencing variable power histories. For ECCS analyses, the GESTR-LOCA model is used to initialize the fuel stored

energy and fuel rod fission gas inventory at the onset of a postulated LOCA. No modifications of this model are required for application to the GNF2 fuel design.

3.11.1 Emergency Core Cooling System Criteria

GESTAR II Section 1.1.10.A: "The criteria in 10 CFR 50.46 shall be met on plant-specific or bounding analyses."

The emergency core cooling system (ECCS) criteria in 10 CFR 50.46 are met by the exposure-dependent maximum average planar linear heat generation rate (MAPLHGR) limit in plant-specific or bounding analyses. GE demonstrates compliance with these ECCS criteria for any new fuel designs using NRC-approved analytical models and analysis procedures.

3.11.2 Plant MAPLHGR

GESTAR II Section 1.1.10.B: "Plant MAPLHGR adjustment factors must be confirmed when a new fuel design is introduced."

Plant MAPLHGR is sometimes adjusted for a specific operational configuration or region. GE will confirm the revised MAPLHGR limit for the GNF2 fuel design for the plant and cycle when it is introduced.

3.12 ROD DROP ACCIDENT ANALYSIS

3.12.1 Cycle Specific Analysis

GESTAR II Section 1.1.11.A: "Plant cycle specific analysis results shall not exceed the licensing limit described in the country specific supplement to this base document."

A generic control rod drop accident analysis confirming that peak fuel enthalpy limits are met was performed and documented in NEDO-10527, "Rod Drop Accident Analysis for Large Boiling Water Reactors," March 1972 (Reference 51). NEDO-21231, "Banked Position Withdrawal Sequence," January 1977 (Reference 52) provides specified control rod sequences that maintain the rod worths to such low values that peak fuel enthalpies do not threaten the design or fuel cladding failure threshold. Plant specific enthalpy calculations are only necessary

for plants that do not follow a generically approved CRDA withdrawal sequence. Plant specific rod worth calculations will be performed for any such reload as part of the reload analysis and will be shown to meet the specified limits. Plant specific rod worth calculations are also performed based on approved withdrawal sequences to confirm that rod worths are bounded, which ensures that the licensing limit in GESTAR II is met. Therefore, compliance to this criterion for GNF2 fueled cores not having a generically approved CRDA withdrawal sequence will be demonstrated as part of the reload license process.

3.12.2 Bounding BPWS Analysis

GESTAR II Section 1.1.11.B: "Applicability of the bounding BPWS analysis must be confirmed."

Rod drop analyses were performed generically for Banked Position Withdrawal Sequence plants in Reference 52. R.E. Engel to D.B. Vassallo, "Elimination of Control Rod Drop Accident Analysis for Banked Position Withdrawal Sequence Plants," MFN-026-82, February 24, 1982 (Reference 53) eliminates the need for CRDA analyses for plants that implement BPWS. In 2004, an alternate BPWS, "Improved BPWS Control Rod Insertion Process," NEDO-33091-A, Revision 2, July 2004, was approved by the USNRC (Reference 54). The analysis performed for GNF2 compliance consists of performing [[

]] The compliance calculations conform with a modified procedure documented in J.S. Charnley (GE) to M. Wayne Hodges (USNRC), "Revised Generic BPWS CRD Analysis," MFN-034-087, April 22,1987, (Reference 55) which more accurately predicts the most reactive control rod, results in a more limiting control rod configuration, and takes credit for the BPWS scram function. The peak fuel enthalpy for the bounding analysis is still significantly lower than the design limit.

[[

]]

This analysis demonstrates the applicability of the generic BPWS analyses. Plant and cycle-specific rod worth calculations will demonstrate that References 51, 52 and 53 are still valid as a part of the reload analysis.

3.12.3 Fuel Enthalpy Analysis

Reference 61 states that based on a bounding postulated Control Rod Drop Accident (CRDA) analysis, it was conservatively determined for the 8x8 fuel designs that approximately 850 fuel rods would reach a fuel enthalpy of 170 cal/g. This is the enthalpy limit for eventual cladding perforation. For the 9x9 GE11 and GE13 fuel designs, approximately 1,000 fuel rods would reach a fuel enthalpy of 170 cal/g, and for the 10x10 GE12 and GE14 fuel designs, approximately 1,200 fuel rods would reach a fuel enthalpy of 170 cal/g.

As with the other 10x10 designs, when the bounding analysis is applied to GNF2, approximately 1,200 fuel rods are calculated to reach a fuel enthalpy of 170 cal/g.

3.13 REFUELING ACCIDENT

GESTAR II Section 1.1.12: "The consequences of a refuel accident as presented in the country-specific supplement or the plant FSAR shall be confirmed as bounding or a new analysis shall be performed (using the methods and assumptions described in the country supplement) and documented when a new fuel design is introduced."

Accidents that result in the release of radioactive materials directly to the containment can occur when the drywell is open and the reactor vessel head has been removed. The only credible accident that could lead to the release of significant quantities of fission products to the containment is one resulting from the accidental dropping of a fuel bundle onto the top of the

core. This results in mechanical damage to the fuel rod cladding both in the dropped bundle and those in the core. This event occurs under non–operating conditions for the fuel with the core in a cold condition.

3.13.1 Fuel Damaged

GE is now manufacturing a new design of the refueling mast with grapple head (NF–500). The new design has a circular cross–section mast versus the previous triangular cross–section mast. The new design is also more "rugged" and weighs more, 280.8 kg compared to 158.8 kg. Additionally, GE has made changes in the fuel bundle configurations. The number of fuel rods has increased from the initial 7x7 array, to the current GNF2 10x10 array with corresponding dimensional changes as well as the inclusion of part length rods.

A damage analysis is performed, taking into consideration the part length rods in the GNF2 design, based on the equivalence of 85.6 full length rods per GNF2 bundle. It is concluded that 172 and 150 rods failed for plants equipped with the NF500 mast and the standard triangular refueling mast, respectively. The smallest number of damaged rods documented in any BWR FSAR refueling accident for 7x7 array is 111 rods.

3.13.2 Radiological Consequences Comparisons

Assuming all other operating parameters remain unchanged, the relative radiological consequence of a refueling accident can be assessed by comparing the equivalent number of fuel bundles damaged. For most BWRs, the FSAR analysis was based on 7x7 array fuel with minimum 111 damaged rods, therefore the activity released is equivalent to that of (111/49) or 2.3 fuel bundles. The accident involving GNF2 with NF500 mast is equivalent to (172/85.6) or 2.0 bundles. With traditional triangular mast, the damage is equivalent to 1.75 bundles. Therefore the damaged GNF2 bundle equivalent is bounded by the 7x7 array of most original plant designs.

3.13.3 Power Peaking Factors

If the radial peaking factor assumed in the FSAR bounds the expected radial peaking of GNF2, and the plant design was based on 7x7 fuel, then the radiological consequence of the GNF2 bundle drop is bounded by the original plant design as shown, and the criterion is met. If the

radial power peaking of the GNF2 core design is greater than that assumed in the FSAR, the effect can be accounted for by taking the ratio of these factors. For example, a GNF2 bundle with an expected radial peaking factor of 1.7, compared to a 7x7 bundle with radial peaking 1.5 typically used in the FSAR, is expected to have an activity release of (1.7/1.5)*(2.0/2.3) = 1.01 times the FSAR values. Because there is typically significant margin to the 10 CFR 100 or 10 CFR 50.67 limits for the refueling accident event, it is expected that most plants can accommodate the ~1% increase in radiological consequence of this event.

Plants may have changed or modified the refueling masts; the FSAR or current licensing basis may be based on fuel types other than GE 7x7 fuel, and the plant specific GNF2 radial peaking will depend on the core design. For these reasons, compliance to the refueling accident criterion is confirmed on a plant-specific basis during preparation for the GNF2 fuel transition.

3.14 ANTICIPATED TRANSIENT WITHOUT SCRAM

GESTAR II Section 1.1.13: "The fuel must meet either criteria A or B below:"

A. "A negative core moderator void reactivity coefficient, consistent with the analyzed range of void coefficients provided in GESTAR II References 1–7 and 1–8, shall be maintained for any operating conditions above the startup critical condition."

B. "If criterion 1.1.13.A is not satisfied, the limiting events (as described in GESTAR II References 1–7 and 1–8) will be evaluated to demonstrate that the plant response is within the ATWS criteria specified in GESTAR II References 1–7 and 1–8."

In response to the requirements of Alternate 3, set forth in NUREG–0460, References 56 and 57 present assessments of the capabilities of representative BWR plants to mitigate the consequences of a postulated ATWS event. Sensitivity studies are provided for the key parameters affecting plant response during the most limiting events requiring ATWS consideration. Values of parameters that fall within the range of characteristics studied have been shown to satisfy the ATWS acceptance criteria.

In terms of core and system response to an ATWS event, the core moderator void reactivity coefficient is the key parameter compared to other fuel and nuclear parameters that may change with a change in fuel type. Maintaining this coefficient within the range of point model void coefficients (or equivalent one–dimensional void coefficients) assumed in the sensitivity studies presented in References 56 and 57 when loading new fuel designs, assures that the conclusions reached regarding BWR mitigation of an ATWS event are still valid. Although the methodology used in References 56 and 57 shows some importance to the void coefficient, the more recent approved methodology in Reference 23 does not show the system response to be sensitive to the void coefficient. This evaluation is shown below in Subsection 3.14.1.

3.14.1 Void Reactivity Coefficient Range

The point model void coefficient must fall within the range of -8 to -14 cents/% voids in order for the new fuel design to meet the acceptance criterion. A preliminary evaluation of the GNF2 void coefficient indicates that the void coefficient is similar to GE14, and may not always fall in this range.

Analyses have also been performed with ODYN with a core-wide [[ ]] increase in ODYN void coefficient magnitude. The results are presented in Table 3-31 for BOC and EOC conditions. [[

]]

In addition, the effect on the peak pool temperature response is also addressed. Sensitivity studies have been performed with a core-wide [[ ]] increase in the ODYN void coefficient magnitude. A sensitivity study was performed for a limiting Pressure Regulator Failure – Open (PRFO) at both BOC and EOC exposure conditions. The results shown in Table 3-32 below

show that the peak pool temperature is [[

]].

Table 3-31 ODYN Peak Vessel Pressure Void Coefficient Study

Event and Description	Exposure	Peak Vessel Pressure (MPa)
PRFO Base Case	BOC	[[
PRFO with [[ ]] void coefficient increase	BOC	
PRFO Base Case	EOC	
PRFO with [[ ]] void coefficient increase	EOC	]]

Table 3-32 Suppression Pool Peak Temperature Void Coefficient Study

Event and Description	Exposure	Peak Suppression Pool Temperature (°C)
PRFO Base Case	BOC	[[
PRFO with [[ ]] void coefficient increase	BOC	
PRFO Base Case	EOC	
PRFO with [[ ]] void coefficient increase	EOC	]]

As the GNF2 void coefficient is in the range is generally similar to GE14 and the sensitivity study above shows very small changes in key results to changes in void coefficient, the introduction of GNF2 will have a small impact on these key ATWS acceptance parameters.

3.14.2 Plant Evaluation

Because the GNF2 void coefficient may not always fall within the prescribed range, additional plant specific ATWS evaluations will be performed for the introduction of GNF2 into a plant. This evaluation will assure that there is acceptable margin to the key ATWS acceptance criteria identified in Table 3-33.

Many plants have implemented power uprates, which have reduced ATWS margins to the acceptance limits and this makes it more difficult to implement a fleet-wide generic analysis. Therefore, plants where margins are less than [[ ]] MPa to the overpressure limit and/or less than [[ ]]°C to the peak suppression pool temperature limit, will be re-analyzed with

the introduction of GNF2. These criteria are approximately a factor of 3 greater than the sensitivity to the void coefficient described in Subsection 3.14.1 above. For BWR/2 plants, the increase in void coefficient magnitude from GE11 to GNF2 may be greater than the sensitivity to the void coefficient described in Section 3.14.1. Therefore, BWR/2 plants will be re-analyzed with the introduction of GNF2. The margin criteria were established for the two parameters whose values may be primarily impacted and are sometimes close to the ATWS acceptance criteria. The PCT and containment pressure have substantial margin for all plants. For example, the observed PCT for all plants has been at least 333 to 389°C below the acceptance criteria. The factor of three provides conservatism to ensure that plants whose key ATWS parameters are close to the limits will be analyzed. If the analyses are required, they will be performed at the time of plant fuel introduction using the References 23 and 28 NRC approved methodology or newer approved methodology, if available.

[[

]]

Table 3-33 Key ATWS Acceptance Criteria

Acceptance Criteria	Limit
Peak Vessel Pressure (MPa)	10.34 (1500psig)
Peak Cladding Temperature (°C)	1204.4 (2200°F)
Peak Local Cladding Oxidation (%)	17
Peak Suppression Pool Temperature	Design Limit
Peak Containment Pressure	Design Limit

4.0 LICENSING APPLICATION

4.1 APPLICABILITY

This report documents the completion of the generic portions of the GESTAR II requirements for the introduction of a new GEH or GNF fuel design into GEH BWRs. Revision 0 of the GNF2 compliance report is [[

]] This document applies the approved PRIME T-M methodology to the GNF2 fuel assembly to revise the T-M design basis. The GESTR-Mechanical basis is included in Appendix A and continues to be applicable, subject to the specified limitations.

The ranges of operation that have been investigated include extended power uprate (EPU) power levels as well as the Maximum Extended Load Line Limit Analysis Plus (MELLLA+) operating domain expansion (Reference 36). Currently licensed operating domains and operational flexibility features have been considered where applicable. [[

]]

The evaluations documented in this report demonstrate that the GNF2 fuel design meets the GESTAR requirements for the introduction of a new fuel design.

4.2 PLANT SPECIFIC APPLICATION PROCESS

In addition to the generic aspect of this GNF2 compliance document, the plant specific application process will confirm that the plant specific cycle-independent aspects of the GNF2 fuel introduction meets the design and licensing basis requirements of the plant. The cycle-independent analyses will be defined and evaluated consistent with the plant licensing basis.

The New Fuel Introduction report will document the cycle-independent plant specific analyses for use by Licensee as input to the plant's 10 CFR 50.59 evaluation of the new fuel introduction. A typical table of contents for a plant specific introduction is shown in Table 4-1.

Table 4-1 Typical Contents of New Fuel Introduction Report

1.0 INTRODUCTION AND SUMMARY
[[
]]
12.0 REFERENCES

5.0 SUMMARY AND CONCLUSION

This report documents the completion of the requirements for a new fuel design per the criteria defined in GESTAR II. Section 1.1 of GESTAR II defines a set of fuel licensing acceptance criteria for evaluating new fuel designs and for determining the applicability of generic analyses to these new designs. As stated in GESTAR II, "Fuel design compliance with the fuel licensing acceptance criteria constitutes USNRC acceptance and approval of the fuel design without specific USNRC review." All of the criteria defined in GESTAR II have been met for the GNF2 fuel design.

[[

]]

6.0 REFERENCES

1. Global Nuclear Fuel, "General Electric Standard Application for Reactor Fuel (GESTAR II)," NEDE-24011-P-A-18, and the US Supplement NEDE–24011–P–A–18–US, April 2011.

2. Global Nuclear Fuel, "GE14 Compliance with Amendment 22 of NEDE-24011-P-A (GESTAR II), NEDE-32868P, Revision 0, December 1998, Revision 1, September 2000, Revision 3, April 2009.

3. Global Nuclear Fuel, "GE12 Compliance with Amendment 22 of NEDE-24011-P-A (GESTAR II)," NEDE-32417, December 1994

4. Global Nuclear Fuel, "GE13 Compliance with Amendment 22 of NEDE-24011-P-A (GESTAR II)," NEDE-32198P, December, 1993.

5. Global Nuclear Fuel, "GE11 Compliance with Amendment 22 of NEDE-24011-P-A (GESTAR II)," NEDE-31917P, April 1991.

6. Letter from AC Thadani (USNRC) to JS Charnley (GE), Subject: Acceptance for Referencing of Amendment 22 to General Electric Licensing Topical Report NEDE-24011-P-A "General Electric Standard Application for Reactor Fuel" (TAC No. 71444), July 23, 1990, MFN 100-90.

7. A. C. Thadani (NRC) to J. S. Charnley (GE), Team Audit of GE11 Fuel Design Compliance with Amendment 22 of NEDE-24011-P-A, March 24, 1992.

8. R.M. Gallo (NRC) to Craig Kipp (GE), Non-Proprietary NRC Inspection Report No 99900003/95-01, March 5, 1996.

9. J. F. Klapproth (GE) to R. C. Jones, Jr. (NRC), Team Audit of GE11 Fuel Design Compliance with Amendment 22 of NEDE-24011-P-A, April 30, 1992.

10. Meeting, NRC/GE, September 22, 1992, Fuel Technology Update.

11. Meeting, NRC/GE, April 14, 1993, Fuel Technology Update.

12. BWR Owners' Group Long-Term Stability Solution Licensing Methodology, NEDO-31960-A, November 1995, and NEDO-31960-A, Supplement 1, November 1995.

13. Impact of Time Varying Axial Power Shape on Pressurization Transients, GENE-666-03-0393, Revision 0, March 1993.

14. Letter from SA Richards (NRC) to GA Watford (GE), Subject: "Amendment 26 to GE Licensing Topical Report NEDE-24011-P-A, GESTAR II Implementing Improved GE Steady-State Methods," (TAC No. MA6481), November 10, 1999.

15. GE Nuclear Energy, "Steady–State Nuclear Methods," NEDE–30130–P–A, April 1985.

16. JF Briesmeister, "MCNP - A General Monte Carlo N-Particle Transport Code, Version 4A," LA-12625-M Manual, Los Alamos National Laboratory, (1993).

17. Letter from DG Eisenhut (USNRC) to RL Gridley (GE), NRC Safety Evaluation RE: "Generic Reload Fuel Application," (GESTAR II, Revision 0) May 12, 1978 (ADAMS Accession No. ML062860426)

18. GE Nuclear Energy, "Methodology and Uncertainties for Safety Limit MCPR Evaluation," NEDC–32601P–A, August 1999.

19. GE Nuclear Energy, "Power Distribution Uncertainties for Safety Limit MCPR Evaluations," NEDC–32694P–A, August 1999.

20. Letter from F Akstulewicz to GA Watford, Acceptance for Referencing of Licensing Topical Reports NEDC-32601P, Methodology and Uncertainties for Safety Limit MCPR Evaluations; NEDC-32694P, Power Distribution Uncertainties for Safety Limit MCPR Evaluation; and Amendment 25 to NEDE-24011-P-A On Cycle-Specific Safety Limit MCPR (TAC Nos. M97490, M99069 & M97491), MFN-003-99, March 11, 1999.

21. GE Nuclear Energy, "Qualification of the One-Dimensional Core Transient Model for BWR's," NEDO-24154, Vol. 1 and 2; October 1978.

22. GE Nuclear Energy, "Qualification of the One-Dimensional Core Transient Model for BWR's," NEDE-24154-P-A, Vol. 3; August 1986.

23. GE Nuclear Energy, "Qualification of the One-Dimensional Core Transient Model (ODYN) for Boiling Water Reactors (Supplement 1-Volume 4)," NEDC-24154P-A, Revision 1, February 2000.

24. GE Nuclear Energy, "TRACG Application for Anticipated Operational Occurrences (AOO) Transient Analyses," NEDE-32906P-A, Revision 3, September 2006.

25. GE Nuclear Energy, "TRACG Application for Anticipated Operational Occurrences (AOO) Transient Analyses," NEDE-32906P Supplement 2-A, March 2006.

26. GE Nuclear Energy, "TRACG Application for Anticipated Transient Without Scram Overpressure Transient Analyses," NEDE-32906P Supplement 1-A, November 2003.

27. GE Nuclear Energy, "Migration to TRACG04 / PANAC11 from TRACG02 / PANAC10 for TRACG AOO and ATWS Overpressure Transients," NEDE-32906P, Supplement 3-A, Revision 1, April 2010.

28. GE Nuclear Energy, "TASC–03A-A computer program for Transient Analysis of a Single Channel," NEDC–32084P–A, Rev. 2, July 2002.

29. GE Nuclear Energy, "ODYSY Application for Stability Licensing Calculations," NEDC–32992P–A, July 2001.

30. Letter, JS Charnley (GE) to RC Jones, Jr. (NRC), Fuel Channel Bow Assessment, MFN086–89, November 15, 1989.

31. Acceptance for Referencing of Licensing Topical Report NEDE-24011-P-A Amendment 7 to Revision 6, GE Standard Application for Reactor Fuel Letter, CO Thomas (NRC) to JS Charnley (GE), MFN-036-85, March 1, 1985.

32. Letter from C. O. Thomas (NRC) to J. S. Charnley (GE), Acceptance for Referencing of LTR NEDE–24011–P–A–6, Amendment 10, GE Standard Application for Reactor Fuel, May 28, 1985.

33. Letter from H. N. Berkow (NRC) to J. S. Charnley (GE), Acceptance for Approval of Fuel Designs Described in LTR NEDE–24011–P–A–6, Amendment 10, For Extended Burnup Operation, December 3, 1985.

34. NRC Information Notice 94-64, Reactivity Insertion Transient and Accident Limits for High Burnup Fuel, August 31, 1994.

35. GE Nuclear Energy, "ATWS Rule Issues Relative to BWR Core Thermal-Hydraulic Stability," NEDO-32047-A, June 1995, (SER includes approval for: "Mitigation of BWR Core Thermal-Hydraulic Instabilities in ATWS," NEDO-32164, December 1992.).

36. GE Nuclear Energy, "General Electric Boiling Water Reactor Maximum Extended Load Line Limit Analysis Plus," NEDC-33006P-A, Revision 3, June 2009.

37. GE Nuclear Energy, "Assessment of Fuel Rod Bowing in General Electric Boiling Water Reactors," NEDE-24284-P-A, March, 1984.

38. GE Nuclear Energy, "GE11 Critical Power Test With Rod Bow to Contact," NEDE-31829P, April 1990.

39. GE Nuclear Energy, "Fuel Assembly Evaluation of Combined Safe Shutdown Earthquake (SSE) and Loss-of-Coolant Accident (LOCA) Loadings (Amendment No. 3)," NEDE-21175-3-P-A, October 1984.

40. American National Standard, Design Requirements for Light Water Reactor Spent Fuel Storage Facilities at Nuclear Power Plants, ANSI/ANS 57.2-1983.

41. GE Nuclear Energy, "General Electric BWR Thermal Analysis Basis (GETAB): Data, Correlation and Design Application," NEDE–10958–PA and NEDO–10958–A, January 1977.

42. Letter, J. S. Charnley (GE) to C. 0. Thomas (NRC), Amendment 15 to General Electric Licensing Topical Report NEDE–24011–P–A, January 25, 1986.

43. Letter GA Watford (GNF) to Document Control Desk (USNRC), Subject: Final Presentation Material for GEXL Presentation – February 11, 2002, FLN–2002–004, February 12, 2002.

44. GE Nuclear Energy, "Analytical Model for Loss-of-Coolant Analysis in Accordance with 10CFR50 Appendix K," NEDE-20566-P-A, Vols. I, II, III, September 1, 1986.

45. Letter, J.F. Klapproth (GE) to USNRC, Transmittal of GE Proprietary Report NEDC-32950P "Compilation of Improvements to GENE's SAFER ECCS-LOCA Evaluation Model," dated January 2000 by letter dated January 27, 2000.

46. Letter, S.A. Richards (NRC) to J.F. Klapproth, "General Electric Nuclear Energy (GENE) Topical Reports GENE (NEDC)-32950P and GENE (NEDC)-32084P Acceptability Review," May 24, 2000.

47. GE Nuclear Energy, "The GESTR–LOCA and SAFER Models for the Evaluation of the Loss–of–Coolant Accident," NEDE–23785–1–P–A,Volumes I - III, February 1985.

48. GE Nuclear Energy, "GESTR–LOCA and SAFER Models for Evaluation of Loss–of–Coolant Accident Volume III, Supplement 1, Additional Information for Upper Bound PCT Calculation," NEDE–23785P–A, Supplement 1, Revision 1, March 2002.

49. GE Nuclear Energy, "SAFER Model for Evaluation of Loss-of-Coolant Accidents for Jet Pump and Non-Jet Pump Plants," NEDE-30996P-A, Volumes 1 and 2, October 1987.

50. SO Akerlund et al, The GESTR–LOCA and SAFER Models for the Evaluation of the Loss–of–Coolant Accident: Volume I - GESTR–LOCA - A Model for the Prediction of Fuel and Thermal Performance, NEDE–23785–1–P–A, February 1985.

51. CJ Paone and JA Woolley, "Rod Drop Accident Analysis for Large Boiling Water Reactors, Licensing Topical Report," NEDO–10527, March 1972.

52. CJ Paone, "Banked Position Withdrawal Sequence," NEDO–21231, January 1977.

53. R.E. Engel to D.B. Vassallo, "Elimination of Control Rod Drop Accident Analysis for Banked Position Withdrawal Sequence Plants," MFN-026-82, February 24, 1982

54. GE Nuclear Energy, "Improved BPWS Control Rod Insertion Process," NEDO-33091-A, Revision 2, July 2004.

55. JS Charnley (GE) to MW Hodges (USNRC), "Revised Generic BPWS CRD Analysis," MFN-034-087, April 22,1987.

56. GE Nuclear Energy, "Assessment of BWR Mitigation of ATWS, Volume I and II (NUREG–0460 Alternate No. 3)," NEDE-24222, December 1979.

57. GE Nuclear Energy, "Assessment of BWR/3 Mitigation of ATWS (Alternate No. 3)," NEDE-24223, December 1979.

58. *Letter* from AA Lingenfelter (GNF) to Document Control Desk (NRC), Subject: *Amendment 32 To NEDE–24011–P, General Electric Standard Application For Reactor Fuel (GESTAR II)*, FLN-2008-011, October 15, 2008, and Letter from TB Blount (NRC) to AA Lingenfelter (GNF), Subject: *Final Safety Evaluation for Amendment 32 to Global Nuclear Fuel Topical Report NEDE-24011-P General Electric Standard Application for Reload (TAC NO. MD9939),* July 30, 2009.

59. Letter from AA Lingenfelter (GNF) to Document Control Desk (USNRC), Subject: GNF Licensing Topical Report, "The PRIME Model for Analysis of Fuel Rod Thermal – Mechanical Performance," NEDC-33256P, NEDC-33257P, and NEDC-33258P, January 2007, FLN-2007-001, January 19, 2007, and Letter from TB Blount (NRC) to AA Lingenfelter (GNF), Subject: Final Safety Evaluation For Global Nuclear Fuel – Americas Topical Reports NEDC-33256P, NEDC-33257P, and NEDC-33258P, "The PRIME Model For Analysis Of Fuel Rod Thermal-Mechanical Performance" (TAC NO. MD4114), January 22, 2010.

60. GE Hitachi Nuclear Energy, "Implementation of PRIME Models and Data in Downstream Methods," NEDO-33173, Supplement 4-A, September 2011.

61. GE Hitachi Nuclear Energy, "General Electric Fuel Bundle Designs," NEDE-31152P, Revision 8, April 2001.

APPENDIX A – GESTR-M THERMAL-MECHANICAL BASES

A.1 THERMAL-MECHANICAL

The Thermal-Mechanical (T-M) analysis of the GNF2 fuel assembly fuel rod and assembly components is performed to demonstrate compliance with the applicable criteria identified in Subsection 1.1.2 of GESTAR II. [[

]]

The GNF2 analyses utilize the following two processes from Section 1.1.2.A. of GESTAR II:

1. Either worst tolerance assumptions are applied or probabilistic analyses are performed to determine statistically bounding results (i.e. upper 95% confidence).
2. Operating conditions are taken to bound the conditions anticipated during normal steady–state operation and anticipated operational occurrences.

The GNF2 fuel rod and assembly component analyses were performed in accordance with the above guidance to demonstrate compliance to the fuel design criteria in Section 1.1.2.B of GESTAR II. The T-M design criteria from GESTAR II are illustrated in Table A-1 with the corresponding subsection of this document. The criteria and subsections that apply to fuel rod T-M design are identified in Table A-2.

The GNF2 fuel rod definition includes three variable application parameters, which may vary for different plants and for different energy utilization plans. The following table illustrates the application parameters and an example of a set that may be applied for a specific design.

Fuel Rod Variable Application Parameters:	Example Values
Fuel rod as fabricated internal fill-gas pressure	[[ ]] MPa
Active fuel column length	Any design reflected in Table 2-1
Local fuel linear heat generation rate [[ ]]	Figure A-1 and Figure A-2

Compliance of the fuel rod response with Subsections A.1.1, A.1.6, A.1.9, and A.1.10 is confirmed for specific sets of the three application parameters by performing exposure-dependent T-M analyses with appropriate consideration of anticipated operational overpower occurrences. The compliance analyses confirm that the criteria are satisfied for all exposures

from beginning of life to design discharge exposure. Compliance with Subsection A.1.8 is confirmed generically for the most limiting set of application parameters. GNF2 compliance with the fuel rod T-M acceptance criteria shall be reconfirmed for each set of application parameters utilized for GNF2 core designs.

The GNF2 fuel rod thermal-mechanical analyses are performed using NRC-approved analytical models. The model applied for the fuel rod analyses was the GESTR-MECHANICAL model as documented in Section 2.2 of NEDE-24011-P-A, General Electric Standard Application For Reactor Fuel: GESTAR II.

Table A-1 GESTAR Fuel Thermal-Mechanical Design Criteria

Section 3.2 Subsection	GESTAR Subsection	GESTAR Criteria
A.1.1 Stress, Strain, Fatigue	1.1.2.B.i	The fuel rod and fuel assembly component stresses, strains, and fatigue life usage shall not exceed the material ultimate stress or strain and the material fatigue capability.
A.1.2 Fretting	1.1.2.B.ii	Mechanical testing will be performed to ensure that loss of fuel rod and assembly component mechanical integrity will not occur due to fretting wear when operating in an environment free of foreign material.
A.1.3 Metal Thinning	1.1.2.B.iii	The fuel rod and assembly component evaluations include consideration of metal thinning and any associated temperature increase due to oxidation and the buildup of corrosion products to the extent that these effects influence the material properties and structural strength of the components.
A.1.4 Fuel Rod Internal Hydrogen Content	1.1.2.B.iv	The fuel rod internal hydrogen content is controlled during manufacture of the fuel rod consistent with ASTM standards C776-83 and C934-85 to assure that loss of fuel rod mechanical integrity will not occur due to internal cladding hydriding.
A.1.5 Fuel Rod/Channel Bow	1.1.2.B.v	The fuel rod is evaluated to ensure that fuel rod or channel bowing does not result in loss of fuel rod mechanical integrity due to boiling transition.
A.1.6 Cladding Pressure Loading	1.1.2.B.vi	Loss of fuel rod mechanical integrity will not occur due to excessive cladding pressure loading.
A.1.7 Control Rod Insertion	1.1.2.B.vii	The fuel assembly (including channel box), control rod and control rod drive are evaluated to assure control rods can be inserted when required.
A.1.8 Cladding Creep Collapse	1.1.2.B.viii	Loss of fuel rod mechanical integrity will not occur due to cladding collapse into a fuel column axial gap.
A.1.9 Fuel Center Temperature	1.1.2.B.ix	Loss of fuel rod mechanical integrity will not occur due to fuel melting.
A.1.10 Cladding Plastic Strain During AOOs	1.1.2.B.x	Loss of fuel rod mechanical integrity will not occur due to pellet-cladding mechanical interaction.

Table A-2 Fuel Rod Thermal-Mechanical Design Criteria

Criterion	Subsection	Governing Equation
The cladding creepout rate ($\dot{\varepsilon}_{cladding\_creepout}$), due to fuel rod internal pressure, shall not exceed the fuel pellet irradiation swelling rate ($\dot{\varepsilon}_{fuel\_swelling}$).	A.1.6	$\dot{\varepsilon}_{cladding\_creepout} \le \dot{\varepsilon}_{fuel\_swelling}$
The maximum fuel center temperature (T_{center}) shall remain below the fuel melting point (T_{melt}).	A.1.9	$T_{center} < T_{melt}$
The cladding circumferential plastic strain (ε_{θ}^{P}) during an anticipated operational occurrence shall not exceed 1.00%.	A.1.10	$\varepsilon_{\theta}^{P} \le 1.00\%$
The fuel rod cladding fatigue life usage ($\sum_i \frac{n_i}{n_f}$ where n_i=number of applied strain cycles at amplitude ε_i and n_f=number of cycles to failure at amplitude ε_i) shall not exceed the material fatigue capability.	A.1.1	$\sum_i \frac{n_i}{n_f} \le 1.0$
Cladding structural instability, as evidenced by rapid ovality changes, shall not occur.	A.1.8	No creep collapse
Cladding effective stresses (σ_e) shall not exceed the failure stress (σ_f) and cladding effective strains (ε_e) shall not exceed the failure stress strain (ε_f).	A.1.1	$\sigma_e < \sigma_f$, $\varepsilon_e < \varepsilon_f$
The as-fabricated fuel pellet evolved hydrogen (C_H is content of hydrogen) at greater than 1800 °C shall not exceed prescribed limits.	A.1.4	[[ ]]

A.1.1 Stress, Strain, Fatigue

GESTAR II Section 1.1.2.B.i: "The fuel rod and fuel assembly component stresses, strains, and fatigue life usage shall not exceed the material ultimate stress or strain and the material fatigue capability."

Fuel Rods

The fuel rod stress analysis was performed for the limiting application parameters as defined in Subsection A.1. The analysis was performed using a Monte Carlo statistical method to calculate the effects of [[

]]

For each calculation, the stresses are combined into an effective stress using the Von Mises theory and compared with the appropriate design limit to produce a design ratio. [[

]] such as shown in Figure A-1 and Figure A-2. Table A-3 summarizes the calculated design ratios for the Power Exposure Envelope of Figure A-1 which is also listed in Appendix C in tabular form.

[[ ]]

Figure A-1 GNF2 for BWR/3-6 Power-Exposure Envelope

[[ ]]

Figure A-2 GNF2 for BWR/2 Power-Exposure Envelope

Table A-3 Results of Cladding Stress Analysis for BWR/3-6 Fuel Rod

Rod Type	Period	Design Ratio at Rated Power	Design Ratio at Overpower
UO_2 Rod	BOL	[[	
	1st Knee		
	2nd Knee		
	EOL		
[[ ]] Gd Rod	BOL		
	1st Knee		
	2nd Knee		
	EOL		
[[ ]] Gd Rod	BOL		
	1st Knee		
	2nd Knee		
	EOL		]]

These analyses demonstrated that the GNF2 fuel rod stresses do not exceed the failure strength of the material. These analyses were explicitly performed for GNF2 for BWR/3-6 and are judged to be applicable to GNF2 for BWR/2 based on the fuel designs and the relative Power-Exposure Envelopes.

Inputs to these fuel rod cladding statistical stress analyses are obtained from the fuel rod thermal-mechanical model GESTR-MECHANICAL as documented in GESTAR II.

Fatigue evaluations of fuel rod designs are performed for the application parameters using the analysis methodology as defined in Subsection A.1 of this document. These evaluations demonstrate with large conservatism that the cladding fatigue usage does not exceed the cladding fatigue capability. Therefore, loss of fuel rod mechanical integrity due to cladding fatigue will not occur.

[[

]]

Channels

The GNF2 fuel channel (Figure A-3) is open at the bottom and makes a sliding seal fit on the lower tieplate surface. At the top of the channel, two opposite corners have welded tabs. These tabs support the weight of the channel on the upper tieplate posts. One of the tabs is drilled for attaching the channel fastener to the bundle. [[

]]

[[

]]

The GNF2 channel has been evaluated by finite element analyses. These analyses demonstrate that the stresses and strains are well below the failure strength at operating conditions. The channel wall pressure differential required to cause material yielding is [[
]] for the thinner and thicker channel offerings, respectively. For each new channel application, it is confirmed that the specific plant pressures do not exceed the channel capability. A fatigue analysis was also performed which addressed the cyclic pressure duty due to normal and transient operation.

[[

]]

Figure A-3 GNF2 Fuel Channel

Spacers

Cyclic testing for seismic loading demonstrates that the GNF2 spacer stresses and strains do not exceed failure values and that the fatigue capability is not exceeded. Because the seismic loads are well in excess of any operational or handling loading and because there is no significant deformation or fracture of the spacer under seismic loadings, the GNF2 spacer is demonstrated to meet the requirements of this Subsection.

The spacer fatigue test consists of loading the spacer in [[

]] The results of the tests are then used to determine the design margin to failure. The test results show the maximum loads that are acceptable, [[

]] and the minimum loads that cause failures. [[

]]

Table A-4 Maximum Successful & Failure Loads

Configuration Description	Maximum Successful Load (kN)	Failure Load (kN)
[[		
		]]

[[

]]

The spacer deformation test consists of testing [[

]] The load is the maximum fuel spacer component load experienced in the postulated combined safe shutdown, earthquake and loss-of-coolant-accident. [[

]] In all cases, the gap changes were small compared to the initial gap; therefore the coolability of the bundle will not be compromised.

Because the seismic loads are in excess of any operational or handling loading and because significant deformation or fracture of the spacer was shown to not occur even under seismic loadings, the GNF2 spacer is demonstrated to meet the requirements of this Subsection.

Water Rods

The GNF2 assembly is designed with two large circular water rods that are centrally located and occupy eight fuel rod lattice positions. A typical spacer–positioning water rod is shown in Figure A-4.

The water rods are hollow Zircaloy tubes with several holes around the circumference near each end to allow coolant to flow through the rod. The number and diameter of the inlet holes at the lower end control the water rod flow. [[

]] Similar to the fuel rods, an expansion spring is located between the water rod shoulder and upper tieplate to allow for differential axial expansion.

Demonstration that the water rod stresses and strains do not exceed failure strength and that the fatigue capability will not be exceeded is shown by stress analyses that address handling and fit up loading.

A limiting pressure differential stress analysis is also provided in response to Subsection A.1.6 requirements. The water rod tubing was evaluated for a steady state differential wall pressure of [[ ]]. The Zircaloy material properties at operating conditions appropriate for this analysis are:

Yield Strength = [[ ]] at 288ºC
Tensile Strength = [[ ]] at 288ºC

The water rod tube membrane stress was determined from S = Pr/t.

Where:

S = membrane stress
P = pressure differential
r = mean tubing radius
t = tubing wall thickness

The maximum stress occurs in the large diameter portion of the water rod.

Therefore;

[[ ]]

Because all stresses are well below yield strength and since there is no significant cyclic loading, the fatigue capability is not exceeded.

[[

]]

Figure A-4 Water Rod

Tie Plates

Demonstration that the GNF2 upper and lower tieplates do not exceed failure strength was shown by stress analyses that addressed the maximum handling loads. The loads are the largest loads on these components except for seismic and fuel lift loadings that are addressed in Subsection A.1.7. The upper and lower tie plates are not subjected to any significant cyclic loadings and fatigue capability is therefore not exceeded.

Upper Tie Plate

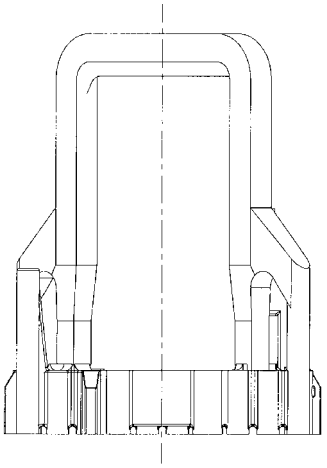

Lower Tie Plate

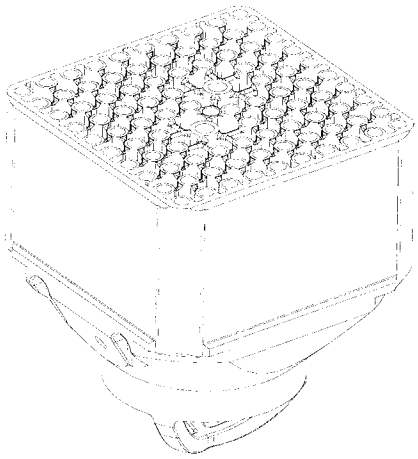

Appropriate material properties for Type-304 Stainless Steel for the upper tieplate stress evaluations are:

Yield Strength = [[ ]] at 38º C
Tensile Strength = [[ ]] at 38º C

The limiting loading on the upper tieplate occurs during fuel handling when the fuel assembly is lifted by the grapple that is attached to the upper tieplate handle. The loads that are evaluated are [[ ]] For this analysis, the GNF2 fuel assembly weight, which includes the fuel bundle, channel, and channel fastener weights, is assumed to be [[ ]] in air (a conservative assumption with respect to the typical weight of an assembly [[ ]]). Therefore, the upward loading on the upper tieplate is [[ ]] for this condition.

The upper tieplate was evaluated by finite element analysis using the ANSYS code. The model utilizes [[

]]

An upward vertical load of [[ ]] was applied at the edge of the grapple interface with the upper tieplate handle (20 mm from the center of the handle). The downward load from the channel of [[ ]] was applied at the channel post location. Note that this is conservative relative to the channel weight of [[ ]]. The upward loading from the expansion springs is also modeled ([[ ]]). The remainder of the upward vertical load was [[

]]

The maximum bending stress in the grid portion of the tieplate (corrected for minimum dimensions) based on these loading was determined to be [[ ]].

A finite element analysis, using three dimensional beam elements, was also used to evaluate the stresses in the handle. The maximum stress in the handle occurs at the center of the horizontal portion of the handle. Correcting the stresses for minimum dimensions results in a stress equal to [[ ]]. This stress is above the yield strength, but much less than the tensile strength. The acceptability of exceeding the yield strength in the center of the handle is addressed by the mechanical handling load test described below.

A mechanical test was performed to assure that excessive deformation or fracture will not occur when the UTP handle is subjected to a [[ ]] load. Tie plates tested were restrained vertically at the eight tie rod locations and an upward load on the handle with a simulated fuel grapple was applied. The test tie plates were subject to a load approximately twice the [[ ]] load and then inspected for grid deformation and deformation of the handle. Previous tests for the GE14

tie plate, which has handle geometry essentially identical to the GNF2 upper tie plate, show a maximum handle deformation of only [[ ]].

The limiting loading condition on the lower tieplate is due to seating of the fuel assembly into the core or into the fuel storage racks. The load that is evaluated is [[ ]] distributed over the tieplate surface. This load is conservative relative to a design basis load of 4.2 times the assembly weight minus the lower tie plate weight i.e., [[ ]]. The lower tieplate was evaluated by a finite element analysis using the ANSYS code. The model utilizes ¼ symmetry and consists of [[ ]] elements. Three dimensional beam elements were used to model the lower tie plate structure. The element cross-section properties were calculated from the nominal drawing dimensions. The side wall was considered as rigid due to its relatively large thickness and depth, therefore no vertical displacement and no rotation along the axis of side wall are assumed. The maximum bending stress (corrected for minimum section dimensions) was determined to be [[ ]]. These lower tieplate analysis results demonstrate that the lower tieplate stresses are well below the yield strength.

The above analysis demonstrates that the GNF2 upper and lower tieplates are not expected to experience excessive deformation or failure during service.

A.1.2 Fretting

GESTAR II Section 1.1.2.B.ii: "Mechanical testing will be performed to ensure that loss of fuel rod and assembly component mechanical integrity will not occur due to fretting wear when operating in an environment free of foreign material."

The GNF2 fuel assembly was tested to assure that the design features do not result in a significant increase in flow induced vibration (FIV) response and thereby do not increase the potential for fretting. The method used to demonstrate the adequacy of the fuel assembly from a FIV perspective was to compare the vibration response of the GNF2 design with the GE14 design during FIV tests. The response comparison was based on accelerometer data from various locations in the fuel assemblies. The GE14 fuel assembly's performance is considered acceptable based upon its reliable performance in reactor operation.

[[

]] The acceleration signals were recorded and then analyzed to perform direct comparisons of RMS and maximum response between GE14 and GNF2 over a range of flow conditions. Each configuration was tested over a range of flow rates, from [[ ]] to approximately [[ ]] of in-reactor rated mass flow.

The results of the FIV tests shown in Figure A-5 show that there are no significant differences in the peak acceleration response of the GNF2 fuel and water rods compared to the performance of the GE14 fuel and water rods. The GNF2 FIV test results also demonstrate the acceptable performance of the part length fuel rods and adjacent rods. The differences in fuel rod, lower tieplate, channel-lower tie plate interface and spacer designs show no significant effect on FIV performance when compared to the GE14 design.

[[

]]

Figure A-5 GNF2 & GE14 FIV Test Result Comparison

Based on the FIV test program, the performance of the GNF2 fuel design meets the fretting design requirements.

A.1.3 Metal Thinning

GESTAR II Section 1.1.2.B.iii: "The fuel rod and assembly component evaluations include consideration of metal thinning and any associated temperature increase due to oxidation and the buildup of corrosion products to the extent that these effects influence the material properties and structural strength of the components."

Metal thinning of the Zircaloy components due to corrosion will result in higher stresses being calculated at end of life if the loading conditions do not change. The increase in stress is more than offset, in this case, by the increase in material strength due to irradiation. However, the fatigue strength of the Zircaloy components is not increased with irradiation. Where the load cycling is potentially significant, the effects of corrosion are explicitly addressed. Corrosion thinning effects were consequently addressed in the fuel rod stress and fatigue analyses and in the channel fatigue analysis described in Subsection A.1.1. Subsections A.1.3.1 and A.1.3.2 describe the methods applied for consideration of metal thinning.

A.1.3.1 Metal Thinning Effects On Zircaloy Cladding

Zircaloy cladding tubes undergo oxidation at slow rates during normal reactor operation. This oxidation causes thinning of the cladding tube wall and introduces a resistance to the fuel rod-to-coolant heat transfer. Corrosion products present in the reactor coolant system also tend to deposit on the fuel rod cladding outer heat transfer surface. This corrosion product deposition also introduces a resistance to the fuel rod-to-coolant heat transfer. In the extensive GNF operational history database, fuel rod failures have not occurred due to cladding corrosion without the presence of an augmenting factor such as an aggressive crud-induced localized corrosion environment. Therefore, no specific limit on cladding corrosion is applied. Although no specific value of cladding oxide thickness can be identified to correspond to fuel rod failure, cladding oxidation does affect the overall strength of the cladding through loss of structural material and reduced material strength due to higher temperature. Therefore, all fuel rod evaluations explicitly include the amount of cladding metal thinning and the cladding temperature increase due to cladding oxidation and the buildup of corrosion products. The amount of cladding oxidation and corrosion product buildup used in the analyses is summarized in Table A-5.

Table A-5 Cladding Oxidation and Corrosion Product Buildup

	Radial Thickness (mm)	
	Mean	**Standard Deviation**
Beginning-of-Life		
Cladding Oxidation	[[	
Corrosion Product Buildup		
End-of-Life (8 years)		
Cladding Oxidation		
Corrosion Product Buildup		]]

These results are based on numerous field measurements through September 2002 at 14 plants, representing normal GNF experience, excluding cases involving specific water chemistry issues outside of normal operating experience. The data above was generated with a best-fit estimate based on the data set mentioned above.

A.1.3.2 Metal Thinning Effects On Zircaloy Channels

The effects of metal thinning have been considered in a GNF channel fatigue and stress rupture analysis. This analysis shows that the GNF2 channel is structurally adequate, with respect to fatigue and stress rupture, for a bounding design basis pressure differential and a maximum lifetime of [[ ]].

Metal thinning as a result of oxidation for the fatigue and stress rupture analysis is modeled by consideration of the thermal and irradiation components in a BWR environment. Metal thinning is modeled according to the following relationship.

[[ ]]

where Z_{total} is the oxidation on each side of the channel wall.

Considering metal thinning, a channel pressure differential of [[ ]] was used to determine the limit of pressure differential that exceeds a total damage of 1.0. The damage is calculated as the sum of the fatigue and rupture stress life consumed under a series of events and

conditions. By definition a damage value of 1.0 indicates failure. Minimum channel thickness is assumed at t=0 in the analysis. An initial thickness of [[ ]] mm is utilized as compared to the nominal values of [[ ]] mm. Figure A-6 depicts a channel cross-section and the nominal thickness.

[[

]]

Figure A-6 Channel Cross Section

As a result of these analysis, which included metal thinning, a fatigue damage and stress rupture damage summation of less than 1.0 for both corner and thickness transitions was determined to be acceptable for differential pressures less than [[ ]].

These analyses demonstrate the adequacy of the GNF2 design and the methods for resisting the effects of metal thinning due to corrosion. The methods are applied for Zircaloy-2 and Zircaloy-4 variants of the GNF2 product.

A.1.4 Fuel Rod Internal Hydrogen Content

GESTAR II Section 1.1.2.B.iv: "The fuel rod internal hydrogen content is controlled during manufacture of the fuel rod consistent with ASTM standards C776-83 and C934-85 to assure that loss of fuel rod mechanical integrity will not occur due to internal cladding hydriding."

The pellet specifications include a requirement that limits the maximum amount of hydrogen that is allowed to be present in the manufactured fuel pellets. This limit is consistent with or less than that specified by ASTM standards C776-83 and C934-85. Manufacturing processes for the fuel rod and its components include controls to ensure that the hydrogen limit is met and are designed to avoid spurious sources of hydrogen in the fuel rod.

A.1.5 Fuel Rod/Channel Bow

GESTAR II Section 1.1.2.B.v: "The fuel rod is evaluated to ensure that fuel rod or channel bowing does not result in loss of fuel rod mechanical integrity due to boiling transition."

Analysis Procedures for Incorporating Channel Bow Effects in Critical Power Evaluations

Channel bow effects are incorporated in critical power evaluations by modifying the bundle R-factor to include changes in local peaking caused by channel bowing. The model is described in the GE report MFN086-89 submitted by letter to the NRC November 15, 1989 and in additional information contained in MFN041-90, May 3, 1990, and MFN109-90, Sep. 26, 1990. The methodology has been approved by the NRC letter, Acceptance for Referencing of Topical Report Titled "GE-Nuclear Energy Report MFN086-89," to J.S. Charnley (GE) from A.C. Thadani (NRC), Jan. 11, 1991.

Channel Bow Compliance

Loss of mechanical integrity due to boiling transition is prevented because all critical power evaluations in the plant process computer and other licensing analyses include an allowance for channel bow effects according to approved methods described above.

Rod Bow Compliance

Reference 37 describes a large program to characterize the extent of rod bowing in BWR fuel along with full scale thermal hydraulic experiments on 8x8 assemblies to investigate the potential impact on Boiling Transition due to rod bow. This program included poolside measurements of over 1000 assemblies and concluded that significant rod bowing did not exist in BWR fuel. Furthermore, the thermal hydraulic testing did not observe any significant impact on critical power.

This original work was supplemented with additional full scale testing of 9x9 assemblies. The results of this testing, described in Reference 38, were verbally communicated to NRC. In summary, a very improbable configuration was tested in which the critical rods in a reference test were bowed to contact just upstream of the onset of Boiling Transition. This testing again

concluded that rod bowing does not degrade the margins to Boiling Transition even in this highly improbable circumstance. The results of these two programs are considered applicable to 10x10 fuel. As such, standard critical power limits are sufficient to prevent loss of mechanical integrity due to Boiling Transition even in the presence of rod bow. As stipulated in Reference 37, NRC will be notified if rod-to-rod gap closures greater than 50% are observed.

Compliance with requirement has been met.

A.1.6 Cladding Pressure Loading

GESTAR II Section 1.1.2.B.vi: "Loss of fuel rod mechanical integrity will not occur due to excessive cladding pressure loading."

Evaluations of fuel rod designs are performed for the application parameters using the analysis methodology as referenced in Subsection A.1 of this document. These evaluations demonstrate that the cladding creepout rate due to fuel rod internal pressure will not exceed the irradiation-swelling rate of the fuel pellet. Therefore, loss of fuel rod mechanical integrity due to excessive pressure loading will not occur.

In this section, cladding lift-off is defined as the separation of the cladding from the pellet. Cladding lift-off evaluations are used to ensure that the criterion in Item 1 of Table A-2 is met. For the cladding lift-off evaluation, fuel rod internal pressure for the maximum duty fuel rods is determined using the GESTR-Mechanical fuel rod thermal-mechanical performance model in conjunction with the standard error propagation statistical method. [[

]]. The standard error propagation analysis results in a mean and standard deviation for the fuel rod internal pressure at uniformly spaced exposure points throughout the design lifetime. [[

]] This design ratio has been calculated at several exposure points for the maximum duty fuel rod for each fuel rod type present in the fuel bundle.

Table A-6 and Table A-7 summarize the GESTR-Mechanical results for the cladding lift-off evaluation for some of the key rod types for BWR/3-6 and BWR/2 respectively. Because all design ratios are less than 1.0, it is assured, [[

]]

Table A-6 GNF2 for BWR/3-6 Fuel rod Cladding Lift-Off Results

		Rod Internal Pressure (MPa)		Critical Pressure (MPa)		
Fuel Rod Type	**Exposure where Design Ratio is Max., GWd/MTU**	**Mean**	**Standard Deviation**	**Mean**	**Standard Deviation**	**Max. 95% Confidence Design Ratio**
UO_2 (Full Length)	[[					
UO_2 (Long Part Length)						
3 w/o Gd						
6 w/o Gd						]]

Table A-7 GNF2 for BWR/2 Fuel Rod Cladding Lift-Off Results

		Rod Internal Pressure (MPa)		Critical Pressure (MPa)		
Fuel Rod Type	**Exposure where Design Ratio is Max., GWd/MTU**	**Mean**	**Standard Deviation**	**Mean**	**Standard Deviation**	**Max. 95% Confidence Design Ratio**
UO_2 (Full Length, Barrier Clad)	[[					
UO_2 (Long Part Length, Barrier Clad)						
4 w/o Gad (Barrier Clad)						
8 w/o Gad (Barrier Clad)						
10 w/o Gad (Barrier Clad)						]]

A.1.7 Control Rod Insertion

GESTAR II Section 1.1.2.B.vii: "The fuel assembly (including channel box), control rod and control rod drive are evaluated to assure control rods can be inserted when required."

The fuel assembly is evaluated to assure that component deformations are not severe enough to prevent control rod insertion and that vertical uplift forces will not unseat the lower tie plate such that the resultant loss of lateral fuel bundle positioning would prevent control rod insertion. This evaluation is performed considering the combined effects of Safe Shutdown, Earthquake and Loss-of-Coolant Accident loadings on fuel assembly deformation and lift-off.

Assurance that component deformations are not excessive is provided by primary load stress analyses and tests of the components. These evaluations are based on un-irradiated material properties at operating temperature. The loads used in the evaluation of the fuel assembly components are derived from enveloping values of combined horizontal and vertical acceleration of the fuel assembly. All component stress evaluations have minimum margins of at least [[ ]] because the limit is specified to be [[ ]] times ultimate. The channel buckling has the same margin as was demonstrated previously in NEDE-21175-3-P-A (Reference 39). The existing plant seismic analysis results for the fuel assembly are checked to assure that fuel loadings do not exceed the enveloping values.

Assurance that vertical uplift forces will not unseat the fuel assembly such that loss of lateral fuel bundle positioning could occur was provided by a nonlinear fuel lift analysis as described in detail in NEDE-21175-3-P-A. The GNF2 fuel design, while visibly different from the previous fuel designs for which the lift analysis was initially performed, is dynamically similar when modeled. Because of this dynamic similarity, no significant difference in the fuel lift behavior was expected. This conclusion was confirmed by explicitly modeling the GNF2 fuel design in a typical BWR plant that has been extensively studied for previous fuel design changes. The study plant was selected because it showed potential fuel lift with previous fuel designs.

Separate from consideration of the combined effects of Safe Shutdown Earthquake and Loss of Coolant Accident loads on control rod insertability, considerations also arise for control rod insertability during normal operation due to any channel-control blade interference that may

result from irradiation-induced channel bulge and channel bow deformations. The primary control for channel-control blade interference is provided by the Plant Technical Specifications surveillance where actions are specified both (1) to ensure control rod drive scram performance is consistent with requirements, and (2) to appropriately disposition instances where control rod operability, including channel control blade interference effects, is less than adequate. These plant technical specification requirements will continue to be applied with GNF2. Additionally, the guidance, as documented in MFN 06-355, "Update to GE Surveillance Program for Channel-Control Blade Interference Monitoring", September 28, 2006, remains applicable and will be similarly applied to operating plants with GNF2 fuel to mitigate any elevated levels of channel-control blade interference.

A.1.8 Cladding Collapse

GESTAR II Section 1.1.2.B.viii: "Loss of fuel rod mechanical integrity will not occur due to cladding collapse into a fuel rod column axial gap."

The condition of an external coolant pressure greater than the fuel rod internal pressure provides the potential for elastic buckling or possibly even plastic deformation if the stresses exceed the material yield strength. Fuel rod failure due to elastic buckling or plastic collapse has never been observed in commercial nuclear reactors. However, a more limiting condition that has been observed in commercial nuclear reactors is cladding creep collapse. This condition occurs at cladding stress levels far below that required for elastic buckling or plastic deformation. In the early 1970s, excessive in-reactor fuel pellet densification resulted in the production of large fuel column axial gaps in some PWR fuel rods. The high PWR coolant pressure in conjunction with thin cladding tubes and low helium fill gas pressure resulted in excessive fuel rod cladding creep and subsequent cladding collapse over fuel column axial gaps. Such collapse occurs due to a slow increase of cladding initial ovality due to creep resulting from the combined effect of reactor coolant pressure, temperature and fast neutron flux on the cladding over the axial gap. Since the cladding is unsupported by fuel pellets in the axial gap region, the ovality can become large enough to result in elastic instability and cladding collapse.

It is noted in this PWR experience that, although complete cladding collapse was observed in some cases, cladding fracture did not occur in any case, therefore fuel rod failure by this mechanism is not expected. However, the GNF design basis includes ensuring that fuel rod failure will not occur due to cladding collapse into a fuel column axial gap. The creep collapse analysis procedure applied to the GNF2 fuel design is documented in NEDC 33139P-A, "Cladding Creep Collapse Licensing Topical Report", July 2005. The analysis consists of a detailed finite element mechanics analysis of the cladding. [[

]] The creep properties employed are the same as are used in GESTR-Mechanical. [[

]]

The analysis performed with the limiting set of application parameters demonstrates that creep collapse of freestanding cladding (cladding unsupported by fuel pellets) will not occur.

A.1.9 Fuel Melting

GESTAR II Section 1.1.2.B.ix: "Loss of fuel rod mechanical integrity will not occur due to fuel melting."

Evaluations of fuel rod designs are performed for the application parameters using the analysis methodology referenced in Subsection A.1 of this document. These evaluations demonstrate that the fuel center temperature will not exceed the fuel melting temperature. Therefore, loss of fuel rod mechanical integrity due to fuel melting will not occur.

Numerous irradiation experiments have demonstrated that extended operation with significant fuel pellet central melting does not result in damage to the fuel rod cladding. However, the fuel rod performance is evaluated to ensure that fuel rod failure due to fuel melting will not occur.

To achieve this objective, the fuel rod is evaluated to ensure that fuel melting during normal steady-state operation and whole core anticipated operational occurrences is not expected to occur. For local anticipated operational occurrences, [[

]] This fuel temperature limit is specified to ensure that sudden shifting of molten fuel in the interior of fuel rods, and subsequent potential cladding damage, can be positively precluded.

The fuel center temperature evaluation is performed using the GESTR-Mechanical fuel rod thermal-mechanical performance model in conjunction with the standard error propagation statistical method [[

]] The standard error propagation analysis results in a mean and standard deviation for the fuel center temperature during the limiting AOO at uniformly spaced exposure points throughout the design lifetime. [[

]]

A.1.10 Pellet-Cladding Mechanical Interaction

GESTAR II Section 1.1.2.B.x: "Loss of fuel rod mechanical integrity will not occur due to pellet-cladding mechanical interaction."

Evaluations of fuel rod designs are performed for the application parameters using the analysis methodology as defined in Subsection A.1 of this document. These evaluations demonstrate that the cladding plastic strain due to pellet-cladding mechanical interaction during an AOO will not exceed the cladding plastic strain limit. Therefore, loss of fuel rod mechanical integrity due to pellet-cladding mechanical interaction will not occur.

After the initial rise to power and the establishment of steady-state operating conditions, the pellet-cladding gap will eventually close due to the combined effects of cladding creep-down, fuel pellet irradiation swelling, and fuel pellet fragment outward relocation. Once hard pellet-cladding contact has occurred, a rapid power increase, such as would occur during an AOO, will

result in cladding outward diametral deformation due to the fuel pellet thermal expansion. The extent of deformation depends on the extent of irradiation exposure, the magnitude of the power increase, and the final peak power level. This (high strain rate) deformation can be a combination of (a) plastic deformation during the power increase due to the cladding stress exceeding the cladding material yield strength, and (b) creep deformation during the elevated power hold time due to creep-assisted relaxation of the high cladding stresses. This cladding deformation (plastic plus creep) during anticipated operational occurrences is limited to a maximum of 1.00%.

The cladding plastic strain evaluation is performed using the GESTR-Mechanical fuel rod thermal-mechanical performance model in conjunction with worst tolerance assumptions. The fabrication parameters important to the analysis are all biased to the fabrication tolerance limit in the direction that produces the most severe result. Other input parameters conservatively biased for this analysis include (a) cladding corrosion (2 sigma), and (b) corrosion product (crud) buildup on the cladding outer surface (2 sigma).

APPENDIX B – PRIME BASED GNF2 LHGR ENVELOPES

BWR/3-6

Tables B-1 and B-2 provide the complete set of UO_2 and gadolinia PRIME based thermal-mechanical LHGR limits applicable to GNF2 fuel bundles for BWR/3-6 plants. The power limit at a given exposure between beginning of life (BOL) and the first knee is equal to the pellet maximum power. The power limit at a given exposure between the first and second knees or between the second knee and end of life (EOL) is determined by interpolation of power with exposure.

Table B-1 BWR/3-6 UO_2 Rod BWREDB_FUEL Limits

[[					
					]]

Table B-2 BWR/3-6 $(U.Gd)O_2$ Rod/Section BWREDB_FUEL Limits

[[						
						]]

BWR/2

Tables B-3 and B-4 provide the complete set of UO_2 and gadolinia PRIME based thermal-mechanical LHGR limits applicable to GNF2 fuel bundles for BWR/2 plants. The power limit at a given exposure between BOL and the first knee is equal to the pellet maximum power. The power limit at a given exposure between the first and second knees or between the second knee and EOL is determined by interpolation of power with exposure.

Table B-3 BWR/2 UO_2 Rod BWREDB_FUEL Limits

[[					
					]]

Table B-4 BWR/2 (U.Gd)O_2 Rod/Section BWREDB_FUEL Limits

[[						
						]]

APPENDIX C – GESTR-M BASED GNF2 LHGR ENVELOPES

BWR/3-6

Tables C-1 and C-2 provide the complete set of UO_2 and gadolinia GESTR-M based thermal-mechanical LHGR limits applicable to GNF2 fuel bundles for BWR/3-6 plants. The power limit at a given exposure between BOL and the first knee is equal to the pellet maximum power. The power limit at a given exposure between the first and second knees or between the second knee and EOL is determined by interpolation of power with exposure.

Table C-1 BWR/3-6 UO_2 Rod BWREDB_FUEL Limits

[[			
			]]

Table C-2 BWR/3-6 $(U.Gd)O_2$ Rod/Section BWREDB_FUEL Limits

[[				
				]]

BWR/2

Tables C-3 and C-4 provide the complete set of UO_2 and gadolinia GESTR-M based thermal-mechanical LHGR limits applicable to GNF2 fuel bundles for BWR/2 plants. The power limit at a given exposure between BOL and the first knee is equal to the pellet maximum power. The power limit at a given exposure between the first and second knees or between the second knee and EOL is determined by interpolation of power with exposure.

Table C-3 BWR/2 UO_2 Rod BWREDB_FUEL Limits

[[			
			]]

Table C-4 BWR/2 (U.Gd)O_2 Rod/Section BWREDB_FUEL Limits

[[				
				]]

Appendix D - Evaluation of PRIME Implementation on GNF2 Amendment 22 Compliance

Discussion

PRIME based thermal mechanical methodology was reviewed and approved in Reference D-1. Implementation of the PRIME basis into downstream safety analysis codes and methods were reviewed and approved in Reference D-2.

This appendix documents the evaluation of PRIME implementation impacts to the downstream safety analysis methodologies for the GNF2 product line. PRIME implementation impacts to the thermal-mechanical analysis were previously documented in Revision 3 to NEDC-33270P as Section 3.2 was updated in its entirety (GESTR-M thermal-mechanical basis moved to Appendix A). The PRIME based LHGR limits were also defined in Revision 3 to NEDC-33270P in Appendix B.

Table D-1 summarizes the evaluation of the fuel licensing acceptance criteria included within GESTAR II (Reference D-3) relative to the change in methodology from GESTR-M to PRIME.

Summary and Conclusions

Evaluation of PRIME implementation for the GNF2 product line has been performed and the impacts were found to be consistent with expectations. The evaluation summary demonstrates compliance to the related GESTAR-II (Reference D-3) fuel licensing criteria for PRIME implementation into the GNF2 product line.

References

D-1 Global Nuclear Fuel, The PRIME Model for Analysis of Fuel Rod Thermal –Mechanical Performance, Technical Bases - NEDC-33256P-A, Qualification - NEDC-33257P-A, and Application Methodology - NEDC-33258P-A, September 2010.

D-2 Global Nuclear Fuel, “Implementation of PRIME Models and Data in Downstream Methods,” NEDO-33173 Supplement 4-A, Revision 1, November 2012.

D-3 Global Nuclear Fuel, “General Electric Standard Application for Reactor Fuel (GESTAR II),” NEDE–24011–P–A–19, May 2012.

Table D-1. PRIME Implementation Summary Evaluation

Report Section	Discussion
3.1 General Criteria	PRIME based thermal mechanical methodology was reviewed and approved in Reference D-1. Implementation of the PRIME basis into downstream safety analysis codes and methods were reviewed and approved in Reference D-2. There are no mechanical or materials changes associated with the use of PRIME that would require a lead use program.
3.2 Thermal–Mechanical	In Revision 3 of the GNF2 Compliance Report, Section 3.2 was updated in its entirety to reflect the PRIME-based evaluations. The LHGR limits for UO_2 and U-GdO_2 rods are shown in Appendix B.
3.3 Nuclear	Use of the PRIME based GNF2 TMOLs and fuel properties does not impact the nuclear evaluations conducted in Section 3.3.
3.4 New Fuel Design Licensing Evaluation	The transition to PRIME fuel properties has been evaluated in the respective sections. The application of PRIME does not affect the new fuel design licensing criteria.
3.5 Thermal–Hydraulic	The transition to PRIME fuel properties is unrelated to this requirement for pressure drop characteristics.
3.6 Safety Limit MCPR	The transition to PRIME fuel properties is unrelated to this requirement for a cycle-specific safety limit MCPR calculation.
3.7 Operating Limit MCPR Licensing Evaluation	The Operating Limit MCPR is evaluated on a cycle specific basis. The generic off-rated thermal limits are a function (multiplier) of the rated power/flow, cycle and plant-unique limits. Generic ARTS off-rated limits are primarily determined by non-fuel plant system parameters which affect core-wide transient responses. Therefore, PRIME implementation has an insignificant effect on these core-wide transient responses. The generic off-rated LHGRFACp limits have been evaluated and remain applicable based on PRIME overpower limits and fuel properties.
3.8 Critical Power Correlation	The transition to PRIME fuel properties is unrelated to the GESTAR requirements for a critical power correlation.
3.9 Stability Licensing Acceptance Criteria	The conclusions of the Amendment 22 stability analysis are not impacted by the use of PRIME. The ODYSY PRIME sensitivity studies and the revised ODYSY benchmarking with the Vermont Yankee test data consistently show that decay ratios calculated with PRIME will either have an insignificant impact on the core decay ratio or will lower the core decay ratio. In addition, stability decay ratio analyses will continue to be analyzed on a plant-/cycle-specific basis. Therefore, the conclusions of the Amendment 22 remain unchanged with the implementation of PRIME.
3.10 Overpressure	The transition to PRIME fuel properties is unrelated to this requirement for plant cycle specific analysis of the ASME

Protection Analysis	overpressure event.
3.11 Loss–of–Coolant Accident Analysis	The change to PRIME based TMOLs does not affect the LOCA limits for UO_2 rods. A generic study has been performed to confirm that the LOCA limits for UO_2 rods bound the U-GdO_2 rods. The impact of the PRIME implementation on ECCS-LOCA response for BWRs utilizing GNF2 fuel is evaluated and estimated by the approved methodology described in PRIME LTR Supplement 4 (Reference D-2).
3.12 Rod Drop Accident Analysis Licensing Evaluation	The current licensing basis control rod drop analysis uses an adiabatic fuel temperature model and constant moderator void, core pressure, and inlet conditions so that there is no effective heat transfer to the coolant, which has been demonstrated to be conservative. The use of PRIME based fuel temperatures in PANAC11 will not change the calculation of the static control rod worth.
3.13 Refueling Accident	The transition to PRIME fuel properties has no effect on the number of rods that fail during the postulated refueling accident or the radiological consequences.
3.14 Anticipated Transient Without Scram	The use of PRIME fuel properties does not significantly affect key ATWS analysis results such as peak vessel pressure, peak cladding temperature, and suppression pool temperature.

Appendix E – Evaluation of GNF2 Slightly Enriched Blankets

Early fuel bundle designs originally included no blankets whatsoever. However, use of natural uranium blankets has been a standard design practice for the past thirty years or so. This practice has been driven by uranium efficiency considerations rather than the need to satisfy generic, plant or cycle specific licensing criteria. [[

]]

GESTAR II provides generic fuel design and licensing acceptance criteria, thermal-hydraulic and thermal-mechanical analyses bases, and methods used to determine reactor limits. This compliance report shows that GNF2 satisfies the acceptance criteria and meet the licensing requirements in GESTAR II. Although the use of slightly enriched blankets is only a minor departure from recent common design practice, it is prudent to evaluate the safety implications within the framework of GESTAR II compliance. GESTAR II fuel licensing acceptance criteria are organized into fourteen generalized categories. Table E-1 summarizes the assessment of the criteria of GESTAR II relative to the change in the blanket enrichment for each compliance category.

Table E-1. Slightly Enriched Blanket Summary Evaluation

GESTAR II Subsection	Compliance Discussion
1.1.1 General Criteria	Since the pellet and lattice enrichments are within the experience base of GNF2, the slightly enriched blanket design is within the methods basis. There are no mechanical or materials changes associated with the use of the slightly enriched blankets that would require a lead use program. Use of slightly enriched blankets does not impact Section 3.1.
1.1.2 Thermal–Mechanical	The use of slightly enriched blankets will not change the reactor power shape, fuel exposure or accumulation of fission products beyond normal cycle to cycle variations. Therefore the generic analyses reported in Section 3.2 remain valid.
1.1.3 Nuclear	The use of slightly enriched blankets will not change the reactor power shape, fuel exposure or accumulation of fission products beyond normal cycle to cycle variations. The effect on nuclear dynamic parameters will be minimal. Therefore the generic analyses reported in Section 3.3 remain valid.

GESTAR II Subsection	Compliance Discussion
New Fuel Design Licensing Evaluation (No corresponding Subsection in GESTAR II)	The use of slightly enriched blankets will not change the reactor power shape, fuel exposure or accumulation of fission products beyond normal cycle to cycle variations. Therefore the compliance statements provided in Section 3.4 remain valid.
1.1.4 Hydraulic	There are no mechanical changes associated with the use of slightly enriched blankets. Approved hydraulic models and fuel assembly ΔP correlations remain valid. Use of slightly enriched blankets does not impact Section 3.5.
1.1.5 Safety Limit MCPR	The approved uncertainties used in the cycle specific SLMCPR analyses are not impacted by the use of slightly enriched blankets. Section 3.6 remains valid.
1.1.6 Operating Limit MCPR	The use of slightly enriched blankets will not change the reactor power shape, fuel exposure or accumulation of fission products beyond normal cycle to cycle variations. Therefore the generic analyses reported in Section 3.7 remain valid.
1.1.7 Critical Power Correlation	There are no mechanical changes associated with the use of slightly enriched blankets. The critical power correlations and associated statistics remain valid. Use of slightly enriched blankets does not impact Section 3.8.
1.1.8 Stability	Use of slightly enriched blankets will not change the reactor power shape or fuel exposure beyond normal cycle to cycle variations. Furthermore, the definition of the fuel product line is not impacted with the change to a slightly enriched blanket. Therefore, the cycle-independent analyses are not impacted nor are the results in Section 3.9.
1.1.9 Overpressure Protection Analysis	Overpressure protection is evaluated on a cycle specific basis. There are no generic analyses performed to demonstrate compliance to this section of GESTAR II. Therefore the use of slightly enriched blankets does not impact Section 3.10.
1.1.10 Loss–of–Coolant Accident Analysis Methods	Approved LOCA models are not impacted by the use of slightly enriched blankets. Section 3.11 remains valid.
1.1.11 Rod Drop Accident Analysis	The use of slightly enriched blankets will not change the reactor power shape, fuel exposure or accumulation of fission products beyond normal cycle to cycle variations. Therefore the generic analyses reported in Section 3.12 remain valid.

GESTAR II Subsection	Compliance Discussion
1.1.12 Refueling Accident Analysis	The use of slightly enriched blankets will not change the reactor power shape, fuel exposure or accumulation of fission products beyond normal cycle to cycle variations. Relative to natural uranium, use of slightly enriched pellets has an insignificant impact on bundle mass, one factor in determining the number of fuel rods calculated to fail in the refueling accident. Therefore the generic analyses reported in Section 3.13 remain valid.
1.1.13 Anticipated Transient Without Scram	The use of slightly enriched blankets will not change the reactor power shape, fuel exposure or accumulation of fission products beyond normal cycle to cycle variations. Therefore the generic analyses reported in Section 3.14 remain valid.
1.1.14 Fuel Loading Error (FLE) Event Analysis	The use of slightly enriched blankets will not change the reactor power shape, fuel exposure or accumulation of fission products beyond normal cycle to cycle variations. Therefore the generic aspects of FLE compliance analyses will remain valid.

All of the GNF2 licensing compliance generic analyses remain valid with the use of slightly enriched blankets.

APPENDIX F EVALUATION OF IMPROVEMENTS TO DEBRIS FILTER AND SPACER

Summary

Consistent with the GNF principles of continuous and evolutionary product improvement, several mechanical design improvements have been developed for application to GNF2 that are motivated to further improve resistance to debris fretting and provide additional durability that increases margin to seismic requirements. In past products, GNF has retrofit improved components to production fuel designs such as filters in the LTP, water rod interface piece parts and throttling devices, channel interface features, et cetera. The improved mechanical components, described herein, are limited to the Defender filter and the spacer and have been demonstrated through testing and analysis to conform to the new fuel licensing requirements of GESTAR II and do not change the applicability of the compliance evaluations.

Description of Changes

The component mechanical design changes are:

Defender Filter

- [[

]]

Spacer

- [[

]]

Component Performance Assessment

[[

]] In summary, the design improvements being applied to the GNF2 spacer result in improved mechanical robustness, and increased margins to accommodate handling and seismic loads, along with reduced debris capture probability, while maintaining the other functions of the spacer.

The design improvements developed for the Defender filter are motivated to further improve filtering effectiveness. The filter [[ ]] is essentially the same, [[

]]

Compliance with Licensing Requirements

The modifications to the spacer geometry that affect the projected area of the spacer [[

]] were evaluated in full scale critical power and pressure drop testing of [[ ]]. This testing confirmed that these changes do not affect the applicability of the GEXL17 correlation, nor the hydraulic models of the GNF2 fuel assembly. As described above, mechanical durability is improved with the subject design changes which further increases margins to licensing requirements. As such, the improved spacer is considered interchangeable.

The modifications to the Defender filter [[

]] Single-phase pressure drop testing of the filter has been performed and affirms that the improved filter design has equivalent flow resistance to the original Defender. As such, the improved filter is considered interchangeable.

The improved mechanical components, described herein, are limited to the Defender filter and the spacer and have been demonstrated through testing and analysis to conform to the new fuel licensing requirements of GESTAR II and do not change the applicability of the compliance evaluations.

[[

Figure F1-A
Modified Spacer Band
[[
]]

Figure F1-B
Current GNF2 Spacer Band

]]

[[

]]

Figure F-2-A
Reference GNF2 Configuration

[[

]]

Figure F-2-B
Modified Configuration

[[

]]

Figure F-3 Defender Strip Design

[[ ]]